Coordination Chemistry Reviews, 63 (1985) 1–125
Elsevier Science Publishers B.V., Amsterdam – Printed in The Netherlands

ORGANOCOBALT B_{12} MODELS: AXIAL LIGAND EFFECTS ON THE STRUCTURAL AND COORDINATION CHEMISTRY OF COBALOXIMES

NEVENKA BRESCIANI-PAHOR [a], MARGHERITA FORCOLIN [a],
LUIGI G. MARZILLI *[b], LUCIO RANDACCIO *[a], MICHAEL F. SUMMERS [b]
and PAUL J. TOSCANO [b]

[a] *Istituto di Chimica, Universita di Trieste (Italy)*
[b] *Department of Chemistry, Emory University, Atlanta, GA 30322 (U.S.A.)*

(Received 1 May 1984)

CONTENTS

ABBREVIATIONS AND DEFINITIONS

α	Bending (from planarity) of the two DH units. Positive values represent bending towards X.
Acacen	N,N'-Bis(acetylacetone)ethylenediamine

---

* Authors to whom correspondence should be addressed.

0010-8545/85/$43.75

5′Ado	5′-Deoxyadenosyl
ASIS	Aromatic solvent-induced shift
But	n-Butyl
Bz	Benzyl
CCA	Calculated cone angle
Chx	Cyclohexyl
d	Displacement of Co out of the 4-nitrogen equatorial plane. Positive values represent displacement towards L.
$(DBF_2)_2$	Bis-boron difluoride derivative of $(DH)_2$
D_{Co-R}	Co–R bond dissociation energy
DEA	Dimethoxyethylamine
$(DH)_2$	Bis(dimethylglyoximato)
E/C	Derived from a four-parameter equation, the ratio provides an estimation of the "softness" (or "hardness") of the Co atom.
ETI	Electronic *trans* influence
$(GH)_2$	Bis(glyoximato)
HI	Hybridization index
i-PrXan	Isopropylxanthinato
K_B	$[H_2OCo(DH)(DH_2)R^+]/[H_2OCo(DH)_2R][H^+]$
K_{cw}	$[\text{"}Co(DH)_2R\text{"}]/[H_2OCo(DH)_2R]$
K_f; K_f'	Formation constant for neutral and deprotonated cobaloximes, respectively.
K_f^{AH}; K_f^{A-}	Formation constant for cobaloximes with neutral and deprotonated R groups, respectively.
k_{off}, k'_{off}	Rate constant for L dissociation from neutral and deprotonated cobaloximes, respectively.
k_{on}, k'_{on}	Rate constant for L ligation to neutral and deprotonated cobaloximes, respectively.
N_a	Equatorial nitrogen closest to the C–R′ bond
N_o	Equatorial nitrogen *trans* to N_a
pK'_{c2}	– Log of the axial H_2O acid dissociation constant.
pK'_{c-L}	– Log of the equatorial O–H–O acid dissociative constant.
pK'_L	– Log of the acid dissociation constant for LH^+
py	Pyridine
R	Mononegative C donor ligand
R′	Alkyl substituent
Salen	*N*,*N*′-Bis(salicylidene)-ethylenediamine
Salophen	*N*,*N*′-Bis(salicylidene)-*o*-phenylenediamine
SCI	Steric *cis* influence
SCS	Substituent chemical shift

STI	Steric *trans* influence
δ^*	Polar substituent constant
δ_I	Inductive substituent constant
δ_R^0	Delocalization substituent constant
tBut	tert-Butyl
TCA	Tolman's cone angle
X	Mononegative ligand, donor atom unspecified
4-X–py	4-Substituted pyridine

A. INTRODUCTION

About 100 X-ray crystal and molecular structures have been reported [1–104] for molecules containing the $Co(DH)_2$ moiety, where DH is the monoanion of dimethylglyoxime. This group of compounds, which contains both metallo-organic and non-metallo-organic members, forms an interesting link between the two types of chemistry. Compounds containing the $Co(DH)_2$ unit make up the bulk of a class of compounds known as cobaloximes, which contain two mono-deprotonated dioxime ligands H-bonded to each other, with the result that the 4-nitrogen donor atoms are nearly co-planar. The two remaining axial coordination sites in these pseudo-octahedral cobalt(III) derivatives can be occupied by two neutral (L), two anionic (X), or one L and X ligand. The last situation is the most common and the resulting charge is zero. When X is a C donor ligand such as an aryl or an alkyl group, it will sometimes be denoted R instead of X. There are no examples of R occupying more than one axial site in a cobaloxime. This can occur for other related Co(III) compounds, however (see, e.g., refs. 105–109).

These compounds are interesting on the one hand because of their extensive coordination chemistry [105,110] and on the other because of the parallels between the chemistry of organometallic derivatives and organocobalamins [105,111–117]. Two organocobalamins, adenosylcobalamin (adenosyl B_{12}, coenzyme B_{12}) and methylcobalamin (methyl B_{12}), are important cofactors for many enzymic processes, including some in mammalian systems [112]. Vitamin B_{12} is a coordination compound, cyanocobalamin, which serves as a metabolic precursor for the cofactors. The biological aspects of these compounds and the relationship of cobaloxime chemistry to B_{12} chemistry have been reviewed extensively recently [112]. In the present work attention will be focused on the coordination chemistry of cobaloximes and, where appropriate, comparisons will be made with other B_{12} models and with B_{12} derivatives.

The remainder of this review will be divided into four sections. The first section will summarize structural data for all cobaloximes (Table 1) for which X-ray structural information is available. The second section will

TABLE 1

References of structurally characterized cobaloximes. The solidus separates the two axial ligands. Data are ordered according to the donor atom of the neutral axial ligand, where possible.

Axial ligands	Ref.	Axial ligands	Ref.
PMe_3/Me	61	$2\text{-}NH_2\text{–}py/i\text{-}C_3H_7$	81
PMe_3/CH_2CMe_3	69	$4\text{-}N(H)\!=\!C(OMe)\text{–}py/CH_2CH_3$	80
$P(OMe)_3/Cl$	45		
$P(OMe)_3/CN$	66	NH_3/NH_3	35, 44, 56
$P(OMe)_3/CH_2CN$	72	NH_3/Cl	8
$P(OMe)_3/Me$	39	$NH_3/SO_2C_6H_4Me$*	92
$P(OMe)_3/CH_2CF_3$	74	NH_3/SO_3*	92
$PO(OMe)_2$/3-benzyladenine	60	NH_3/CH_2Cl*	92
$P(OMe)_2Ph/Cl$	71	NH_3/Me*	92
$P(OMe)_2Ph/Me$	73	NH_3/C_6H_5*	92
$P(OMe)Ph_2/Cl$	71	$NHMe_2/Cl$	78
$P(OMe)Ph_2/Me$	73	NH_2Ph/NH_2Ph	9, 20
$P(OCH_2)_3CMe/i\text{-}C_3H_7$	68	NH_2Ph/Cl	18
$PBut_3/5\text{-}CF_3$–tetrazolate	48	NH_2Ph/I	37
$PBut_3/Cl$	45	NH_2Ph/SO_3	34, 42
$PBut_3$/xanthinato	16	$NH_2(C_6H_4p\text{-}Cl)/Cl$	23
$PBut_3/\text{–}C_5H_4N$	4	$NH_2(C_6H_4p\text{-}NH_2SO_2)/Cl$	23
$PPh_3/\text{–}NCS$	36		
PPh_3/Cl	8, 19, 22	Morpholine/Cl	70
PPh_3/Br	59	Morpholine/CH_2Ph	65
PPh_3/NO_2	38	(*S*)-PhCH(Me)NH_2–/(*R*)-Me(CN)CH–	26, 31, 52
PPh_3/CH_2CF_3	74	(*S*)-PhCH(Me)NH_2–/(*S*)-Me(CN)CH–	32, 53
PPh_3/CH_2CN	77	(*R*)-PhCH(Me)NH_2–/Me	27
PPh_3/CH_2Br	77	(*R*)-PhCH(Me)NH_2–/(*R*)-MeOOC(Me)CH–	28
$PPh_3/i\text{-}C_3H_7$	49	N-iminopyridine/Me	55
PPh_3/Me	40	3-N-Me–imidazole/OH	25
PPh_3/CH_2CH_3	79	3-N-Me–imidazole/Me	25
$PPh_3/CH(Me)Et$	79	imidazole/*trans*-3,3,4,4-tetracyano-2-phenylcyclopentyl	15, 29
$PPh_3/CH_2C(Me)(COOEt)_2$	79		

PPh_3/CH_2CMe_3	62
$PChx_3/Cl$	40
$PChx_3/CH_2CN$	72
$PChx_3/Me$	61
Py/py	10
Py/Cl	2
Py/N_3	33, 75
$Py/{-}O{-}O{-}CMe_2Ph$	24
$Py/{-}O{-}O{-}CH(Me)(C_6H_4\textit{p}\text{-}Me)$	3
Py/CH_2NO_2	58
Py/CH_2COOMe	1
$Py/{-}CH{=}C{=}C{=}CPh_2$	64
$Py/CH{=}CH_2$	54
$Py/{-}C(Cl){=}C(C_6H_4\textit{p}\text{-}Cl)_2$	14
Py/CH(Me)COOMe*	67
Py/Me	12, 25
Py/CH_2CH_3	51
Py/CH(Me)(COOMe)	82
Py/(*S*)-CH(CN)(Me)*	83
$Py/S(Me)(HgI_2)$*	84
4-CN–py/(*R*)-CH(CN)(Me)	85
4-Cl–py/(*R*)-CH(Me)(COOMe)*	86
$PBut_3$/(*R*)-CH(CN)(Me)*	87
PPh_3/(*R*)-CH(CN)(Me)*	87
H_2O/CN*	89
H_2O/NC*	89
$Py/C_6H_4\text{-}\textit{p}\text{-}SO_2{-}C_6H_4\text{-}\textit{p}\text{-}OEt$*	90
$Py/C_{15}H_{10}Br$*	91
$Py/C_{15}H_{11}$*	91
$Py/CH_2C(Me)(COOEt)_2$	79
Py/CH_2CMe_3	57
Py/CH_2SiMe_3	57
$Py/i\text{-}C_3H_7$	41
$4\text{-}CN{-}Py/CH_2CF_3$	74
$NH_2CH(Ph)CH(OH)Ph/CH_2CH_2CN$	5
NO_2/NO_2	38, 43
NO_2/I	47
H_2O/Br	76
H_2O/NO_2	46
H_2O/CN	63
H_2O/Me	11, 13
H_2O/CH_2CMe_3	62
Cl/Cl*	94
SeCN/SeCN*	93
SCN/SCN*	93
$-CH(NC_5H_5)CO(Ph)/Me$	50
$-CH(NC_5H_5)CO(Ph)/Cl$	30
CH_2CH_3/Cl	6
$SbPh_3/Cl$	7
Br/Br	17, 21
$[Me(DH)_2]_2$	39
$Cl/i\text{-}C_3H_7$*	95
Thiourea/*p*-Cl–aniline*	96
Thiosemicarbazide/thiosemicarbazide*	97
$[(NH_3)_2Co(DH)_2]^+[Co(DH)_2Cl_2]^-$*	98
Me(Ph)As(O)/Cl*	99
Co^{II}-containing compounds	
cis-$Co^{II}(DH_2)_2(CF_3COO)_2$*	100
$[Pyrazine\ Co^{II}(DH)_2]_\infty$*	101
$[4,4'\text{-}Bipyridine\ Co^{II}(DH)_2]_\infty$*	102
$(py)_2Co^{II}(DH)_2$*	103
$[Me(Ph)As(O)Co^{III}(DH)(DH)_2PBut_3]_2Co^{II}$*	104

summarize solution data. A correlation of structural and solution results is given in a third section. Finally, the implications of this work for B_{12} biochemistry will be described.

B. X-RAY STRUCTURES

This section is divided into two parts. First, the $Co(DH)_2$ equatorial unit will be considered and then the axial ligands will be evaluated. A statistical survey of the results presented in Table 1 was undertaken. Starred structures in Table 1 were excluded from the survey for various reasons, including the presence of Co in oxidation state II.

(i) Equatorial moiety

Calculations

The bond lengths and angles of the $Co(DH)_2$ moiety do not differ appreciably from compound to compound. The structural parameters have been collected (with standard deviations) in four Tables (2–5) which will be described below. The compounds in these Tables are identified only by the reference numbers in Table 1 and have been placed into two groups: (1) metallo-organic and (2) non-metallo-organic.

The data given in Tables 2–5 were utilized in the following calculations, with the exception of those structures having estimated standard deviations of Co–N distances greater than 0.01 Å. The means were obtained assuming that the $Co(DH)_2$ unit, without hydrogen atoms, has D_{2h} symmetry, as shown in Fig. 1. The averages were calculated by weighting each measurement by the inverse square of its individual standard deviation.

In a first step, all equivalent bond lengths and angles were averaged, using the data of Tables 2–5, to obtain the values (M_{tot}) of each independent bond length and angle. These values, together with their corresponding estimated standard deviations in parentheses, range (R_{tot}), and number of averaged individual measurements (N_{tot}), are given in Table 6. The relative distributions are represented in Figs. 2–5, in which the intervals are almost equal to the estimated standard deviations of the means of the bond lengths and bond angles. The distributions involving bond angles are comparatively "sharper" than those involving bond lengths. Note that the C–C and O–O means, as well as the means of the C–N–O angles, exhibit broader distributions since N_{tot} for these parameters is about one-half that of the other averages in Table 6. However, the distribution of the O–O distance appears to be particularly broad.

Since the σ-donating power of the axial ligand could influence the electron distribution and hence bond lengths in the equatorial moiety [127],

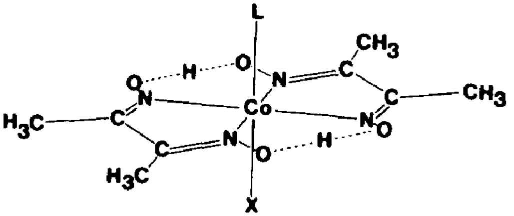

Fig. 1. A general sketch of the cobaloximes $LCo(DH)_2X$.

the means have been calculated for groups of axial ligands of approximately similar σ-donating power. Thus, all available measurements were divided into two groups, one of metallo-organic (organometallic) compounds (group I) and the other of non-metallo-organic (non-organometallic) complexes (group II). The calculated means, M_{mo} and M_{nmo}, respectively, and the corresponding statistical parameters are also given in Table 6.

Results

A comparison of the data collected in Table 6 shows the following points:

(a) the various averages of each independent bond angle appear to be essentially the same within their estimated standard deviations, i.e. the values of M_{mo} and M_{nmo} for bond angles do not differ from the values of M_{tot}.

(b) The averages of the distances for organometallic derivatives, especially those of Co–N and O–O, appear to be slightly different from those of non-organometallic complexes. For example, the Co–N mean for the latter is 0.010 Å longer than that of its organometallic analogue. Similarly, the O–O mean is 0.015 Å longer.

These points, in addition to the kind of distribution of individual measurements shown in Figs. 2 and 3, led us to evaluate the significance of the different values of the bond lengths of the $Co(DH)_2$ moiety. Points (a) and (b) above were checked by dividing all the Co–N distances and all the Co–N–O angles into two groups, each containing about the same number of organometallic and non-organometallic compounds, and averaging each group of values. This trial was repeated four times. The means calculated for each trial are given in Table 7 and are almost all equal to each other and to M_{tot}.

Assuming that the differences in the bond length between groups I and II are significant, a shortening of the Co–N bond length should correspond to a lengthening of the N–O and C–N distances. A comparison of the bond lengths in group I with the corresponding bond lengths in group II illustrates this relationship. Furthermore, the lengthening of the C–N and N–O distances in group I should induce a shortening of the O–O distance, since the bond angles are equal in both groups I and II. The latter distance is actually

TABLE 2

Bond lengths for metallo-organic cobaloximes

Ref.	Co ··· N	C ··· N	N ··· O	C ··· Me	C ··· C	O ··· O
4	1.890 (2)	1.294 (2)	1.359 (2)	1.516 (4)	1.461 (3)	2.470 (2)
	1.894 (1)	1.311 (2)	1.344 (2)	1.509 (3)	1.449 (3)	2.477 (2)
	1.888 (1)	1.308 (2)	1.351 (2)	1.508 (3)		
	1.892 (1)	1.309 (2)	1.343 (2)	1.512 (3)		
25	1.877 (2)	1.319 (6)	1.345 (6)	1.503 (6)	1.478 (9)	2.484 (9)
	1.918 (5)	1.301 (5)	1.351 (6)	1.514 (8)	1.486 (10)	2.481 (4)
	1.877 (4)	1.307 (7)	1.357 (7)	1.492 (7)		
	1.905 (5)	1.300 (5)	1.355 (6)	1.523 (9)		
25	1.886 (6)	1.316 (9)	1.378 (9)	1.513 (13)	1.463 (13)	2.514 (8)
	1.917 (6)	1.302 (11)	1.361 (10)	1.525 (12)	1.472 (12)	2.483 (8)
	1.882 (7)	1.313 (9)	1.359 (9)	1.499 (13)		
	1.903 (5)	1.328 (10)	1.359 (9)	1.519 (10)		
15	1.896 (8)	1.300 (10)	1.360 (10)	1.500 (20)	1.460 (10)	2.518 (9)
	1.909 (8)	1.290 (10)	1.330 (10)	1.500 (20)	1.450 (10)	2.455 (10)
	1.882 (8)	1.300 (10)	1.350 (10)	1.500 (20)		
	1.888 (7)	1.310 (10)	1.340 (10)	1.500 (20)		
39	1.898 (8)	1.301 (13)	1.354 (10)	1.517 (16)	1.486 (15)	2.616 (10)
	1.879 (8)	1.306 (14)	1.343 (11)	1.493 (16)	1.478 (16)	2.470 (10)
	1.873 (8)	1.322 (14)	1.324 (12)	1.493 (17)		
	1.892 (8)	1.295 (14)	1.372 (11)	1.504 (17)		
41	1.891 (2)	1.299 (4)	1.348 (3)	1.503 (5)	1.456 (4)	
	1.882 (2)	1.317 (4)	1.345 (3)	1.504 (4)	1.459 (4)	
	1.892 (2)	1.299 (4)	1.352 (3)	1.507 (5)		
	1.884 (3)	1.316 (4)	1.349 (3)	1.496 (4)		
32	1.889 (5)	1.294 (9)	1.346 (9)	1.504 (11)	1.456 (10)	2.505 (8)
	1.878 (5)	1.307 (9)	1.351 (7)	1.503 (11)	1.468 (10)	2.478 (8)

	1.887 (5)	1.320 (8)	1.343 (8)	1.477 (11)		
	1.893 (5)	1.307 (8)	1.329 (7)	1.499 (10)		
54	1.881 (5)	1.313 (8)	1.332 (7)	1.505 (10)	1.444 (9)	2.495 (5)
	1.872 (5)	1.299 (7)	1.331 (5)	1.488 (10)	1.464 (8)	2.462 (5)
	1.895 (4)	1.298 (7)	1.365 (6)	1.487 (8)		
	1.882 (4)	1.284 (7)	1.369 (6)	1.508 (9)		
57	1.867 (4)	1.330 (7)	1.341 (7)	1.508 (9)	1.438 (10)	2.476 (6)
	1.891 (5)	1.297 (7)	1.352 (7)	1.494 (9)	1.459 (9)	2.470 (6)
	1.893 (2)	1.309 (7)	1.332 (7)	1.492 (8)		
	1.874 (5)	1.301 (6)	1.353 (7)	1.506 (9)		
57	1.914 (5)	1.314 (8)	1.330 (8)	1.498 (10)	1.455 (11)	2.499 (6)
	1.892 (6)	1.312 (8)	1.352 (9)	1.519 (11)	1.450 (11)	2.488 (7)
	1.873 (4)	1.322 (9)	1.339 (9)	1.498 (10)		
	1.903 (6)	1.291 (7)	1.352 (8)	1.505 (10)		
58	1.892 (2)	1.291 (5)	1.355 (3)	1.499 (5)	1.467 (4)	2.460 (4)
	1.887 (3)	1.301 (4)	1.348 (3)	1.488 (6)	1.476 (4)	2.495 (4)
	1.886 (2)	1.302 (2)	1.346 (3)	1.498 (5)		
	1.894 (3)	1.294 (4)	1.356 (3)	1.495 (5)		
61	1.882 (4)	1.315 (6)	1.355 (6)	1.495 (7)	1.455 (8)	2.472 (6)
	1.879 (4)	1.300 (6)	1.353 (6)	1.505 (9)	1.449 (8)	2.456 (6)
	1.874 (4)	1.316 (7)	1.352 (6)	1.506 (8)		
	1.883 (4)	1.311 (6)	1.354 (5)	1.497 (9)		
61	1.884 (4)	1.309 (7)	1.352 (4)	1.492 (8)	1.463 (6)	2.477 (5)
	1.882 (4)	1.290 (6)	1.360 (5)	1.500 (8)	1.462 (7)	2.478 (5)
	1.879 (4)	1.305 (7)	1.361 (5)	1.486 (8)		
	1.883 (4)	1.297 (7)	1.358 (5)	1.497 (8)		
61	1.885 (3)	1.300 (7)	1.345 (5)	1.501 (8)	1.460 (7)	2.492 (5)
	1.895 (4)	1.299 (7)	1.358 (5)	1.505 (8)	1.465 (7)	2.500 (5)
	1.889 (3)	1.282 (6)	1.352 (5)	1.511 (7)		
	1.894 (3)	1.298 (6)	1.364 (5)	1.507 (8)		

TABLE 2 (continued)

Ref.	Co · · · N	C · · · N	N · · · O	C · · · Me	C · · · C	O · · · O
62	1.907 (6)	1.322 (11)	1.317 (8)	1.500 (13)	1.452 (12)	2.517 (8)
	1.869 (6)	1.279 (10)	1.399 (8)	1.474 (13)	1.462 (10)	2.534 (8)
	1.897 (6)	1.303 (10)	1.335 (8)	1.526 (12)		
	1.887 (6)	1.273 (9)	1.370 (7)	1.517 (12)		
62	1.891 (4)	1.301 (7)	1.363 (6)	1.505 (8)	1.466 (8)	2.507 (5)
	1.884 (4)	1.309 (7)	1.358 (5)	1.504 (8)	1.467 (7)	2.501 (5)
	1.885 (4)	1.301 (7)	1.364 (6)	1.503 (8)		
	1.896 (4)	1.312 (7)	1.349 (5)	1.503 (8)		
31	1.898 (5)	1.276 (9)	1.352 (7)	1.507 (11)	1.457 (10)	2.492 (7)
	1.883 (5)	1.302 (9)	1.347 (8)	1.494 (10)	1.485 (10)	2.520 (8)
	1.874 (6)	1.333 (9)	1.307 (8)	1.486 (11)		
	1.901 (5)	1.304 (9)	1.347 (7)	1.466 (11)		
28	1.877 (5)	1.303 (9)	1.358 (7)	1.474 (13)	1.474 (13)	2.477 (8)
	1.880 (6)	1.275 (9)	1.358 (8)	1.505 (14)	1.474 (11)	2.491 (8)
	1.885 (6)	1.312 (10)	1.344 (8)	1.478 (14)		
	1.888 (5)	1.288 (9)	1.340 (8)	1.519 (13)		
40	1.889 (5)	1.313 (8)	1.371 (6)	1.516 (11)	1.451 (9)	2.497 (6)
	1.921 (5)	1.305 (9)	1.354 (7)	1.505 (10)	1.461 (8)	2.477 (6)
	1.887 (5)	1.303 (8)	1.356 (6)	1.508 (9)		
	1.866 (5)	1.334 (8)	1.349 (6)	1.493 (9)		
64	1.881 (5)	1.295 (11)	1.347 (8)	1.523 (9)	1.477 (10)	
	1.878 (7)	1.287 (8)	1.369 (7)	1.555 (13)	1.465 (12)	
	1.872 (5)	1.299 (11)	1.358 (8)	1.514 (9)		
	1.877 (7)	1.286 (9)	1.344 (8)	1.517 (15)		
64	1.872 (8)	1.298 (9)	1.339 (8)	1.513 (15)	1.501 (13)	
	1.882 (5)	1.266 (12)	1.348 (9)	1.533 (10)	1.458 (11)	

	1.903 (5)	1.282 (11)	1.363 (8)	1.495 (9)		
	1.914 (7)	1.294 (9)	1.339 (7)	1.522 (13)		
77	1.892 (9)	1.290 (20)	1.360 (10)	1.500 (20)	1.430 (20)	2.470 (10)
	1.882 (9)	1.320 (20)	1.360 (10)	1.510 (20)	1.440 (20)	2.487 (10)
	1.895 (9)	1.280 (20)	1.350 (10)	1.540 (20)		
	1.896 (9)	1.310 (20)	1.350 (10)	1.520 (20)		
77	1.881 (3)	1.305 (4)	1.360 (3)	1.494 (6)	1.458 (5)	2.488 (3)
	1.888 (3)	1.309 (5)	1.347 (3)	1.499 (5)	1.455 (4)	2.475 (3)
	1.886 (3)	1.301 (4)	1.368 (3)	1.501 (6)		
	1.891 (3)	1.309 (5)	1.340 (3)	1.497 (5)		
74	1.879 (5)	1.330 (20)	1.355 (4)	1.508 (11)	1.448 (7)	2.485 (4)
	1.881 (3)	1.270 (20)	1.349 (5)	1.510 (7)	1.452 (7)	2.499 (5)
	1.884 (5)	1.350 (20)	1.357 (4)	1.510 (11)		
	1.895 (3)	1.270 (20)	1.341 (5)	1.508 (7)		
55	1.878 (7)	1.290 (10)	1.380 (10)	1.510 (10)	1.450 (10)	2.455 (10)
	1.890 (6)	1.300 (10)	1.340 (10)	1.510 (10)	1.450 (10)	2.485 (10)
	1.881 (7)	1.310 (10)	1.340 (10)	1.500 (10)		
	1.893 (7)	1.300 (10)	1.340 (10)	1.520 (10)		
66	1.882 (7)	1.287 (10)	1.357 (7)	1.498 (19)	1.461 (10)	2.483 (7)
	1.898 (5)	1.297 (12)	1.337 (7)	1.491 (11)	1.433 (10)	2.480 (7)
	1.880 (8)	1.296 (10)	1.359 (7)	1.491 (17)		
	1.885 (5)	1.303 (12)	1.351 (7)	1.492 (11)		
66	1.903 (7)	1.302 (10)	1.338 (12)	1.503 (13)	1.460 (15)	2.461 (11)
	1.892 (6)	1.304 (9)	1.326 (11)	1.475 (12)	1.450 (15)	2.487 (11)
	1.896 (6)	1.278 (9)	1.360 (11)	1.508 (13)		
	1.886 (6)	1.299 (9)	1.351 (11)	1.495 (12)		
67	1.880 (8)	1.318 (12)	1.315 (11)	1.506 (10)	1.459 (14)	2.508 (10)
	1.876 (8)	1.305 (12)	1.350 (10)	1.491 (10)	1.464 (14)	2.501 (10)
	1.874 (7)	1.294 (12)	1.342 (10)	1.523 (10)		
	1.890 (8)	1.282 (13)	1.343 (10)	1.528 (10)		

TABLE 2 (continued)

Ref.	Co ··· N	C ··· N	N ··· O	C ··· Me	C ··· C	O ··· O
11	1.884 (3)	1.298 (5)	1.347 (3)	1.488 (6)	1.456 (5)	2.486 (4)
	1.896 (3)	1.306 (5)	1.358 (4)	1.499 (7)	1.471 (7)	
13	1.888 (6)	1.275 (11)	1.339 (8)	1.489 (13)	1.509 (12)	2.484 (9)
	1.884 (7)	1.316 (11)	1.351 (9)	1.503 (15)	1.468 (15)	
14	1.867 (10)	1.321 (13)	1.368 (11)	1.503 (16)	1.454 (15)	2.499 (11)
	1.871 (9)	1.305 (13)	1.334 (10)	1.501 (15)	1.405 (15)	2.505 (11)
	1.871 (9)	1.267 (13)	1.372 (11)	1.515 (17)		
	1.886 (10)	1.296 (13)	1.338 (11)	1.479 (16)		
14	1.884 (10)	1.303 (13)	1.348 (10)	1.488 (16)	1.457 (15)	2.497 (11)
	1.879 (10)	1.280 (13)	1.368 (11)	1.482 (16)	1.435 (16)	2.505 (11)
	1.894 (11)	1.305 (13)	1.362 (11)	1.488 (16)		
	1.861 (10)	1.326 (13)	1.343 (11)	1.481 (16)		
27	1.906 (10)	1.306 (17)	1.349 (13)	1.540 (22)	1.447 (19)	2.474 (12)
	1.883 (11)	1.280 (17)	1.328 (14)	1.484 (21)	1.483 (17)	2.454 (12)
	1.886 (9)	1.306 (14)	1.350 (12)	1.480 (20)		
	1.887 (8)	1.257 (16)	1.318 (12)	1.514 (12)		
50	1.890 (10)	1.300 (10)	1.350 (10)	1.520 (20)	1.470 (20)	2.460 (10)
	1.890 (10)	1.280 (10)	1.370 (10)	1.520 (20)	1.490 (10)	2.450 (10)
	1.870 (10)	1.290 (10)	1.370 (10)	1.510 (20)		
	1.870 (10)	1.300 (10)	1.350 (10)	1.530 (20)		
30	1.880 (10)	1.310 (20)	1.360 (10)	1.500 (20)	1.480 (20)	2.490 (10)
	1.920 (10)	1.260 (10)	1.340 (10)	1.480 (20)	1.470 (20)	2.480 (10)
	1.860 (10)	1.300 (20)	1.350 (10)	1.490 (20)		
	1.900 (10)	1.270 (10)	1.330 (10)	1.540 (20)		
39	1.889 (12)	1.293 (19)	1.362 (18)	1.479 (26)	1.465 (22)	2.458 (18)
	1.898 (12)	1.337 (23)	1.332 (20)	1.487 (26)	1.432 (23)	2.455 (17)

	1.868 (12)	1.323 (22)	1.384 (18)	1.504 (27)		
	1.868 (12)	1.329 (23)	1.349 (20)	1.536 (26)		
49	1.861 (12)	1.330 (20)	1.350 (16)	1.530 (30)	1.420 (20)	
	1.926 (11)	1.270 (20)	1.353 (16)	1.530 (30)	1.410 (30)	
	1.817 (11)	1.350 (20)	1.326 (15)	1.540 (30)		
	1.822 (13)	1.270 (20)	1.377 (16)	1.570 (30)		
65	1.880 (10)	1.330 (20)	1.340 (10)	1.470 (20)	1.470 (20)	2.500 (20)
	1.880 (10)	1.310 (20)	1.360 (20)	1.490 (20)	1.450 (20)	2.551 (20)
	1.900 (10)	1.300 (20)	1.330 (10)	1.510 (20)		
	1.870 (10)	1.310 (20)	1.370 (10)	1.510 (20)		
74	1.889 (3)	1.304 (4)	1.347 (4)	1.501 (5)	1.469 (5)	2.446 (6)
	1.888 (3)	1.295 (4)	1.359 (4)	1.500 (6)	1.467 (5)	2.464 (6)
	1.889 (3)	1.306 (4)	1.351 (4)	1.494 (6)		
	1.895 (3)	1.308 (4)	1.351 (4)	1.492 (6)		
74	1.888 (5)	1.295 (8)	1.353 (5)	1.503 (12)	1.464 (7)	2.480 (10)
	1.890 (4)	1.312 (9)	1.337 (5)	1.495 (9)	1.455 (8)	2.503 (10)
	1.888 (5)	1.296 (8)	1.368 (5)	1.508 (13)		
	1.893 (4)	1.297 (8)	1.350 (5)	1.503 (10)		
74	1.886 (3)	1.307 (8)	1.341 (6)	1.516 (6)	1.447 (7)	2.476 (10)
	1.884 (5)	1.314 (5)	1.343 (5)	1.488 (10)	1.454 (8)	2.488 (10)
	1.882 (3)	1.307 (7)	1.357 (5)	1.495 (6)		
	1.895 (5)	1.302 (6)	1.352 (5)	1.503 (11)		
73	1.885 (4)	1.313 (6)	1.351 (5)	1.503 (8)	1.446 (7)	2.470 (5)
	1.885 (3)	1.300 (6)	1.332 (5)	1.513 (7)	1.483 (6)	2.484 (5)
	1.881 (3)	1.295 (5)	1.347 (4)	1.497 (7)		
	1.875 (3)	1.302 (6)	1.347 (4)	1.490 (7)		
73	1.876 (5)	1.331 (8)	1.327 (7)	1.510 (9)	1.448 (9)	2.472 (7)
	1.859 (5)	1.303 (8)	1.367 (6)	1.497 (11)	1.450 (9)	2.466 (6)
	1.900 (5)	1.320 (8)	1.342 (7)	1.500 (10)		
	1.891 (4)	1.313 (9)	1.355 (7)	1.493 (10)		

TABLE 2 (continued)

Ref.	Co · · · N	C · · · N	N · · · O	C · · · Me	C · · · C	O · · · O
72	1.886 (9)	1.324 (15)	1.357 (12)	1.484 (21)	1.424 (17)	2.508 (1)
	1.892 (9)	1.286 (17)	1.359 (14)	1.541 (20)	1.462 (18)	2.474 (1)
	1.866 (9)	1.311 (17)	1.363 (13)	1.483 (21)		
	1.866 (9)	1.300 (16)	1.317 (14)	1.507 (20)		
72	1.891 (5)	1.287 (7)	1.346 (5)	1.499 (10)	1.472 (7)	2.485 (7)
	1.885 (4)	1.292 (9)	1.361 (6)	1.515 (8)	1.461 (9)	2.507 (7)
	1.900 (6)	1.294 (8)	1.339 (6)	1.509 (12)		
	1.891 (4)	1.292 (9)	1.350 (6)	1.509 (9)		
72	1.884 (4)	1.299 (7)	1.341 (7)	1.488 (8)	1.464 (10)	2.482 (5)
	1.878 (5)	1.309 (7)	1.363 (7)	1.492 (9)	1.476 (10)	2.497 (5)
	1.883 (4)	1.292 (7)	1.348 (8)	1.501 (8)		
	1.897 (5)	1.303 (7)	1.353 (7)	1.499 (8)		
68	1.885 (3)	1.317 (5)	1.347 (4)	1.490 (7)		2.498 (8)
	1.891 (4)	1.294 (6)	1.355 (5)	1.505 (8)		

69	1.875 (3)	1.312 (4)	1.354 (3)	1.503 (5)		2.485 (5)
	1.875 (2)	1.300 (4)	1.353 (3)	1.506 (5)		2.485 (5)
	1.876 (3)	1.301 (4)	1.356 (3)	1.508 (5)		
	1.871 (2)	1.308 (4)	1.355 (3)	1.506 (5)		
51	1.886 (7)	1.310 (10)	1.340 (10)	1.500 (10)	1.470 (20)	2.470 (10)
	1.880 (7)	1.320 (10)	1.360 (10)	1.500 (10)	1.460 (10)	2.450 (10)
	1.899 (8)	1.320 (10)	1.350 (10)	1.500 (10)		
	1.896 (8)	1.310 (10)	1.340 (10)	1.510 (20)		
51	1.872 (7)	1.320 (10)	1.350 (8)	1.540 (10)	1.480 (10)	2.460 (10)
	1.883 (7)	1.290 (10)	1.322 (9)	1.500 (20)	1.470 (10)	2.450 (10)
	1.869 (7)	1.300 (10)	1.324 (7)	1.520 (10)		
	1.878 (6)	1.310 (10)	1.351 (7)	1.530 (10)		
79	1.880 (4)	1.297 (6)	1.359 (5)	1.505 (7)	1.470 (7)	2.500 (7)
	1.884 (4)	1.307 (4)	1.349 (5)	1.482 (7)	1.462 (8)	2.491 (7)
	1.883 (4)	1.300 (5)	1.358 (5)	1.499 (7)		
	1.883 (4)	1.304 (5)	1.356 (5)	1.499 (7)		
80	1.887 (4)	1.286 (7)	1.371 (5)	1.506 (7)	1.460 (7)	2.496 (7)
	1.879 (4)	1.307 (6)	1.360 (5)	1.502 (8)	1.485 (7)	2.478 (7)
	1.885 (3)	1.280 (6)	1.367 (5)	1.503 (7)		
	1.883 (3)	1.307 (6)	1.352 (5)	1.481 (7)		

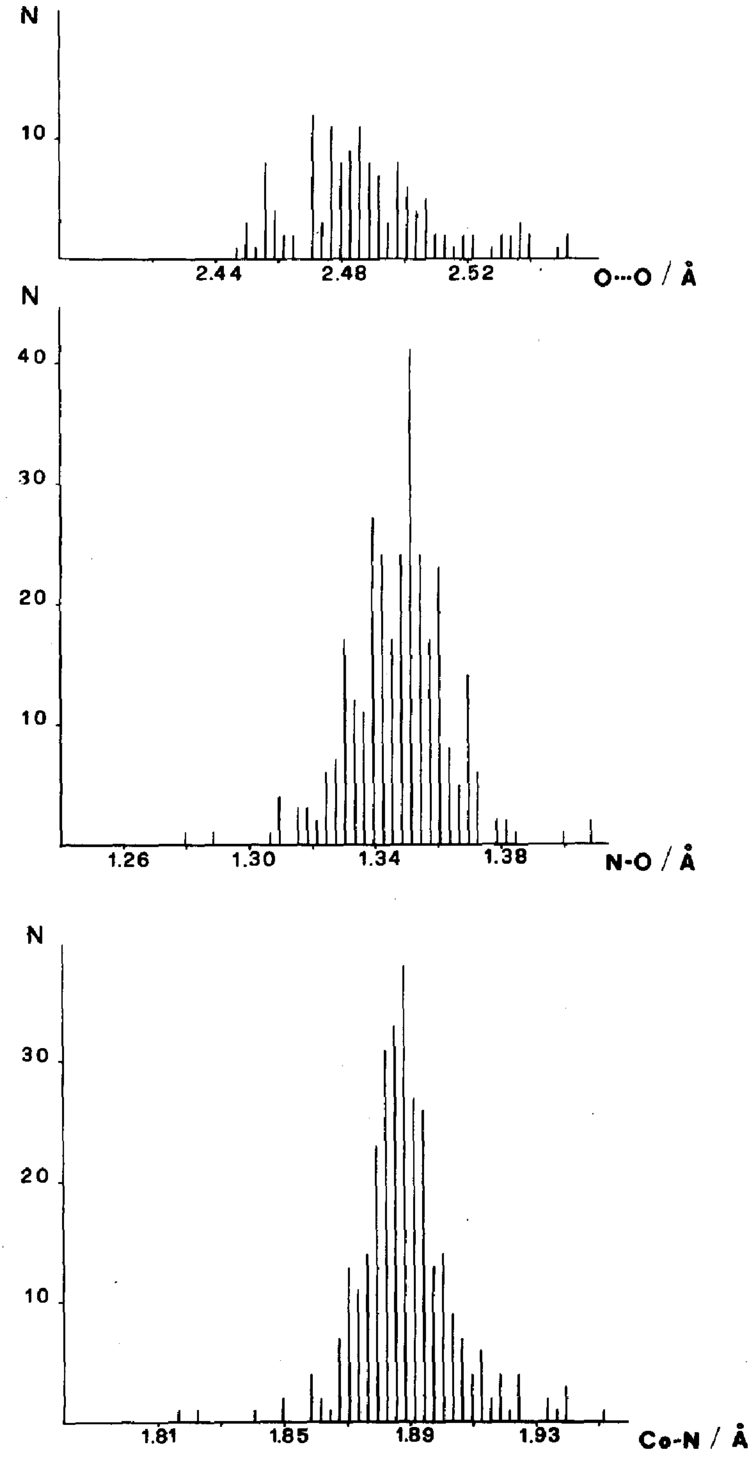

Fig. 2. Distribution of values of the Co–N, N–O, and O · · · O distances.

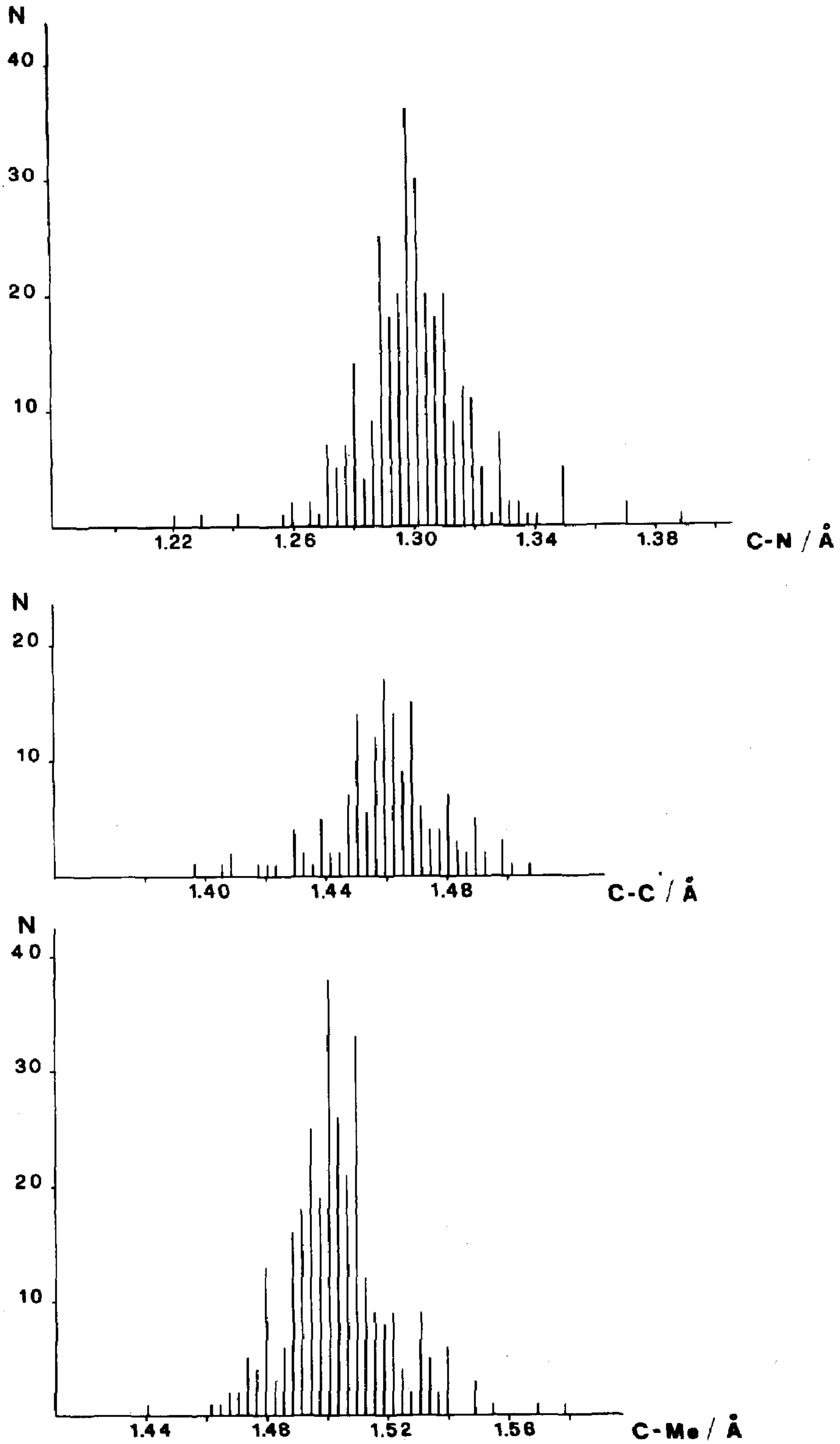

Fig. 3. Distribution of values of the C–Me, C–C, and C–N bond lengths.

TABLE 3

Bond angles of metallo-organic cobaloximes

Ref.	Co··N··C	Co··N··O	N··C··C	C··N··O	Me··C··C	Me··C··N
4	116.5 (2)	122.5 (1)	113.2 (2)	121.0 (2)	124.8 (2)	121.9 (3)
	116.1 (2)	123.2 (1)	112.5 (2)	120.8 (2)	124.2 (2)	123.3 (3)
	116.5 (2)	122.5 (1)	112.8 (2)	121.0 (2)	124.7 (2)	122.5 (2)
	116.2 (2)	123.3 (1)	113.0 (2)	120.4 (2)	125.4 (3)	121.6 (3)
25	117.0 (3)	121.8 (2)	113.1 (3)	121.2 (3)	124.0 (5)	122.9 (5)
	117.7 (4)	122.6 (2)	111.1 (4)	119.7 (5)	125.0 (4)	123.8 (6)
	116.3 (4)	122.0 (3)	113.7 (4)	121.6 (4)	122.3 (6)	123.9 (6)
	117.8 (4)	122.6 (2)	110.7 (5)	119.5 (5)	125.7 (4)	123.6 (6)
25	117.5 (6)	122.0 (4)	112.8 (6)	120.5 (6)	124.3 (6)	123.0 (8)
	117.5 (6)	122.5 (6)	111.8 (6)	120.0 (6)	123.9 (8)	124.3 (8)
	116.9 (6)	122.0 (4)	113.5 (6)	121.1 (6)	122.7 (6)	123.8 (8)
	117.0 (5)	123.4 (4)	111.0 (6)	119.7 (5)	125.0 (6)	123.9 (8)
15	116.0 (6)	122.9 (6)	113.4 (8)	120.7 (8)	124.8 (10)	121.8 (10)
	116.1 (6)	122.2 (6)	113.1 (8)	121.8 (8)	124.7 (10)	122.1 (10)
	118.0 (6)	121.4 (6)	118.8 (8)	120.6 (8)	125.1 (8)	123.1 (8)
	116.8 (6)	121.5 (5)	112.6 (8)	121.6 (6)	124.0 (8)	123.4 (8)
39	115.7 (6)	121.9 (6)	112.6 (6)	122.4 (6)	123.2 (8)	124.2 (8)
	117.0 (8)	123.6 (6)	111.6 (8)	119.2 (6)	123.6 (8)	124.7 (6)
41	117.0 (2)	122.3 (2)	112.4 (3)	120.7 (3)	124.1 (3)	123.5 (3)
	116.4 (2)	122.5 (2)	112.8 (2)	121.2 (2)	124.4 (3)	122.9 (3)
	117.4 (2)	123.0 (2)	112.4 (3)	119.5 (2)	123.4 (3)	124.2 (3)
	117.3 (2)	122.8 (2)	111.9 (2)	119.9 (3)	124.3 (3)	123.7 (3)
32	116.7 (5)	122.9 (5)	113.1 (6)	120.5 (6)	123.5 (6)	123.4 (6)
	117.3 (5)	122.3 (4)	111.8 (6)	120.3 (6)	124.8 (6)	123.3 (6)
	116.8 (4)	123.2 (4)	111.8 (6)	120.0 (6)	125.2 (6)	123.0 (6)
	116.2 (5)	122.5 (4)	113.4 (6)	121.3 (5)	122.8 (6)	123.8 (6)
54	115.5 (4)	122.3 (4)	113.7 (5)	122.1 (5)	122.4 (6)	123.0 (6)
	117.6 (4)	122.7 (4)	111.7 (4)	119.7 (5)	124.7 (6)	123.6 (6)
	117.2 (4)	122.9 (3)	111.9 (5)	120.8 (4)	123.6 (5)	124.5 (5)
	118.0 (4)	122.3 (4)	112.4 (5)	119.7 (4)	123.1 (5)	124.5 (5)
57	115.5 (4)	123.0 (3)	113.4 (5)	121.5 (4)	124.8 (6)	121.9 (6)
	116.5 (4)	122.7 (3)	112.6 (5)	120.7 (5)	123.3 (6)	124.1 (6)
	116.6 (4)	122.9 (3)	111.9 (4)	120.2 (4)	125.8 (6)	122.3 (6)
	117.0 (4)	122.4 (3)	112.9 (5)	120.5 (5)	124.0 (5)	123.1 (6)
57	115.6 (5)	123.1 (4)	112.9 (5)	121.3 (5)	125.6 (6)	121.5 (6)
	116.0 (5)	122.3 (4)	113.6 (6)	121.7 (6)	124.2 (6)	122.3 (6)
	116.5 (5)	123.1 (4)	112.4 (5)	120.4 (5)	124.9 (6)	122.7 (8)
	116.2 (5)	122.7 (3)	113.3 (6)	121.1 (6)	123.9 (6)	122.7 (6)

TABLE 3 (continued)

Ref.	Co··N··C	Co··N··O	N··C··C	C··N··O	Me··C··C	Me··C··N
58	116.9 (2)	121.6 (3)	112.7 (3)	121.3 (3)	123.4 (4)	123.9 (3)
	116.0 (2)	122.3 (2)	112.2 (3)	120.8 (3)	124.1 (3)	123.6 (3)
	117.0 (2)	122.6 (3)	112.2 (3)	120.6 (2)	123.8 (4)	124.0 (3)
	117.0 (2)	122.4 (2)	112.4 (3)	120.6 (3)	123.3 (3)	124.3 (2)
61	117.1 (4)	122.6 (3)	111.8 (4)	120.3 (4)	124.9 (5)	123.6 (6)
	117.2 (2)	122.5 (3)	112.8 (5)	120.3 (4)	122.9 (4)	124.3 (5)
	116.9 (4)	122.5 (3)	112.5 (4)	120.5 (4)	124.2 (5)	123.2 (6)
	117.1 (4)	122.2 (3)	112.1 (5)	120.7 (4)	124.9 (4)	123.0 (5)
61	116.4 (3)	122.8 (3)	112.5 (4)	120.8 (4)	124.4 (5)	123.1 (4)
	117.5 (3)	122.5 (3)	112.3 (4)	120.0 (4)	122.8 (4)	124.9 (4)
	117.4 (3)	122.6 (3)	112.1 (4)	120.0 (4)	124.2 (5)	123.7 (5)
	117.6 (3)	122.1 (3)	112.1 (4)	120.3 (4)	124.8 (5)	123.1 (4)
61	116.7 (3)	122.9 (3)	112.9 (4)	120.3 (4)	124.2 (5)	122.8 (5)
	116.6 (3)	123.7 (3)	112.5 (4)	119.2 (4)	124.5 (5)	122.9 (5)
	116.9 (3)	122.6 (3)	113.1 (4)	120.4 (4)	124.2 (5)	122.6 (5)
	116.6 (3)	123.0 (3)	112.3 (4)	119.9 (4)	125.3 (5)	122.4 (5)
62	114.9 (5)	122.9 (5)	113.4 (6)	122.2 (6)	124.1 (8)	122.4 (8)
	119.3 (5)	122.9 (4)	111.5 (6)	117.5 (6)	124.7 (8)	123.9 (8)
	115.6 (5)	122.1 (5)	113.2 (6)	121.8 (6)	124.1 (6)	122.6 (6)
	117.9 (5)	123.7 (4)	112.2 (6)	118.4 (6)	123.4 (6)	124.5 (6)
62	116.8 (4)	123.4 (3)	112.4 (5)	119.8 (4)	123.8 (5)	123.8 (5)
	116.6 (4)	122.9 (3)	112.5 (5)	120.4 (4)	125.4 (5)	122.1 (5)
	117.3 (4)	122.9 (3)	112.7 (5)	119.8 (4)	123.2 (5)	124.1 (5)
	116.9 (3)	122.8 (3)	111.9 (5)	120.3 (4)	124.6 (5)	123.5 (5)
31	116.4 (5)	122.3 (4)	113.7 (6)	121.1 (5)	122.1 (6)	124.0 (6)
	117.0 (5)	122.7 (4)	111.8 (6)	119.9 (6)	127.3 (6)	120.9 (6)
	115.7 (5)	124.1 (5)	112.8 (6)	120.0 (6)	124.4 (6)	122.7 (6)
	116.3 (5)	122.8 (4)	112.0 (6)	120.5 (5)	121.6 (6)	120.0 (6)
28	117.7 (5)	123.6 (4)	110.9 (6)	118.6 (6)	125.0 (6)	124.1 (6)
	117.5 (5)	121.9 (4)	113.0 (6)	120.4 (6)	122.1 (6)	124.9 (8)
	116.4 (4)	122.8 (5)	111.6 (6)	120.7 (6)	125.9 (8)	122.5 (8)
	116.0 (5)	122.6 (4)	113.6 (6)	121.0 (6)	122.4 (6)	124.0 (6)
40	117.7 (4)	122.8 (4)	111.9 (6)	119.3 (5)	124.8 (6)	123.2 (6)
	115.9 (4)	122.6 (4)	113.7 (5)	121.5 (5)	124.7 (6)	121.6 (6)
	115.8 (4)	124.0 (4)	112.6 (5)	119.6 (5)	124.7 (6)	122.7 (6)
		123.0 (4)	112.6 (5)	120.8 (5)	123.9 (6)	123.3 (6)
64	116.7 (5)	121.5 (5)	112.5 (6)	121.2 (5)	124.4 (8)	123.1 (6)
	116.9 (5)	122.2 (4)	112.9 (6)	120.8 (6)	124.5 (6)	122.6 (6)
	117.2 (5)	122.0 (5)	111.2 (6)	120.7 (5)	124.4 (8)	124.3 (8)
	116.4 (6)	123.3 (4)	113.4 (8)	120.3 (6)	123.6 (6)	123.0 (8)

TABLE 3 (continued)

Ref.	Co··N··C	Co··N··O	N··C··C	C··N··O	Me··C··C	Me··C··N
64			110.1 (8)	119.1 (6)	124.7 (6)	125.3 (8)
			114.1 (6)	120.6 (6)	122.3 (8)	123.6 (8)
			112.9 (6)	121.1 (5)	124.1 (6)	123.1 (6)
			112.7 (8)	122.5 (6)	125.1 (6)	122.2 (6)
77	117.0 (2)	122.3 (6)	113.0 (10)	120.6 (8)	123.0 (10)	124.0 (10)
	116.4 (8)	121.9 (6)	113.0 (10)	121.7 (8)	127.0 (10)	121.0 (10)
	116.3 (8)	121.1 (6)	114.0 (10)	123.0 (10)	123.0 (10)	123.0 (10)
	115.2 (8)	122.8 (6)	113.0 (10)	121.9 (8)	126.0 (10)	121.0 (10)
77	117.0 (2)	123.5 (2)	112.2 (3)	119.4 (3)	124.8 (12)	123.0 (3)
	116.3 (2)	122.3 (2)	112.9 (3)	121.5 (3)	124.0 (4)	123.1 (3)
	117.4 (2)	122.6 (2)	112.0 (3)	119.8 (3)	124.6 (3)	123.3 (3)
	116.2 (2)	122.8 (2)	113.2 (3)	120.9 (3)	124.5 (4)	122.3 (3)
74	116.8 (3)	122.9 (3)	112.8 (5)	120.4 (5)	124.7 (5)	122.6 (5)
	116.7 (3)	122.4 (3)	112.4 (4)	120.9 (3)	124.6 (6)	122.9 (5)
	117.0 (3)	123.3 (3)	112.6 (5)	119.7 (5)	124.2 (5)	123.3 (4)
		122.6 (3)	113.1 (4)	121.3 (3)	124.1 (6)	122.8 (5)
55	116.8 (6)	122.4 (5)	112.8 (8)	120.7 (6)	124.7 (8)	122.5 (8)
	115.7 (6)	122.8 (5)	113.1 (6)	121.6 (6)	123.7 (8)	123.2 (8)
	116.8 (6)	123.5 (5)	111.7 (8)	119.6 (6)	126.1 (8)	122.2 (8)
	115.5 (6)	122.5 (5)	114.1 (8)	121.9 (6)	124.7 (8)	121.1 (8)
66	117.2 (5)	122.0 (5)	112.9 (8)	120.7 (6)	124.2 (6)	122.9 (6)
	116.6 (4)	121.9 (5)	112.3 (6)	121.5 (5)	123.6 (8)	124.1 (6)
	116.6 (5)	122.1 (5)	113.4 (8)	121.0 (6)	125.3 (8)	121.3 (6)
	117.1 (4)	122.4 (5)	112.0 (6)	120.5 (5)	124.4 (8)	123.6 (6)
66	115.6 (6)	122.5 (4)	113.5 (6)	121.9 (6)	124.1 (8)	122.4 (10)
	116.4 (6)	122.1 (4)	112.7 (6)	121.6 (6)	123.0 (6)	124.2 (8)
	116.1 (6)	121.1 (4)	114.1 (6)	122.7 (6)	122.6 (6)	123.3 (8)
	116.9 (6)	122.9 (4)	111.8 (6)	120.2 (6)	124.4 (6)	123.7 (8)
67	115.6 (6)	124.4 (6)	113.2 (8)	120.0 (8)	124.8 (8)	121.7 (8)
	117.5 (6)	123.4 (6)	113.5 (8)	119.1 (8)	123.7 (8)	124.9 (8)
	116.3 (6)	123.1 (6)	111.5 (8)	120.6 (8)	124.1 (8)	123.2 (8)
	116.0 (6)	123.9 (6)	112.6 (8)	120.1 (8)	121.8 (8)	124.8 (8)
11	116.0 (2)	122.0 (2)	113.0 (3)	122.0 (3)	123.3 (3)	123.7 (3)
	117.3 (3)	123.3 (2)	112.2 (3)	119.4 (3)	123.5 (4)	124.3 (4)
13	116.7 (5)	122.0 (5)	112.3 (6)	121.3 (6)	123.1 (6)	124.6 (6)
	116.9 (5)	124.2 (5)	112.3 (8)	119.0 (6)	123.2 (8)	124.6 (8)
14	117.6 (8)	124.0 (6)	110.5 (11)	118.2 (8)	125.4 (11)	124.0 (10)
	116.2 (8)	122.6 (6)	113.3 (11)	120.3 (8)	122.8 (10)	123.8 (8)
	117.0 (8)	121.2 (6)	114.2 (11)	121.7 (8)	123.0 (11)	122.5 (11)
	116.3 (8)	122.8 (6)	112.4 (11)	120.9 (8)	124.3 (11)	123.1 (10)

TABLE 3 (continued)

Ref.	Co··N··C	Co··N··O	N··C··C	C··N··O	Me··C··C	Me··C··N
14	116.2 (8)	123.9 (6)	112.5 (11)	120.0 (8)	123.0 (11)	124.4 (10)
	117.2 (8)	122.9 (6)	112.4 (11)	119.6 (8)	122.5 (11)	125.0 (10)
	115.5 (8)	122.3 (6)	114.2 (12)	122.2 (10)	126.0 (11)	119.3 (11)
	117.5 (8)	123.0 (6)	111.3 (11)	119.5 (8)	125.2 (11)	123.2 (10)
27	115.2 (8)	121.8 (6)	113.7 (12)	112.9 (10)	124.9 (12)	121.4 (12)
	118.2 (8)	122.8 (8)	112.1 (12)	119.5 (11)	123.0 (12)	124.9 (12)
	115.5 (8)	119.8 (6)	112.1 (10)	124.6 (8)	120.2 (11)	118.0 (11)
	117.6 (8)	124.1 (6)	112.7 (11)	118.9 (10)		126.9 (12)
50			111.0 (10)	119.0 (10)	123.0 (10)	126.0 (10)
			111.0 (10)	120.0 (10)	125.0 (10)	124.0 (10)
			111.0 (10)	121.0 (10)	123.0 (10)	123.0 (10)
				121.0 (10)	125.0 (10)	
30	117.0 (8)	124.2 (6)	112.0 (10)	118.0 (10)	125.0 (10)	123.0 (10)
	117.0 (8)	121.4 (6)	113.0 (10)	122.0 (10)	122.0 (10)	125.0 (10)
	117.1 (8)	123.8 (6)	111.0 (10)	119.0 (10)	125.0 (10)	124.0 (10)
	115.0 (8)	121.0 (6)	115.0 (10)	124.0 (10)	123.0 (10)	122.0 (10)
39	117.4 (10)	121.4 (8)	112.8 (8)	120.9 (11)	122.3 (15)	124.8 (11)
	115.5 (12)	123.0 (11)	122.2 (10)	120.9 (12)	123.5 (10)	122.5 (16)
49	116.0 (10)	123.5 (8)	113.0 (10)	120.0 (10)	125.0 (20)	122.0 (20)
	116.0 (10)	121.7 (8)	114.0 (20)	122.0 (10)	125.0 (20)	122.0 (20)
	114.0 (10)	127.6 (8)	113.0 (20)	118.0 (10)	123.0 (20)	121.0 (20)
	118.0 (10)	123.9 (8)	112.0 (20)	118.0 (10)	126.0 (20)	125.0 (20)
65			118.0 (10)	120.0 (10)	125.0 (20)	123.0 (20)
			111.0 (10)	117.0 (10)	125.0 (10)	124.0 (20)
			114.0 (10)	123.0 (10)	123.0 (10)	123.0 (10)
			110.0 (10)	118.0 (10)	127.0 (10)	122.0 (10)
74	116.9 (2)	122.4 (2)	112.1 (3)	120.7 (3)	124.5 (3)	123.4 (4)
	116.9 (3)	122.5 (2)	112.8 (3)	120.5 (3)	123.3 (3)	123.9 (4)
	117.1 (2)	122.8 (2)	112.5 (3)	120.0 (3)	124.5 (3)	123.0 (4)
	117.0 (2)	122.5 (2)	112.2 (3)	120.5 (3)	124.3 (3)	123.5 (4)
74	116.9 (2)	123.1 (2)		120.0 (3)		
		122.9 (2)				
73	116.4 (3)	123.1 (3)	113.4 (4)	120.5 (4)	125.5 (4)	122.2 (5)
	116.3 (3)	123.2 (3)	112.7 (4)	120.6 (4)	123.4 (4)	123.2 (6)
	116.9 (3)	122.9 (3)	112.4 (4)	120.5 (3)	124.7 (4)	122.6 (4)
	116.4 (4)	120.4 (3)	112.0 (4)	120.5 (4)	125.5 (4)	122.5 (4)
73	117.3 (4)	123.1 (4)	112.8 (6)	119.1 (5)	124.5 (6)	122.0 (6)
	114.6 (4)	123.6 (3)	113.5 (5)	122.2 (5)	123.4 (6)	124.5 (6)
	117.3 (4)	123.7 (4)	112.0 (6)	119.9 (5)	123.7 (6)	123.5 (6)
	116.4 (4)	122.1 (4)	112.4 (5)	120.6 (5)	124.3 (6)	123.3 (6)

TABLE 3 (continued)

Ref.	Co··N··C	Co··N··O	N··C··C	C··N··O	Me··C··C	Me··C··N
72	115.9 (8)	123.8 (6)	112.0 (10)	120.0 (8)	126.0 (10)	122.0 (10)
	115.6 (8)	122.9 (4)	115.0 (10)	121.3 (8)	123.0 (10)	122.0 (10)
	117.7 (8)	122.2 (6)	111.0 (10)	119.7 (8)	125.0 (10)	124.0 (10)
	116.5 (8)	124.3 (8)	113.0 (10)	119.0 (10)	123.0 (10)	124.0 (10)
72	117.0 (4)	122.2 (4)	112.2 (6)	120.6 (5)	122.6 (5)	125.2 (5)
	116.7 (5)	122.7 (4)	112.7 (5)	120.5 (4)	122.7 (6)	124.6 (5)
	116.8 (4)	122.1 (4)	112.6 (6)	121.1 (6)	124.2 (6)	123.2 (6)
	117.1 (4)	122.8 (4)	112.8 (5)	120.1 (5)	124.0 (6)	123.1 (6)
72	116.7 (5)	123.0 (3)	113.1 (5)	120.7 (5)	122.9 (5)	124.0 (6)
	116.4 (5)	123.5 (3)	112.1 (5)	119.8 (5)	124.0 (5)	123.9 (6)
	116.6 (5)	123.0 (3)	113.6 (5)	120.6 (5)	123.0 (6)	123.3 (6)
	116.3 (4)	123.4 (3)	111.5 (5)	119.7 (5)	124.9 (5)	123.5 (6)
69	116.9 (2)	123.1 (2)	111.9 (3)	120.0 (3)	125.8 (3)	122.3 (3)
	116.9 (2)	122.9 (2)	112.6 (3)	120.1 (3)	125.1 (3)	122.0 (3)
	117.2 (2)	122.9 (2)	112.3 (3)	119.8 (3)	124.3 (3)	123.3 (3)
	117.1 (2)	123.2 (3)	112.1 (3)	119.5 (2)	125.2 (3)	122.6 (3)
51	117.1 (6)	121.2 (6)	112.4 (8)	121.3 (8)	125.2 (8)	123.1 (8)
	117.8 (6)	122.2 (6)	111.4 (8)	120.0 (8)	125.2 (8)	124.0 (8)
	116.3 (6)	121.6 (6)	113.1 (8)	122.5 (8)	124.5 (8)	122.2 (8)
	117.3 (6)	122.8 (6)		120.0 (8)	124.7 (6)	123.5 (10)
51	116.4 (6)	122.2 (5)	112.1 (6)	121.3 (6)	122.9 (8)	122.8 (8)
	117.4 (6)	122.7 (5)	112.1 (8)	119.9 (6)	123.4 (6)	125.0 (8)
	118.1 (5)	123.6 (5)	111.5 (6)	118.3 (6)	125.2 (6)	125.1 (6)
	117.0 (5)	121.7 (5)	112.1 (6)	121.2 (6)		122.7 (6)
79	117.4 (3)	122.7 (3)	112.4 (4)	119.9 (4)	123.6 (5)	124.0 (5)
	117.2 (3)	123.5 (3)	111.8 (4)	119.2 (4)	123.9 (4)	124.3 (5)
	117.0 (3)	123.2 (3)	112.2 (4)	119.8 (4)	125.0 (5)	122.8 (5)
	116.5 (4)	122.7 (3)	112.7 (4)	120.8 (4)	123.7 (5)	123.7 (5)

shorter in group I. In addition, the general constancy of the bond angles suggests that the above changes in the bond lengths could reflect variations of π-electron density distribution in the equatorial DH ligands rather than changes in hybridization.

It is worthwhile to compare the geometry of the DH ligand in the complexes with that of the free ligand DH_2 and its deprotonated dianion D^{2-} [118]. These data, together with those relative to the parent ligand glyoxime (GH_2) [119], are given in Table 8. In addition to the expected large variations in the conformation and the N–C–C–N chain bond angles of the ligand upon coordination, the N–O distance decreases by 0.05 Å and the

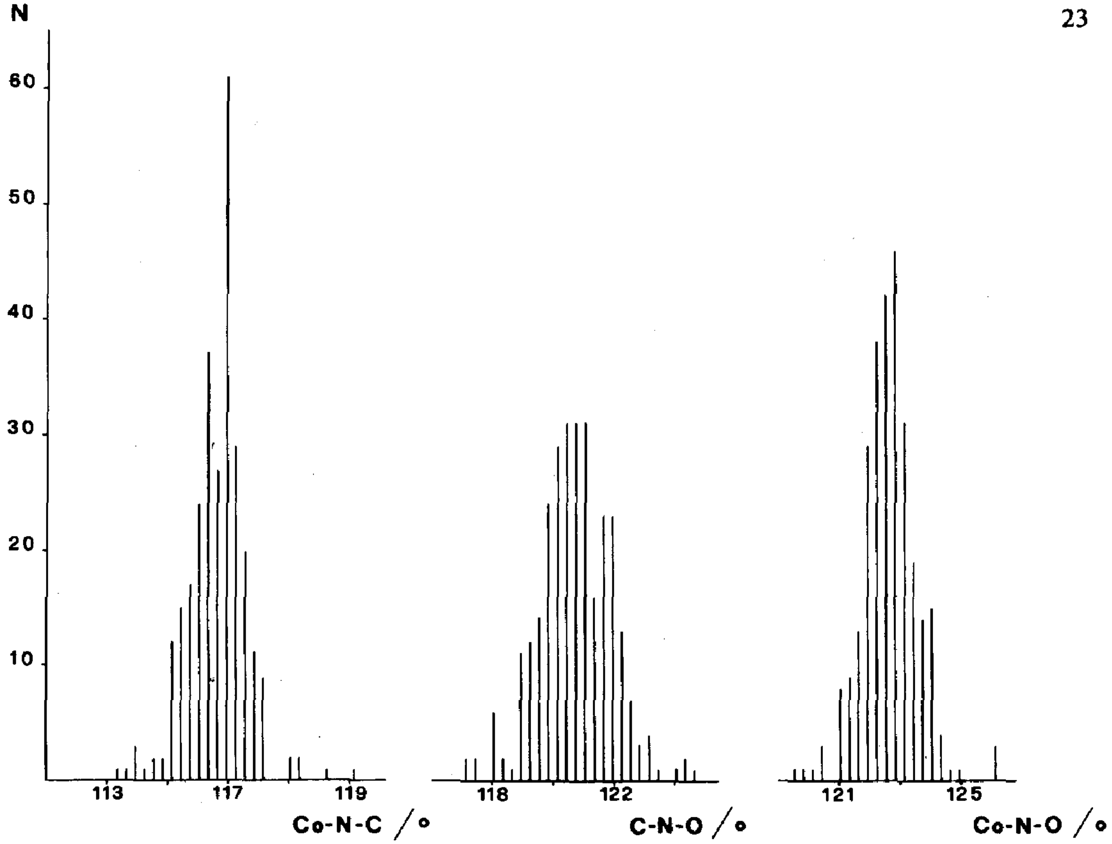

Fig. 4. Distribution of values of the Co–N–C, C–N–O, and Co–N–O bond angles.

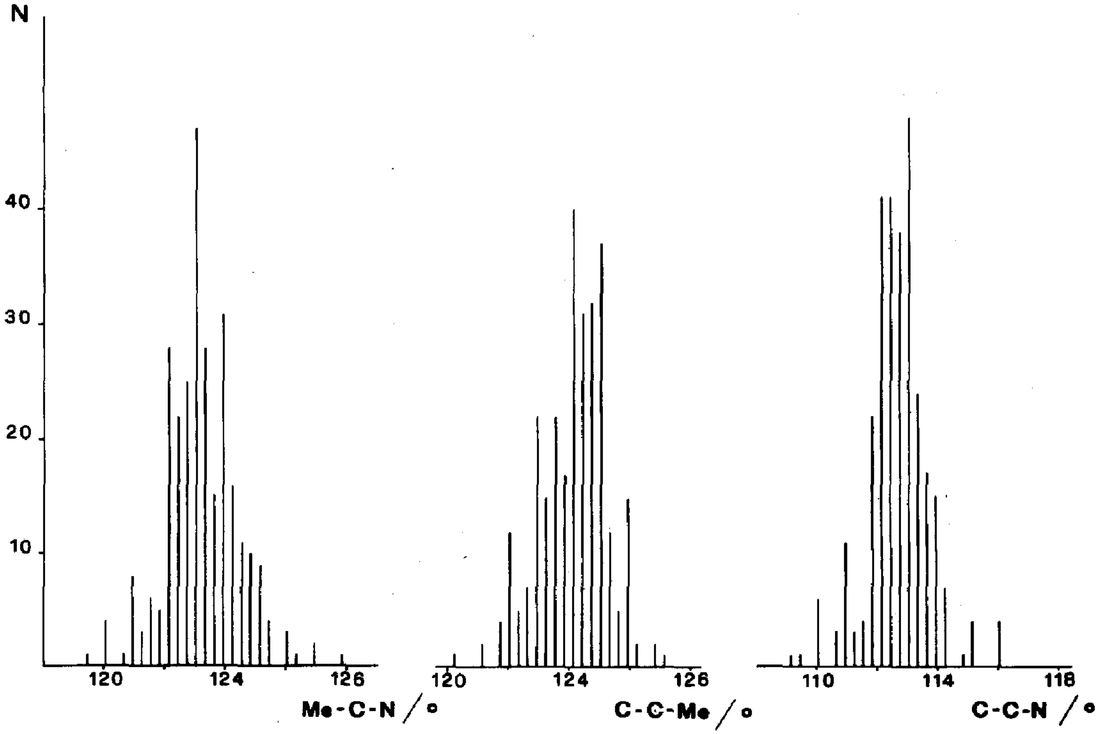

Fig. 5. Distribution of values of the Me–C–N, C–C–Me, and C–C–N bond angles.

TABLE 4

Bond lengths of non-metallo-organic cobaloximes

Ref.	Co ··· N	C ··· N	N ··· O	C ··· Me	C ··· C	O ··· O
8	1.870 (10)	1.300 (20)	1.340 (10)	1.490 (20)	1.470 (20)	2.490 (10)
	1.890 (10)	1.290 (20)	1.350 (10)	1.520 (20)	1.500 (20)	2.500 (10)
	1.890 (10)	1.290 (20)	1.350 (10)	1.500 (20)		
	1.890 (10)	1.320 (20)	1.330 (10)	1.500 (20)		
8	1.883 (5)	1.276 (8)	1.343 (6)	1.501 (10)	1.489 (8)	2.491 (6)
	1.883 (5)	1.278 (8)	1.345 (6)	1.501 (8)	1.477 (8)	2.480 (6)
	1.909 (5)	1.291 (7)	1.335 (6)	1.498 (8)		
	1.887 (5)	1.285 (8)	1.361 (5)	1.503 (9)		
9	1.885 (6)	1.286 (10)	1.353 (6)	1.482 (12)	1.463 (7)	
	1.889 (5)	1.303 (10)	1.333 (6)	1.476 (11)		
16	1.898 (5)	1.283 (8)	1.337 (7)	1.504 (10)	1.462 (10)	2.506 (7)
	1.887 (5)	1.280 (8)	1.357 (7)	1.486 (10)	1.452 (10)	2.507 (7)
	1.880 (5)	1.302 (8)	1.338 (7)	1.509 (10)		
	1.879 (5)	1.304 (8)	1.325 (7)	1.501 (10)		
18	1.876 (2)	1.306 (4)	1.332 (4)	1.494 (4)	1.463 (4)	2.490 (4)
	1.884 (3)	1.293 (3)	1.334 (4)	1.487 (5)	1.476 (4)	2.513 (4)
	1.899 (2)	1.302 (4)	1.353 (4)	1.493 (4)		
	1.925 (2)	1.277 (3)	1.343 (4)	1.495 (5)		
19	1.913 (11)		1.289 (15)	1.504 (29)	1.460 (28)	2.470 (30)
	1.935 (14)		1.328 (14)	1.533 (30)	1.419 (28)	2.484 (30)
	1.897 (11)		1.328 (16)	1.498 (29)		
	1.901 (18)		1.331 (25)	1.500 (31)		
20	1.910 (5)	1.301 (10)	1.356 (7)	1.489 (11)	1.468 (10)	
	1.937 (6)	1.323 (9)	1.310 (7)	1.474 (12)	1.468 (9)	
	1.953 (6)	1.317 (10)	1.317 (7)	1.478 (10)		
	1.933 (6)	1.294 (9)	1.352 (7)	1.491 (11)		
22	1.885 (7)	1.300 (10)	1.342 (9)	1.500 (10)	1.470 (10)	2.478 (9)
	1.885 (7)	1.320 (10)	1.315 (9)	1.510 (10)	1.450 (10)	2.536 (9)
	1.890 (7)	1.330 (10)	1.332 (9)	1.500 (10)		
	1.897 (7)	1.300 (10)	1.339 (9)	1.500 (10)		
23	1.870 (8)	1.289 (14)	1.323 (11)	1.532 (17)	1.494 (16)	2.510 (11)
	1.884 (8)	1.293 (13)	1.344 (11)	1.488 (16)	1.447 (17)	2.536 (11)
	1.905 (8)	1.292 (12)	1.326 (10)	1.494 (17)		
	1.896 (8)	1.290 (12)	1.338 (11)	1.488 (16)		
23	1.872 (5)	1.311 (8)	1.337 (6)	1.488 (10)	1.457 (9)	2.498 (6)
	1.884 (5)	1.308 (8)	1.329 (6)	1.487 (10)	1.468 (9)	2.480 (6)
	1.908 (5)	1.280 (8)	1.348 (6)	1.486 (11)		
	1.906 (5)	1.288 (8)	1.359 (6)	1.498 (11)		

TABLE 4 (continued)

Ref.	Co···N	C···N	N···O	C···Me	C···C	O···O
24	1.887 (3)	1.297 (5)	1.336 (4)	1.475 (6)	1.458 (6)	2.480 (5)
	1.890 (3)	1.296 (5)	1.344 (4)	1.468 (6)	1.459 (6)	2.486 (5)
	1.892 (3)	1.299 (6)	1.342 (5)	1.502 (6)		
	1.887 (3)	1.293 (5)	1.343 (4)	1.465 (6)		
25	1.896 (5)	1.292 (8)	1.331 (7)	1.485 (8)	1.466 (9)	2.483 (6)
	1.908 (5)	1.289 (8)	1.342 (6)	1.493 (9)	1.472 (9)	2.500 (6)
	1.896 (5)	1.296 (8)	1.342 (7)	1.514 (9)		
	1.913 (5)	1.273 (8)	1.336 (6)	1.494 (10)		
37	1.900 (10)	1.290 (20)	1.320 (20)	1.510 (20)	1.480 (20)	2.450 (10)
	1.890 (10)	1.230 (20)	1.340 (20)	1.530 (20)	1.490 (20)	2.450 (10)
	1.900 (10)	1.290 (20)	1.330 (20)	1.500 (20)		
	1.890 (10)	1.290 (20)	1.330 (20)	1.490 (20)		
34	1.893 (5)	1.307 (9)	1.334 (8)	1.511 (8)	1.470 (10)	2.523 (8)
	1.889 (7)	1.288 (9)	1.362 (8)	1.490 (10)	1.480 (10)	2.485 (8)
	1.892 (6)	1.290 (10)	1.315 (8)	1.511 (9)		
	1.881 (7)	1.302 (9)	1.366 (9)	1.510 (10)		
38	1.918 (2)	1.295 (5)	1.371 (4)	1.496 (4)	1.494 (5)	2.549 (4)
	1.918 (2)	1.297 (3)	1.366 (3)	1.496 (5)	1.482 (5)	2.496 (4)
	1.903 (2)	1.297 (5)	1.350 (4)	1.505 (4)		
	1.902 (2)	1.301 (3)	1.353 (3)	1.497 (5)		
38	1.891 (9)	1.320 (20)	1.350 (10)	1.500 (20)	1.450 (20)	2.483 (10)
	1.924 (9)	1.280 (20)	1.310 (10)	1.550 (20)	1.460 (20)	2.535 (10)
	1.904 (9)	1.330 (20)	1.340 (10)	1.480 (20)		
	1.914 (9)	1.320 (20)	1.330 (10)	1.500 (20)		
42	1.910 (10)	1.280 (20)	1.350 (10)	1.530 (20)	1.480 (20)	2.480 (10)
	1.890 (10)	1.390 (20)	1.310 (10)	1.550 (30)	1.410 (20)	2.540 (10)
	1.850 (10)	1.350 (20)	1.340 (10)	1.550 (20)		
	1.900 (10)	1.340 (20)	1.330 (10)	1.510 (20)		
43	1.904 (3)	1.300 (6)	1.353 (4)	1.495 (9)	1.473 (9)	2.540 (4)
	1.908 (3)	1.301 (7)	1.350 (4)	1.495 (9)	1.464 (8)	2.492 (4)
	1.892 (3)	1.298 (7)	1.333 (4)	1.512 (9)		
	1.893 (3)	1.299 (7)	1.335 (4)	1.502 (9)		
40	1.913 (12)	1.220 (20)	1.410 (20)	1.480 (30)	1.500 (20)	2.527 (30)
	1.849 (13)	1.370 (20)	1.370 (20)	1.510 (30)	1.460 (20)	2.522 (30)
	1.924 (12)	1.240 (20)	1.410 (20)	1.520 (20)		
	1.901 (12)	1.370 (20)	1.370 (20)	1.470 (30)		
45	1.876 (5)	1.305 (7)	1.349 (7)	1.530 (10)	1.460 (10)	2.455 (7)
	1.887 (4)	1.317 (8)	1.350 (7)	1.510 (10)	1.480 (10)	2.482 (7)
	1.886 (5)	1.301 (7)	1.366 (7)	1.510 (10)		
	1.888 (4)	1.276 (7)	1.359 (7)	1.530 (10)		

TABLE 4 (continued)

Ref.	Co···N	C···N	N···O	C···Me	C···C	O···O
45	1.876 (5)	1.313 (11)	1.335 (7)	1.534 (9)	1.441 (10)	2.486 (7)
	1.889 (5)	1.303 (8)	1.330 (5)	1.535 (12)	1.458 (8)	2.493 (7)
	1.894 (4)	1.299 (9)	1.353 (6)	1.518 (9)		
	1.892 (6)	1.310 (8)	1.344 (5)	1.518 (11)		
45	1.940 (10)	1.280 (20)	1.340 (20)	1.540 (20)	1.430 (20)	2.472 (20)
	1.940 (10)	1.260 (20)	1.380 (20)	1.480 (30)		2.408 (20)
	1.840 (10)	1.290 (20)	1.350 (20)	1.580 (30)		
	1.900 (10)	1.300 (20)	1.280 (20)	1.520 (30)		
45	1.870 (10)	1.310 (20)	1.370 (20)	1.440 (20)		2.506 (20)
	1.860 (10)	1.350 (20)	1.360 (20)	1.490 (30)		2.553 (20)
	1.940 (10)	1.350 (20)	1.310 (20)	1.460 (30)		
	1.880 (10)	1.290 (20)	1.340 (20)	1.480 (20)		
46	1.908 (6)	1.292 (8)	1.350 (8)	1.493 (11)	1.439 (11)	2.538 (8)
	1.885 (5)	1.292 (8)	1.325 (7)	1.474 (10)	1.470 (10)	
48	1.860 (6)	1.320 (10)	1.340 (10)	1.510 (10)	1.430 (10)	2.456 (7)
	1.877 (5)	1.310 (10)	1.330 (10)	1.530 (10)	1.440 (10)	2.498 (8)
	1.875 (6)	1.310 (10)	1.340 (10)	1.490 (10)		
	1.896 (5)	1.270 (10)	1.320 (10)	1.510 (10)		
60	1.879 (7)	1.290 (10)	1.346 (8)	1.480 (10)	1.470 (10)	2.532 (9)
	1.869 (7)	1.300 (10)	1.355 (8)	1.480 (10)	1.480 (10)	2.531 (9)
	1.915 (7)	1.290 (10)	1.357 (8)	1.500 (10)		
	1.902 (7)	1.290 (10)	1.342 (9)	1.480 (10)		
70	1.896 (4)	1.312 (6)	1.330 (5)	1.494 (9)	1.397 (8)	2.472 (5)
	1.902 (4)	1.265 (7)	1.347 (6)	1.504 (8)	1.473 (7)	2.492 (5)
	1.889 (4)	1.292 (6)	1.373 (5)	1.472 (7)		
	1.882 (4)	1.286 (6)	1.345 (5)	1.489 (7)		
25	1.884 (6)	1.288 (9)	1.373 (9)	1.505 (11)	1.466 (12)	2.490 (9)
	1.895 (6)	1.295 (11)	1.341 (10)	1.506 (11)	1.459 (10)	2.457 (9)
	1.875 (6)	1.292 (9)	1.349 (8)	1.505 (11)		
	1.886 (5)	1.305 (8)	1.325 (8)	1.498 (9)		
3	1.890 (7)	1.289 (15)	1.359 (10)	1.505 (15)	1.489 (15)	2.460 (10)
	1.897 (7)	1.274 (15)	1.342 (10)	1.501 (15)	1.472 (15)	2.478 (10)
	1.867 (7)	1.284 (15)	1.353 (10)	1.504 (15)		
	1.884 (7)	1.272 (15)	1.341 (10)	1.536 (15)		
59	1.889 (11)	1.334 (17)	1.335 (15)	1.508 (22)	1.423 (20)	2.470 (10)
	1.891 (11)	1.318 (17)	1.343 (15)	1.499 (23)	1.464 (20)	2.510 (10)
	1.887 (11)	1.299 (18)	1.333 (15)	1.533 (20)		
	1.888 (11)	1.289 (18)	1.344 (15)	1.498 (24)		

TABLE 4 (continued)

Ref.	Co···N	C···N	N···O	C···Me	C···C	O···O
71	1.901 (5)	1.306 (9)	1.344 (7)	1.511 (11)	1.442 (10)	2.468 (13)
	1.898 (5)	1.316 (8)	1.325 (7)	1.502 (11)	1.462 (12)	2.473 (13)
	1.898 (5)	1.316 (9)	1.351 (8)	1.508 (12)		
	1.887 (6)	1.278 (10)	1.346 (8)	1.512 (14)		
71	1.898 (4)	1.300 (7)	1.343 (6)	1.513 (9)	1.456 (8)	2.480 (8)
	1.895 (4)	1.298 (7)	1.353 (6)	1.514 (8)	1.463 (7)	2.473 (8)
	1.894 (4)	1.295 (7)	1.338 (5)	1.513 (8)		
	1.890 (4)	1.292 (7)	1.362 (6)	1.509 (8)		

TABLE 5

Bond angles of non-metallo-organic cobaloximes

Ref.	Co··N··C	Co··N··O	N··C··C	C··N··O	Me··C··C	Me··C··N
8	119.2 (8)	123.5 (8)	109.3 (11)	117.3 (10)	125.0 (13)	125.0 (12)
	115.8 (8)	122.2 (8)	114.8 (12)	122.0 (10)	123.0 (10)	122.0 (10)
	117.9 (8)	122.2 (8)	111.8 (12)	119.6 (10)	125.3 (12)	122.9 (12)
	116.7 (8)	123.6 (8)	111.8 (12)	119.7 (11)	121.6 (12)	125.5 (12)
8	116.7 (4)	123.0 (4)	112.6 (5)	120.2 (5)	121.9 (6)	125.4 (5)
	117.0 (4)	122.4 (4)	112.0 (5)	120.6 (5)	123.7 (6)	124.2 (6)
	117.0 (4)	122.0 (4)	111.8 (5)	121.1 (5)	123.1 (5)	125.0 (5)
	117.3 (4)	121.8 (4)	113.0 (5)	120.9 (5)	123.7 (6)	123.3 (6)
9	117.8 (8)	122.9 (6)	112.2 (8)	119.2 (10)	122.9 (12)	125.0 (16)
	116.8 (8)	121.4 (6)	112.4 (10)	121.8 (12)	123.0 (12)	124.6 (16)
16	115.7 (5)	122.3 (5)	113.8 (5)	121.9 (5)	122.1 (5)	124.0 (5)
	117.2 (5)	123.1 (5)	112.1 (5)	119.5 (5)	124.8 (5)	123.1 (5)
	115.7 (5)	123.5 (5)	113.5 (5)	120.6 (5)	123.6 (5)	122.8 (5)
	116.5 (5)	123.6 (5)	112.3 (5)	119.9 (5)	124.6 (5)	123.1 (5)
18	116.1 (2)	122.2 (2)	112.6 (4)	121.7 (2)	124.7 (4)	122.6 (3)
	116.0 (2)	121.9 (2)	113.1 (4)	122.0 (3)	123.9 (4)	123.1 (3)
	117.2 (2)	123.7 (2)	112.2 (4)	119.1 (2)	123.7 (4)	123.9 (3)
	116.8 (2)	123.2 (2)	112.5 (4)	120.8 (2)	124.3 (4)	122.7 (3)
19	113.7 (13)	124.4 (11)	114.0 (20)	121.5 (12)	124.0 (20)	122.3 (16)
	116.4 (11)	121.7 (8)	114.0 (20)	124.3 (17)	126.0 (20)	120.0 (20)
	114.3 (11)	121.5 (10)	112.0 (20)	120.0 (12)	125.0 (20)	123.0 (20)
	114.6 (11)	122.0 (13)	116.0 (20)	122.6 (15)	123.0 (20)	121.0 (20)
20	117.0 (10)	124.0 (10)	113.0 (10)	118.0 (10)	125.0 (10)	122.0 (10)
	115.0 (10)	126.0 (10)	114.0 (10)	119.0 (10)	124.0 (10)	122.0 (10)
	124.0 (10)	124.0 (10)	114.0 (10)	121.0 (10)		122.0 (10)
	117.0 (10)	124.0 (10)	113.0 (10)	119.0 (10)		122.0 (10)

TABLE 5 (continued)

Ref.	Co··N··C	Co··N··O	N··C··C	C··N··O	Me··C··C	Me··C··N
22	115.9 (6)	122.8 (6)	113.0 (10)	121.3 (6)	122.1 (6)	124.7 (8)
	115.5 (6)	122.9 (6)	113.0 (10)	121.4 (6)	124.0 (10)	123.1 (8)
	116.7 (6)	122.4 (6)	112.0 (10)	120.9 (6)	124.0 (10)	124.0 (8)
	116.4 (6)	121.5 (6)	114.0 (10)	121.9 (6)	125.0 (10)	121.7 (8)
23	116.4 (8)	123.0 (6)	113.3 (10)	120.5 (8)	121.7 (8)	125.0 (11)
	117.4 (6)	122.7 (6)	110.7 (8)	119.9 (8)	125.3 (8)	124.0 (10)
	116.3 (6)	121.3 (6)	113.1 (8)	122.2 (8)	126.0 (8)	120.7 (8)
	116.8 (6)	123.1 (6)	113.0 (8)	120.1 (8)	123.6 (10)	122.9 (10)
23	116.0 (4)	121.9 (4)	112.8 (6)	122.1 (6)	124.2 (6)	123.0 (6)
	115.6 (4)	122.2 (4)	113.1 (6)	122.2 (5)	124.3 (6)	122.5 (6)
	116.5 (5)	123.2 (4)	113.5 (6)	120.2 (6)	124.0 (6)	122.5 (6)
	117.0 (4)	123.3 (5)	112.3 (6)	119.7 (5)	124.4 (6)	123.3 (6)
24	116.1 (3)	122.9 (2)	112.8 (4)	121.0 (3)	124.8 (4)	122.2 (4)
	115.8 (3)	122.4 (2)	113.2 (4)	121.4 (3)	124.4 (4)	122.3 (4)
	115.8 (3)	122.7 (3)	113.4 (4)	121.5 (4)	125.2 (4)	121.4 (4)
	116.8 (3)	123.0 (2)	112.4 (4)	120.2 (3)	125.0 (4)	122.6 (4)
75	116.1 (4)	122.2 (4)	113.4 (5)	121.7 (5)	123.7 (6)	122.8 (6)
	116.1 (4)	121.7 (4)	112.9 (6)	122.2 (5)	124.2 (6)	122.7 (6)
	115.3 (4)	122.3 (6)	114.1 (6)	122.5 (5)	123.9 (6)	122.6 (6)
	116.6 (4)	122.7 (4)	112.4 (5)	120.7 (5)	123.4 (6)	122.6 (5)
37	118.0 (10)	122.0 (10)	112.0 (10)	124.3 (10)	125.0 (20)	121.0 (10)
	115.0 (10)	122.0 (10)	113.0 (20)	120.9 (10)	119.0 (20)	126.0 (10)
	117.0 (10)	121.0 (10)	114.0 (10)	122.0 (10)	122.0 (20)	123.0 (10)
	115.0 (10)	120.0 (10)	110.0 (20)	119.0 (10)	125.0 (20)	124.0 (10)
34	116.0 (6)	123.9 (5)	113.2 (8)	120.0 (5)	123.6 (8)	123.3 (4)
	117.8 (6)	121.8 (5)	111.8 (8)	120.4 (6)	124.0 (6)	124.0 (6)
	116.8 (6)	122.5 (5)	112.5 (8)	120.7 (6)	122.7 (8)	124.7 (6)
	116.6 (6)	123.6 (6)	112.5 (6)	119.8 (6)	124.0 (10)	123.7 (6)
38	117.1 (2)	123.9 (2)	112.4 (5)	119.0 (2)	125.0 (3)	122.6 (3)
	116.8 (2)	123.1 (2)	112.7 (3)	120.1 (2)	124.0 (3)	123.2 (3)
	115.6 (2)	122.4 (2)	113.1 (3)	122.1 (3)	124.6 (3)	122.4 (3)
	115.2 (2)	122.6 (2)	113.6 (3)	122.2 (2)	124.4 (3)	122.0 (3)
38	116.8 (8)	121.8 (6)	111.0 (10)	121.3 (8)	125.0 (10)	123.0 (10)
	114.7 (8)	122.1 (6)	116.0 (10)	122.9 (8)	124.0 (10)	120.0 (10)
	116.9 (8)	122.3 (6)	112.0 (10)	120.3 (8)	126.0 (10)	122.0 (10)
	116.8 (8)	122.0 (6)	113.0 (10)	121.2 (8)	125.0 (10)	122.0 (10)
42	115.0 (10)	121.0 (10)	116.0 (20)		122.0 (20)	
	114.0 (10)	125.0 (10)	111.0 (20)		126.0 (20)	
	118.0 (10)	126.0 (10)	111.0 (20)		126.0 (20)	
	114.0 (10)	124.0 (10)	115.0 (20)		125.0 (20)	

TABLE 5 (continued)

Ref.	Co··N··C	Co··N··O	N··C··C	C··N··O	Me··C··C	Me··C··N
43	117.8 (5)	123.1 (2)	112.3 (6)	119.2 (6)	124.7 (8)	123.1 (6)
	117.7 (5)	122.6 (2)	112.1 (6)	119.7 (6)	124.1 (8)	123.8 (6)
	116.1 (5)	122.1 (2)	113.0 (6)	121.8 (6)	124.4 (8)	122.5 (6)
	116.2 (5)	122.1 (2)	112.9 (6)	121.7 (6)	124.5 (8)	122.7 (6)
40	118.0 (10)	121.0 (10)	112.0 (20)	122.0 (10)	123.0 (20)	125.0 (20)
	118.0 (10)	126.0 (10)	109.0 (10)	118.0 (10)	124.0 (20)	127.0 (20)
	118.0 (10)	119.5 (8)	114.0 (10)	121.0 (10)	122.0 (10)	114.0 (10)
	121.0 (10)	122.8 (8)	110.0 (10)	119.0 (10)	126.0 (20)	123.0 (20)
45	116.0 (5)	123.0 (3)	113.6 (6)	121.0 (5)	123.7 (6)	122.7 (6)
	116.1 (4)	122.7 (3)	111.9 (5)	121.0 (5)	125.6 (6)	122.5 (6)
	116.8 (5)	122.5 (3)	111.9 (5)	120.2 (5)	124.8 (6)	123.3 (6)
	117.5 (5)	121.6 (3)	112.5 (5)	120.9 (5)	122.7 (6)	124.8 (6)
45	115.3 (5)	123.3 (5)	113.3 (6)	121.2 (5)	124.5 (8)	122.2 (2)
	115.3 (4)	122.1 (4)	113.4 (6)	122.5 (6)	125.1 (6)	121.5 (5)
	117.1 (3)	123.3 (4)	112.6 (5)	119.5 (5)	123.4 (6)	124.1 (6)
	116.8 (4)	123.1 (5)	112.4 (6)	119.7 (6)	123.4 (5)	124.2 (5)
45	113.4 (11)	123.7 (11)	116.0 (10)	122.8 (12)	121.0 (10)	123.0 (10)
	115.0 (12)	115.5 (8)	115.0 (10)	129.0 (10)	126.0 (20)	120.0 (20)
	117.2 (10)	122.5 (8)	113.0 (10)	120.0 (10)	125.0 (20)	122.0 (20)
	115.0 (11)	124.1 (10)	112.0 (20)	121.0 (10)	124.0 (20)	124.0 (20)
45	120.2 (10)	120.4 (8)	110.0 (10)	119.0 (10)	124.0 (10)	126.0 (10)
	118.9 (10)	128.7 (8)	110.0 (10)	112.0 (10)	122.0 (10)	128.0 (10)
	116.9 (10)	123.5 (8)	115.0 (10)	122.0 (10)	121.0 (20)	123.0 (20)
	115.8 (11)	121.2 (10)	113.0 (10)	123.0 (10)	125.0 (10)	122.0 (10)
46	117.5 (6)	123.5 (5)	112.7 (8)	118.9 (8)	123.9 (8)	123.9 (8)
	116.9 (6)	121.1 (5)	112.5 (6)	122.0 (8)	122.1 (8)	125.5 (8)
48	115.4 (5)	123.7 (4)	112.6 (6)	120.5 (6)	126.1 (6)	121.0 (6)
	115.5 (5)	122.1 (4)	113.9 (6)	122.2 (5)	122.7 (8)	123.4 (8)
	116.8 (5)	123.3 (4)	111.9 (6)	119.3 (6)	125.1 (6)	122.9 (6)
	116.7 (5)	121.9 (4)	113.6 (6)	121.3 (5)	123.2 (6)	123.1 (6)
60	116.9 (6)	121.4 (5)	112.2 (6)	121.5 (6)	124.4 (8)	123.3 (8)
	116.9 (6)	121.7 (5)	112.1 (6)	121.3 (6)	124.6 (8)	123.2 (8)
	117.3 (6)	123.6 (5)	113.0 (8)	119.1 (6)	123.6 (8)	123.4 (8)
	118.9 (6)	124.1 (5)	110.9 (8)	117.0 (6)	122.8 (8)	126.2 (8)
70	115.0 (6)	121.5 (5)	114.2 (5)	123.5 (6)	123.3 (5)	122.5 (6)
	117.1 (6)	120.5 (6)	113.7 (5)	122.5 (5)	125.1 (6)	121.2 (6)
	117.0 (6)	121.8 (5)	112.0 (4)	121.1 (6)	124.9 (5)	123.2 (5)
	117.2 (6)	123.0 (5)	112.6 (4)	119.8 (6)	124.0 (5)	123.3 (5)
25	117.5 (6)	122.3 (4)	112.1 (6)	120.2 (6)	124.1 (6)	123.9 (6)
	116.2 (6)	123.1 (5)	113.1 (6)	120.7 (6)	123.2 (8)	123.8 (8)
	116.8 (5)	122.7 (4)	112.5 (6)	120.5 (6)	124.4 (6)	123.1 (6)
	115.4 (4)	122.6 (4)	113.3 (5)	122.0 (5)	123.7 (6)	123.0 (6)

TABLE 5 (continued)

Ref.	Co··N··C	Co··N··O	N··C··C	C··N··O	Me··C··C	Me··C··N
3	117.2 (5)	121.6 (5)	112.4 (5)	120.8 (5)	123.4 (5)	124.2 (5)
	116.5 (5)	123.0 (5)	111.9 (5)	119.2 (5)	123.6 (5)	124.5 (5)
	117.7 (5)	122.5 (5)	112.2 (5)	120.4 (5)	123.2 (5)	124.6 (5)
	117.1 (5)	121.3 (5)	112.7 (5)	122.1 (5)	122.7 (5)	124.5 (5)
59	117.4 (8)	122.0 (9)	113.0 (10)	122.3 (11)	126.0 (10)	121.0 (10)
	115.5 (8)	122.1 (11)	113.0 (10)	121.1 (11)	123.0 (10)	124.0 (10)
	116.6 (8)	124.6 (8)	114.0 (10)	119.7 (11)	124.0 (10)	122.0 (10)
	115.7 (8)	122.7 (8)	112.0 (10)	119.9 (11)	124.0 (10)	125.0 (10)
71	116.2 (4)	122.1 (4)	113.4 (6)	121.6 (6)	123.5 (6)	123.1 (6)
	116.1 (4)	122.9 (4)	113.0 (6)	121.0 (5)	124.6 (6)	122.4 (6)
	115.2 (5)	122.2 (4)	112.6 (6)	122.6 (6)	125.3 (4)	122.1 (8)
	116.4 (5)		113.8 (6)	121.6 (6)	123.3 (6)	122.9 (8)
71	116.3 (3)	121.9 (5)	113.0 (5)	122.0 (4)	124.8 (6)	122.2 (6)
	116.6 (3)	121.7 (3)	112.8 (5)	120.9 (4)	124.4 (5)	122.8 (5)
	116.5 (4)	122.6 (3)	112.6 (4)	121.5 (4)	124.4 (5)	123.0 (5)
	116.3 (4)	121.9 (3)	113.1 (4)	121.6 (4)	124.2 (5)	122.7 (5)

TABLE 6

Averages with their ESDs in parentheses, ranges, number of averaged measurements for bond lengths and angles of the Co(DH)$_2$ unit

	Co–N	C–N	N–O	C–C	C–Me	O ··· O	∠Co–N–O
M_{tot}	*1.8901 (9)*	*1.301 (1)*	*1.3492 (9)*	*1.462 (3)*	*1.501 (1)*	*2.487 (2)*	*122.63 (7)*
R_{tot}	0.136	0.170	0.130	0.112	0.140	0.208	13.2
N_{tot}	306	302	306	157	306	140	282
M_{mo}	*1.887 (2)*	*1.304 (1)*	*1.351 (1)*	*1.460 (2)*	*1.503 (1)*	*2.482 (3)*	*122.72 (6)*
R_{mo}	0.109	0.093	0.092	0.104	0.104	0.170	7.8
N_{mo}	182	182	182	94	182	81	158
M_{nmo}	*1.897 (2)*	*1.296 (2)*	*1.345 (2)*	*1.466 (3)*	*1.498 (2)*	*2.497 (4)*	*122.6 (1)*
R_{nmo}	0.113	0.170	0.130	0.112	0.140	0.145	13.2
N_{nmo}	124	120	124	63	124	59	124

	∠Co–N–C	∠C–N–O	∠N–C–Me	∠N–C–C	∠Me–C–C	∠N_1–Co–N_2	∠N_1–Co–N_4
M_{tot}	*116.6 (7)*	*120.61 (9)*	*123.11 (8)*	*112.62 (7)*	*124.23 (7)*	*81.38 (5)*	*98.57 (8)*
R_{tot}	10.6	17.0	14.0	13.2	8.3	4.3	10.4
N_{tot}	279	293	283	294	285	154	149
M_{mo}	*116.76 (6)*	*120.49 (9)*	*123.18 (9)*	*112.6 (1)*	*124.28 (9)*	*81.37 (6)*	*98.60 (6)*
R_{mo}	5.3	11.7	8.9	12.2	7.1	2.9	3.6
N_{mo}	155	173	163	170	163	87	87
M_{nmo}	*116.4 (1)*	*120.8 (2)*	*123.0 (1)*	*112.8 (1)*	*124.1 (1)*	*81.4 (1)*	*98.5 (2)*
R_{nmo}	10.6	17.0	14.0	7.0	7.1	4.3	10.4
N_{nmo}	124	120	124	124	122	67	62

TABLE 7

Means for two groups, a and b, of Co–N bond lengths and Co–N–O bond angles, randomly chosen

	Co–N bond lengths (Å)		Co–N–O bond angles (°)	
	a	b	a	b
1	1.890 (2)	1.890 (1)	122.66 (8)	122.72 (9)
2	1.891 (2)	1.890 (1)	122.6 (1)	122.74 (7)
3	1.892 (1)	1.888 (1)	122.75 (9)	122.61 (9)
4	1.890 (1)	1.890 (1)	122.67 (9)	122.72 (9)

O–N–C angle increases by 7°. A slight but significant lengthening (~ 0.01 Å) of the C–N bond length is also observed. The N–O bond length in the DH species, shorter by about 0.06 Å than that in the DH_2 species, is also shorter (~ 0.04 Å) than that observed in the dianion D^{2-}. The variation of the O–N–C angle can be attributed to the formation of the strong O–H–O hydrogen bond.

The comparison in Table 8 suggests that delocalization in the $Co(DH)_2$ plane is small. It is interesting to recall that comparison of the geometry of some quadridentate Schiff bases, such as $SalenH_2$, $AcacenH_2$, and $SalophenH_2$ before and after ionization and coordination to cobalt [120–122] indicates that the π-electron delocalization in the Co(Salophen), Co(Salen) and Co(Acacen) units is significantly greater than that in cobaloximes.

As far as the O–H–O bridge is concerned, the two equatorial ligands are occasionally present as D^{2-} and DH_2 species [23], i.e. both protons are attached to one of the two dimethylglyoxime ligands as in (a) (Scheme 1), although more often the cobaloximes have the arrangement represented by (b). This shift from (b) to (a) is often accompanied by a small lengthening of the Co–N and N–O distances of the DH_2 unit with respect to those of the

TABLE 8

Comparison of bond lengths (Å) and angles (°) of the DH unit in $Co(DH)_2$, DH_2, D^{2-} and GH_2

	DH(M_{tot})	DH_2	D^{2-}	GH_2
C–C	1.462 (3)	1.474 (3)	1.478 (4)	1.453 (1)
C–N	1.301 (1)	1.288 (3)	1.289 (3)	1.2849 (8)
N–O	1.3492 (9)	1.410 (3)	1.388 (3)	1.3854 (8)
C–Me	1.501 (1)	1.487 (2)	1.501 (5)	–
∠C–C–N	112.62 (7)	114.1 (1)	116.3 (2)	118.00 (5)
∠C–N–O	120.61 (9)	113.2 (1)	116.8 (2)	112.31 (5)
∠Me–C–N	123.11 (8)	124.8 (2)	123.7 (3)	–
∠Me–C–C	124.27 (7)	121.1 (2)	120.1 (2)	–

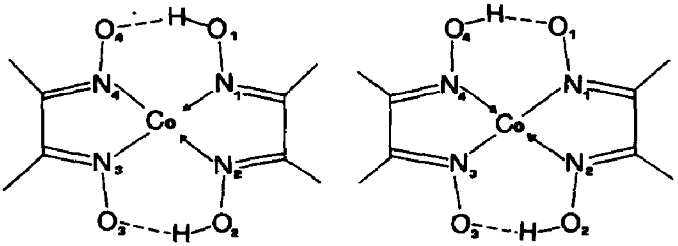

a DDH$_2$ b (DH)$_2$

Scheme 1

D^{2-} unit [38] (Table 9). The proton shift has been attributed to the involvement of additional interactions, such as extra hydrogen bond formation, of the oxygen atoms [60] or to localized π–π interaction between the DH ligand and phenyl groups of the axial ligands [38].

Note that the proton shift may occur in cases other than those of Table 9. However, because of the positional disorder of the equatorial ligands in the crystal (about one-half of the molecules have the structure (a) and one-half have the same structure but rotated by 180°), X-ray analysis gives only the average structure, which has the hydrogen atom positioned nearly in the middle of the bridge, and all Co–N and N–O distances approximately equal [56].

The Co(DH)$_2$ unit may undergo other geometrical deformations, which may be roughly represented by the displacement of the cobalt out of the plane of the 4-nitrogen equatorial donors, d, and by the bending angle between the two DH units, α. These two parameters will be discussed in the section which is concerned with axial ligands, since they appear to be influenced by properties of the axial ligands.

Clear evidence of the influence of the equatorial ligand on the axial ligands is shown in Table 10, where axial bond lengths of some LCo(DH)$_2$X complexes are compared with those reported for LCo(chel)X where chel represents the dianion of tetradentate Schiff bases, namely Salen, Acacen, and Salophen. In each comparable pair of complexes, large variations in Co–L distances are observed, while Co–X distances are almost the same. The N$_3^-$ derivatives represent an exception, since the Co–py axial bond lengths are essentially equal. Since N$_3^-$ is a very poor *trans*-influencing ligand and the other X ligands are essentially strong *trans*-influencing groups, it may be assumed that the change of the equatorial ligand influences the Co–L bond (*cis*-influence) primarily when one axial group exerts an appreciable *trans* influence [126].

Two principal effects of the equatorial ligands may influence the Co–N(py) distances given in Table 10. First, the different electronic nature of the chelate macrocycle could change the metal-orbital mix involved in the axial

TABLE 9

Variation of Co–N and N–O distances attributed to the shift of the oxime bridging hydrogen atom

Axial ligands	$Co{-}N_1$(Å) $Co{-}N_2$	$Co{-}N_3$(Å) $Co{-}N_4$	$N_1{-}O_1$(Å) $N_2{-}O_2$	$N_3{-}O_3$(Å) $N_4{-}O_4$	Interaction of the O bond
NO_2/NO_2	1.918 (2)	1.903 (2)	1.369 (4)	1.352 (4)	O_1, O_3, O_4 interact with Na^+
Cl/ $NH_2(C_6H_4$*p*-$NH_2SO_2)$	1.900 (8)	1.877 (8)	1.33 (1)	1.33 (1)	$\pi-\pi$ interaction
$Cl/NH_2(C_6H_4$*p*-Cl)	1.907 (5)	1.879 (5)	1.353 (6)	1.334 (6)	$\pi-\pi$ interaction
Me/H_2O	1.896 (3)	1.884 (3)	1.358 (4)	1.347 (3)	O_3, O_4 involved in H bond
Cl/NH_3	1.898 (3)	1.883 (5)	1.348 (6)	1.344 (6)	O_2, O_3, O_4 involved in H bond
NO_2/H_2O	1.908 (6)	1.885 (5)	1.358 (8)	1.328 (7)	O_3, O_4 involved in H bond
(*R*)-MeOOC(Me)CH–/ (*R*)-PhCH(Me)NH_2	1.887 (5)	1.879 (5)	1.358 (8)	1.342 (8)	$\pi-\pi$ interaction
$PO(OMe)_2$/3-benzyladenine	1.914 (7)	1.875 (7)	1.349 (9)	1.351 (8)	O_3, O_4 involved in H bond

TABLE 10

Influence of the equatorial macrocycle on the axial bond lengths in octahedral $Co(DH)_2$ and Co(Schiff base) complexes

	Co–C(N)	Co–N (Py)	α (°)
N_3Co(acacen)py [a]	1.955 (6)	1.980 (5)	+20
$N_3Co(DH)_2py$	1.952 (5)	1.973 (5)	+3
MeCo(acacen)py [b]	1.99 (1)	2.16 (1)	+7
$MeCo(DH)_2py$	1.998 (5)	2.068 (3)	+3
CH_2=CHCo(Salen)py [c]	1.93 (2)	2.12 (1)	+17
$CH_2=CHCo(DH)_2py$	1.966 (6)	2.073 (3)	+6
CH_3CH_2Co(Salophen)py [d]	2.042 (6)	2.215 (4)	−25
$CH_3CH_2Co(DH)_2$4-N(H)=C(OMe)py	2.035 (5)	2.081 (3)	+9
$NCCH_2$Co(Salophen)py [d]	1.999 (5)	2.098 (5)	+18
$NO_2CH_2Co(DH)_2py$	2.002 (3)	2.028 (3)	~0
F_3CCH_2Co(Salophen)py [e]	1.988 (11)	2.124 (8)	+17
$F_3CCH_2Co(DH)_2$4-CNpy	2.010 (3)	2.041 (3)	−1

[a] Ref. 123. [b] Ref. 124. [c] Ref. 125. [d] Ref. 126. [e] Ref. 74.

ligand bonding. This effect is identified here as the electronic *cis* influence (ECI). Second, the more flexible macrocycle may bend towards the axial ligand, thus increasing the axial bond length. This effect is identified here as the steric *cis* influence (SCI) [25,61]. In ref. 61, the relationship of the SCI to the steric *trans* influence (STI) and electronic *trans* influence [16,113] (ETI) is described. The cobaloximes listed in Table 10 exhibit α values that are significantly smaller than those of the Schiff base complexes. Since the bending is away from py (i.e. α is positive), the only significant exception being the pyCo(Salophen)CH_2CH_3 derivative [126], it may be suggested that the main influence on the Co–N bond length is due to the ECI. However, the bending of the equatorial macrocycle (SCI) may further increase the Co–N bond length, as in the case of the ethyl (Salophen) derivative, where the difference of about 0.14 Å in the Co–N(py) distance relative to the cobaloxime analogue should be compared with those of about 0.07 Å in other pairs of organocobalt complexes.

(ii) Axial ligands

Structural data which characterize the bonding of axial ligands to cobalt are collected in Tables 11–14, together with α and d values. For the sake of clarity, the data are ordered according to the atom bonded to cobalt, e.g. C, N, P or O. Since each Table reports the axial Co–X and Co–L bond lengths and the X–Co–L angle, some values are duplicated over two Tables, but this arrangement will facilitate the following discussion. The α and d values are reported only once.

The sign of α is defined in such a way that it is positive when the intersection of the DH planes is above the 4-N equatorial plane towards the neutral ligand L (bending is away from L). However, it should be noted that sometimes the DH planes are tilted with respect to each other, so that the angle α is due in part to the bending and in part to the tilt of these planes.

Co–P bonding

Co–P bond lengths are reported in Table 11; for each P ligand, they are grouped in order of increasing value. The following trends can be clearly derived from these data [128]: (a) For the same P ligand, the bond lengths increase with increasing σ-donating power of X. For example, in PPh_3 complexes, the Co–P distance varies from 2.286(8) Å for X = NCS to 2.460(1) Å for X = CH_2CMe_3. (b) For a given X ligand, a lengthening of the Co–P distance is observed with increasing bulk of the P ligand. (c) The increase in the Co–P distance that is due to the same *trans* ligand X, relative to a weak *trans*-influencing ligand such as Cl, is nearly equal for the different P ligands. Result (a) is called the electronic *trans* influence (ETI),

TABLE 11

Structural parameters of the X–Co–PR_3 moiety of cobaloximes
(The positive sign of *d* indicates displacement towards the neutral axial ligand.)

P ligand	X ligand	Co–P (Å)	Co–X (Å)	∠X–Co–P (°)	*d* (Å)	α (°)
PMe_3	Me	2.291 (1)	2.011 (3)	179.2 (2)	0.04	2.2
		2.295 (1)	2.019 (3)	178.5 (2)	0.06	6.0
	CH_2CMe_3	2.316 (1)	2.084 (3)	173.68 (9)	~0	−5
$P(OMe)_3$	Cl	2.211 (4)	2.298 (5)	175.3 (2)	0.01	1
		2.165 (4)	2.272 (4)	178.2 (1)	0.03	7
	CN	2.222 (2)	1.914 (7)	178.4 (3)	0.02	7
		2.227 (3)	1.903 (9)	177.2 (2)	0.02	1
	CH_2CN	2.236 (2)	2.030 (7)	175.1 (2)	0.05	7
		2.252 (2)	2.042 (7)	177.5 (2)	0.05	6.5
	Me	2.256 (4)	2.014 (14)	177.2 (5)	0.10	10
	CH_2CF_3	2.255 (2)	2.028 (7)	172.8 (1)	0	4.5
		2.257 (2)	2.035 (6)	175.3 (2)	0.02	0.9
$PO(OMe)_2$	3-Benzyladenine	2.229 (3)	2.101 (7)	176.4 (2)	0.10	7.7
$P(OMe)_2Ph$	Cl	2.213 (2)	2.288 (2)	179.6 (1)	0.02	2.3
	Me	2.287 (1)	2.013 (5)	178.4 (2)	0.06	4.8
$P(OMe)Ph_2$	Cl	2.242 (1)	2.290 (1)	178.3 (1)	0.01	0.9
	Me	2.352 (1)	2.019 (6)	175.1 (2)	0.09	8.8
$P(OCH_2)_3CMe$	i-C_3H_7	2.270 (1)	2.12 (1)	173.1 (3)	0.01	4.2
			2.13 (1)	169.6 (4)		
$PBut_3$	5-CF_3–tetrazolate	2.263 (2)	1.979 (6)	177.8 (2)	0.03	10.4
	Cl	2.271 (2)	2.295 (2)	179.2 (1)	0.04	11
		2.258 (2)	2.293 (2)	177.6 (1)	0.04	12
	Xanthinato	2.285 (2)	1.999 (5)	177.4 (3)	0.02	3.6
	–C_5H_4N	2.342 (1)	1.979 (1)	179.2 (2)	0.03	4.4
PPh_3	–NCS	2.286 (8)	1.93 (4)	175.0 (3)	–	–
	Cl	2.309 (7)	2.272 (6)	178.4 (3)	–	–
	Cl	2.327 (4)	2.277 (4)	176.5 (1)	0.05	6
	Cl	2.330 (2)	2.287 (2)	176.5 (1)	–	–
	Br	2.331 (4)	2.445 (2)	177.0 (1)	0.07	7
	CH_2CF_3	2.383 (1)	2.036 (3)	170.9 (1)	0.04	1.7
	CH_2CN	2.391 (1)	2.043 (3)	177.7 (1)	0.08	11.1
	NO_2	2.392 (3)	1.980 (9)	175.6 (3)	0.04	7.7
	CH_2Br	2.399 (3)	1.998 (15)	175.1 (4)	0.07	2.7
	i-C_3H_7	2.412 (4)	2.22 (2)	170.3 (6)	0.17	14
	CH_2CH_3	2.415 (1)	2.045 (5)	175.7 (3)	0.06	1.4
	Me	2.418 (1)	2.026 (6)	175.4 (2)	0.11	14
	CH(Me)Et	2.436 (2)	2.11 (1)	177.1 (3)	0.03	5.5
	$CH_2C(Me)$-$(COOEt)_2$	2.460 (1)	2.062 (2)	173.32 (7)	0.02	5.2
	CH_2CMe_3	2.460 (1)	2.104 (8)	165.0 (2)	0.04	2.2
			2.128 (12)	168.2 (3)		
$PChx_3$	Cl	2.369 (5)	2.294 (5)	178.9 (2)	0.10	16
	CH_2CN	2.433 (3)	2.065 (12)	178.7 (5)	0.11	14.5
	Me	2.463 (5)	2.016 (5)	179.1 (2)	0.12	12

TABLE 12

Structural parameters of the X–Co–N moiety of cobaloximes

N ligand	X ligand	Co–N (Å)	Co–X (Å)	∠X–Co–N (°)	d (Å)	α (°)
NH_3	NH_3	1.952 (4)	–	–	–	–
	NH_3	1.951 (2)	–	–	–	–
	NH_3	1.957 (2)	–	–	–	–
	NH_3	1.960 (2)	–	–	–	–
	Cl	1.965 (4)	2.251 (1)	177.4 (2)	~ 0	3.7 [a]
NH_2Ph	NH_2Ph	2.001 (5)	–	–	–	–
	NH_2Ph	2.009 (5)	2.007 (5)	–	–	–
	Cl	2.019 (2)	2.261 (1)	178.4 (2)	–	–
	I	2.053 (8)	2.558 (3)	177 (1)	–	–
	SO_3	2.105 (9)	2.207 (5)	173.4 (9)	0.05	–
	SO_3	2.117 (7)	2.225 (2)	177.9 (4)	0.02	7.0
$NH_2(C_6H_4p\text{-}Cl)$	Cl	1.999 (6)	2.257 (2)	178.0 (2)	–	–
$NH_2(C_6H_4p\text{-}NH_2SO_2)$	Cl	2.023 (8)	2.235 (2)	179.7 (2)	–	–
Morpholine	Cl	2.022 (3)	2.256 (1)	176.1 (1)	0.05	7
	CH_2Ph	2.11 (1)	2.13 (1)	180.0	0.03	7
$NHMe_2$	Cl	1.994 (5)	2.248 (2)	176.1 (1)	–	–
(S)-PhCH(Me)NH_2	(S)-Me(CN)CH–	2.054 (5)	2.070 (8)	177.2 (3)	~ 0	–
		2.064 (7) [b]	2.059 (9) [b]	177.4 (3) [b]	~ 0 [b]	–
	(R)-Me(CN)CH–	2.088 (6)	2.036 (8)	178.8 (2)	0.01	–
		2.070 (6) [b]	2.056 (6) [b]	179.1 (2) [b]	~ 0	–
(R)-PhCH(Me)NH_2	(R)-MeOOC(Me)CH–	2.066 (6)	2.067 (8)	171.7 (3)	−0.04	–
	Me	2.087 (9)	1.988 (19)	–	0.04	–
Py	Py	1.946	1.954	180	–	–
	Cl	1.97 (2)	2.222 (8)	–	–	–
	N_3	1.973 (1)	1.950 (2)	176.93 (6)	–	–
	N_3	1.973 (5)	1.955 (6)	177.3 (2)	0.02	2.9
	–O–O–C(Me)$_2$Ph	1.994 (3)	1.909 (3)	175.9 (1)	–	–

	O–O–CH(Me)–(C_6H_4p-Me)	2.013 (7)	1.897 (7)	174.1 (5)	0.03	–
	CH_2NO_2	2.028 (3)	2.002 (3)	176.0 (1)	0.02	0.2
	CH_2COOMe	2.039 (6)	2.024 (6)	175.6 (3)	–	–
	–CH=C=C=CPh_2	2.041 (6) 2.043 (5)	1.956 (8) 1.943 (7)	177.5	–	–
	–C(Cl)=C(C_6H_4p-Cl)$_2$	2.04 (1)	1.97 (1)	178.0 (4)	–	–
	CH(Me)COOMe	2.058 (7)	2.083 (7)	176.3 (3)	–	–
	Me	2.068 (3)	1.998 (5)	178.0 (2)	0.04	3.2
	CH=CH_2	2.073 (3)	1.966 (6)	178.1 (2)	0.04	6.3
	$CH_2C(Me)(COOEt)_2$	2.075 (4)	2.047 (5)	176.0 (2)	−0.03	−12.3
	CH_2CMe_3	2.081 (4)	2.060 (6)	174.7 (2)	~0	−5.2
	CH_2CH_3	2.084 (7)	2.065 (10)	–	–	–
	CH_2SiMe_3	2.091 (5)	2.031 (6)	174.1 (2)	~0	−1.2
	i-C_3H_7	2.099 (2)	2.085 (3)	174.1 (2)	0.02	4.0
4-CN–Py	CH_2CF_3	2.041 (4)	2.010 (3)	174.6 (1)	0.01	1
4-N(H)=C(OMe)–py	CH_2CH_3	2.081 (3)	2.035 (5)	177.1 (2)	0.05	9.1[a]
2-NH_2–Py	i-C_3H_7	2.194 (4)	2.097 (6)	173.9 (2)	0.04	5.2
Imidazole	*trans*-3,3,4,4-tetracyano-2-phenylcyclopentyl	2.007 (7)	2.049 (9)	174.9 (3)	−0.02	–
5-CF_3–Tetrazolate	$PBut_3$	1.979 (6)	2.263 (2)	177.8 (2)	–	–
N-iminopyridine	Me	2.038 (6)	2.006 (8)	172.6 (3)	0.06	2.3
3-N-Me–imidazole	OH	2.043 (3)	2.190 (3)	176.9 (2)	0.05	4.4
	Me	2.058 (5)	2.009 (7)	178.0 (3)	0.05	4.4
3-Benzyladenine	$PO(OMe)_2$	2.101 (7)	2.229 (3)	176.4 (2)	–	–
–NCS	PPh_3	1.93 (4)	2.286 (8)	175 (3)	–	–
Xanthinato	$PBut_3$	1.999 (5)	2.285 (2)	177.4 (3)	–	–
NO_2	H_2O	1.881 (9)	1.980 (5)	–	–	–
	NO_2	1.943 (3)	1.949 (3)	179.6 (1)	0.001	–
	NO_2	1.945 (3)	1.944 (3)	179.0 (7)	–	–
	PPh_3	1.980 (9)	2.392 (3)	175.6 (3)	–	–

---

[a] The two DH units are tilted. [b] At 173 K.

TABLE 13

Structural parameters of the X–Co–O moiety of cobaloximes

O ligand	X ligand	Co–O (Å)	Co–X (Å)	∠O–Co–X (°)	d (Å)	α (°)
–O–O–CH(Me)($C_6H_4$$p$-Me)	Py	1.897 (7)	2.013 (7)	174.1 (5)		
–O–O–CMe_2Ph	Py	1.909 (3)	1.994 (3)	175.9 (1)		
H_2O	Br	1.955 (11)	2.364 (2)	180.0	–	–
	NO_2	1.980 (5)	1.881 (9)	–	–	–
	CN	1.992 (4)	1.906 (5)	–	–	–
	Me	2.055 (8)	1.978 (11)	178.0 (3)	0	–4
	CH_2CMe_3	2.056 (5)	2.044 (7)	172.4 (3)	–0.04	–7
	Me	2.058 (3)	1.990 (5)	178.0 (2)	–	–
OH	3-N–Me–imidazole	2.190 (3)	2.043 (3)	176.9 (2)		

TABLE 14

Structural parameters of the C–Co–L moiety in cobaloximes

C ligand	X ligand	Co–C (Å)	Co–X (Å)	C–C (Å)	∠C–Co–X (°)	∠Co–C–C (°)
CN	$P(OMe)_3$	1.903 (9)	2.227 (3)	–	177.2 (2)	
		1.914 (7)	2.222 (2)		178.4 (3)	
	H_2O	1.906 (5)	1.992 (4)	–	–	–
Me	H_2O	1.978 (11)	2.055 (8)	–	178.0 (3)	–
	(*R*)-$PhCH(Me)NH_2$-	1.988 (19)	2.087 (9)	–	–	–
	H_2O	1.990 (5)	2.058 (3)	–	178.0 (2)	–
	py	1.998 (5)	2.068 (3)	–	178.0 (2)	–
	N-iminopyridine	2.006 (8)	2.038 (6)	–	172.6 (3)	–
	3-N–Me–imidazole	2.009 (7)	2.058 (5)	–	178.0 (3)	–
	PMe_3	2.011 (3)	2.291 (1)	–	179.2 (2)	–
		2.019 (3)	2.295 (1)		178.5 (2)	
	$P(OMe)_2Ph$	2.013 (5)	2.287 (1)	–	178.4 (2)	–
	$P(OMe)_3$	2.014 (14)	2.256 (4)	–	177.2 (5)	–
	$PChx_3$	2.016 (5)	2.463 (2)	–	179.1 (2)	
	$P(OMe)Ph_2$	2.019 (6)	2.352 (1)	–	175.1 (2)	–
	PPh_3	2.026 (6)	2.418 (1)	–	175.4 (2)	–
	$-CH(NC_5H_5)CO(Ph)$	2.04 (1)	2.19 (1)	1.43 (2)	174.9 (4)	110.4 (7)
$[Me(DH_2)]_2$	O	2.019 (11)	2.058 (3)			
CH_2Br	PPh_3	1.998 (15)	2.399 (3)	1.842 (14) (C–Br)	175.1 (4)	125.2 (9)
CH_2NO_2	Py	2.002 (3)	2.028 (3)	1.455 (6) (C–N)	176.0 (1)	113.7 (2)
CH_2CN	$P(OMe)_3$	2.030 (7)	2.236 (2)	1.461 (10)	175.1 (2)	114.7 (3)
		2.042 (7)	2.252 (2)	1.440 (7)	177.5 (2)	115.0 (0)
	PPh_3	2.043 (3)	2.391 (1)	1.424 (5)	177.7 (1)	116.5 (3)
	$PChx_3$	2.065 (12)	2.433 (3)	1.42 (2)	178.7 (5)	119.0 (1)

TABLE 14 (continued)

C ligand	X ligand	Co–C (Å)	Co–X (Å)	C–C (Å)	∠C–Co–X (°)	∠Co–C–C (°)
CH_2CH_3	4-N(H)=C(OMe)–py	2.035 (5)	2.081 (3)	1.519 (8)	177.1 (2)	117.8 (4)
	Py	2.065 (10)	2.084 (7)	–	–	–
	PPh_3	2.045 (5)	2.415 (1)	1.317 (9)	175.7 (3)	126.2 (5)
CH(Me)Et	PPh_3	2.11 (1)	2.436 (2)	1.51 (2) 1.45 (2)	177.1 (3)	114.4 (7) 116.6 (9)
CH_2CF_3	4-CN–py	2.010 (3)	2.041 (2)	1.469 (5)	174.6 (1)	122.6 (3)
	$P(OMe)_3$	2.028 (7) 2.035 (6)	2.255 (2) 2.257 (2)	1.469 (12) 1.428 (8)	172.8 (1) 175.3 (2)	124.7 (5) 124.4 (5)
	PPh_3	2.036 (3)	2.383 (1)	1.405 (5)	170.9 (1)	121.1 (3)
(*R*)-Me(CN)CH–	(*S*)-PhCH(Me)NH_2	2.036 (8)	2.088 (6)	1.478 (13) 1.465 (11)	177.2 (3)	119.8 (6) 111.9 (5)
(*S*)-Me(CN)CH–	(*S*)-PhCH(Me)NH_2	2.070 (8)	2.054 (5)	1.495 (13) 1.419 (10)	177.2 (3)	117.7 (6) 110.8 (5)
$-CH_2Ph$	Morpholine	2.13 (1)	2.11 (1)	1.45	180.0 (5)	
$-CH=CH_2$	Py	1.966 (6)	2.073 (3)	–	178.1 (2)	
$C(Cl)=C(C_6H_4\text{-}p\text{-}Cl)_2$	Py	1.97 (1)	2.04 (1)	1.37 (2)	178.0 (4)	133.0 (1)
$-CH=C=C=CPh_2$	Py	1.956 (8) 1.943 (7)	2.041 (6) 2.043 (5)	1.319 (10) 1.312 (10)	177.5 (3)	126.0 (5)
$i\text{-}C_3H_7$	Py	2.085 (3)	2.099 (2)	1.507 (4) 1.507 (4)	174.1 (2)	114.0 (2) 114.4 (2)
	$2\text{-}NH_2\text{–}py$	2.097 (6)	2.194 (4)	1.512 (8) 1.515 (9)	173.9 (2)	114.5 (4) 113.6 (4)

	$P(OCH_2)_3CMe$	2.12 (1) 2.13 (1)	2.270 (1)		173.1 (3) 169.6 (4)	
	PPh_3	2.22 (2)	2.412 (4)	1.49 (3) 1.58 (5)	170.3 (6)	118.0 (2) 112.0 (2)
(*R*)-MeOOC(Me)CH–	(*R*)-PhCH(Me)NH_2	2.067 (8)	2.066 (6)	1.501 (13) 1.466 (13)	171.7 (3)	115.7 (6) 112.4 (6)
	Py	2.083 (7)	2.058 (7)	1.501 (17) 1.466 (17)	176.3 (3)	115.5 (7) 104.8 (7)
$-CH_2COOMe$	Py	2.024 (6)	2.039 (6)	1.48		
$-CH(NC_5H_5)CO(Ph)$	Cl	2.07	2.285 (4)	1.45 (1)	175.5 (3)	112.7 (7)
	Me	2.19 (1)	2.04 (1)	1.43 (2)	174.9 (4)	110.4 (7)
CH_2CMe_3	H_2O	2.044 (7)	2.056 (5)	1.530 (10)	172.4 (3)	126.9 (5)
	Py	2.060 (6)	2.081 (4)	1.529 (7)	174.1 (2)	130.3 (4)
	PMe_3	2.084 (3)	2.316 (1)	1.523 (5)	173.68 (9)	113.2 (2)
	PPh_3	2.104 (10) 2.118 (12)	2.460 (1)	1.555 (10) 1.484 (13)	165.0 (2) 168.2 (3)	127.7 (5) 130.7 (8)
CH_2SiMe_3	Py	2.031 (6)	2.091 (5)	1.863 (6) (C–Si)	174.1 (2)	127.7 (3)
$-C_5H_4N$	PBu^t_3	1.979 (1)	2.342 (1)	1.397 (2) 1.397 (2)	179.2 (2)	122.7 (1) 122.1 (2)
trans-3,3,4,4-tetra-cyano-2-phenyl-cyclopentyl	imidazole	2.049 (9)	2.007 (7)	1.55 (1) 1.53 (1)	174.9 (3)	115.6 (6) 117.9 (6)
$CH_2C(Me)(COOEt)_2$	Py	2.047 (5)	2.075 (4)	1.537 (7)	176.0 (2)	125.4 (4)
	PPh_3	2.062 (2)	2.460 (1)	1.550 (4)	173.32 (7)	127.2 (2)

since it is due primarily to the σ-electron-donating power of X [25,61]. Thus, the lengthening of the Co–P bond should be a measure of the ETI of X. Result (b) is best illustrated by the plot in Fig. 6, where the Co–P distances for different P ligands are reported against Tolman's cone angles [129], except for PPh_3, where a value of the cone angle (156°) different from that obtained by Tolman (145°) has been used [71]. This lengthening with increased cone angle, resulting from the steric interaction between the axial P ligand and the equatorial DH units, is another example of the SCI. However, the principal factor is the bulk of the axial ligand. Finally, result (c) is best illustrated by Fig. 7, where the Co–P distances in $LCo(DH)_2X$ ($X = Me$, CH_2CN) are reported against those found in the corresponding

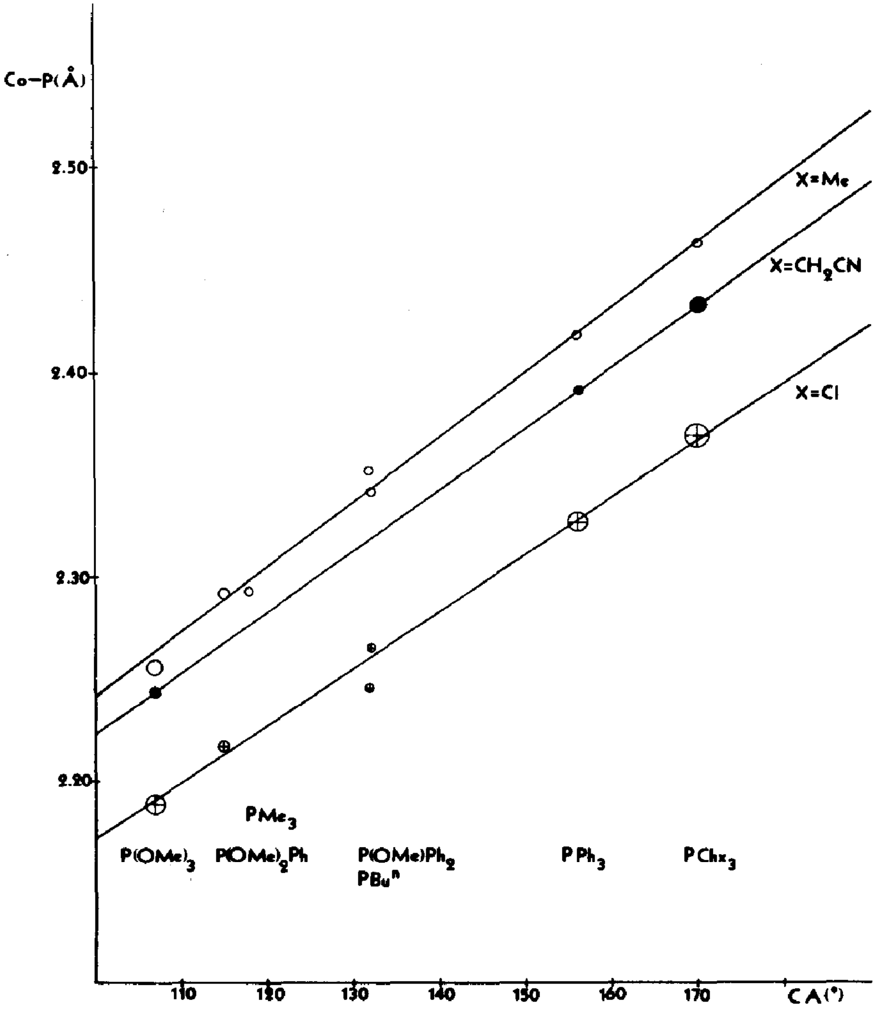

Fig. 6. Co–P distances against Tolman's cone angles in $PR_3Co(DH)_2X$ with $X = Cl$, CH_2CN, and Me (see ref. 71 for details).

$LCo(DH)_2Cl$. The linear relationship, with a slope of about unity indicates that the lengthening due to the greater *trans*-influencing power of Me or CH_2CN is little influenced by the bulk of the P ligand. Only the point relative to $P(OMe)Ph_2$ is significantly off the line. There is some evidence that the Co–P bond length may be influenced to some extent by the crystal packing [45]. Thus, the ratio Co–P(Me)/Co–P(Cl) is much more influenced than are the individual distances by this effect which, on the other hand, does not substantially modify the overall trends shown in Figs. 6 and 7.

The Co–Cl and Co–Me bond lengths do not vary greatly when the P ligand is changed. They range from 2.272(4) to 2.298(5) with a mean of

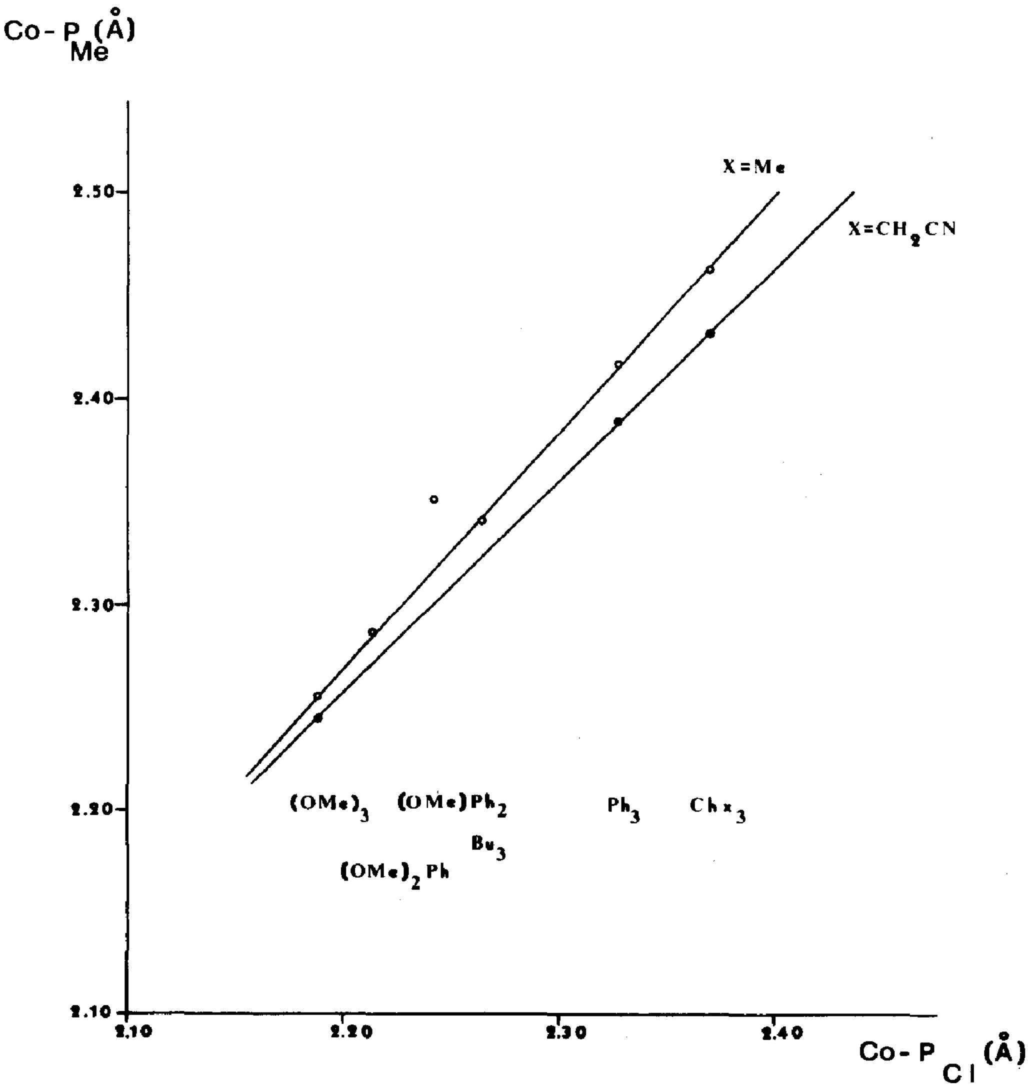

Fig. 7. Co–P distances in $PR_3Co(DH)_2Cl$ complexes against the corresponding distances in $PR_3Co(DH)_2Me$ and $PR_3Co(DH)_2CH_2CN$ complexes.

2.289(29) and from 2.011(3) to 2.026(6) with a mean of 2.016(12), respectively. However, the Co–Cl bond lengths appear to be slightly, but significantly, longer by about 0.04 Å than those found for the analogous chlorocobaloximes containing N ligands (see below). Although negatively charged, the $PO(OMe)_2^-$ ligand *trans* to 3-benzyladenine has a Co–P distance (2.229(3) Å) which is not far from that expected on the basis of its bulk. On the other hand, it has a *trans* influence which is significantly larger than that of the phosphines. In fact, the *trans* Co–N(3-benzyladenine) distance (2.101(7) Å) is longer than that found for the $PBut_3Co(DH)_2$(xanthinato) complex (1.999(5) Å).

The values of d and α, reported in Table 11 indicate that distortions of the $Co(DH)_2$ moiety are related in some degree to the bulk of the axial ligands. In fact, d and α generally have the largest values when only one of the two axial ligands is bulky. The displacement d is towards and the bending is away from the bulkiest of the two axial ligands. However, if both the axial ligands are sufficiently bulky, the d and α values are significantly smaller, with some "tilt" of the DH units. When L is a bulky P donor ligand, the values of d and α are the largest observed in cobaloximes. However, these values are not very large in an absolute sense and the $Co(DH)_2$ moiety is probably fairly rigid.

Co–N bonding

Known Co–N bond lengths are collected in Table 12. In this case, data are available for both $N(sp^3)$– and $N(sp^2)$–Co bonds. The amine derivatives exhibit trends of Co–N bond lengths similar to those found for phosphines, although the limited data available do not indicate a systematic relationship. However, the $Co–N(sp^3)$ distance is 1.958 Å (mean) in those NH_3 derivatives which have poor *trans* σ-donors, such as NH_3 or Cl. When the bulk of the amine increases, as in NH_2Ph or $NHMe_2$, the Co–N distance increases by about 0.05 Å if the *trans* ligand is still a poor σ-donor. This result illustrates the SCI. For a given N ligand, the Co–N bond is significantly influenced by the nature of the *trans* ligand, as illustrated in Table 12 by the series of aniline derivatives. An increase of about 0.1 Å is observed when X varies from Cl to SO_3^{2-}. A similar variation (~ 0.09 Å) is observed in the morpholine derivatives having Cl and CH_2Ph, respectively, as the *trans* ligands. These comparisons are best understood in terms of the ETI.

The Co–Cl bond lengths are rather insensitive to changes in the nature of the amine ligand. The values range from 2.235(2) to 2.261(1) Å, with a mean value of 2.254(20). Such values appear shorter than the values obtained for Co–Cl *trans* to P ligands (mean 2.289(29) Å). A large number of cobaloximes containing pyridine and several *trans* X ligands has been reported. Clear evidence of a *trans*-influence effect is shown in Table 12, where the

Co–N(py) bond length varies from 1.973(5) Å for X = N_3 to 2.099(5) Å for X = i-C_3H_7. It is noteworthy that the Co–N(py) bond length is sensitive to the electronic nature of the substituents at the C bonded to cobalt. For X = CH_2NO_2, where NO_2 is an electron-withdrawing group, the Co–N(py) distance of 2.028(3) Å is significantly shorter than that of 2.081(4) Å for X = CH_2CMe_3, where CMe_3 is an electron-donating group.

When py is replaced by the bulkier 2-NH_2–py, which coordinates to cobalt through the endocyclic N atom, a pronounced lengthening of the Co–N distance from 2.099(2) to 2.194(4) Å occurs when X = i-C_3H_7 [81]. As shown for the P ligands, this result suggests that the steric and electronic effects affecting the Co–N distance can both occur in the same compound. This enormous lengthening of about 0.2 Å relative to a weak *trans*-influencing X ligand brings the Co(III)–py bond length very close to the value of the Co(II)–py distance of 2.25(2) Å reported for pyCo(DH)$_2$py [103].

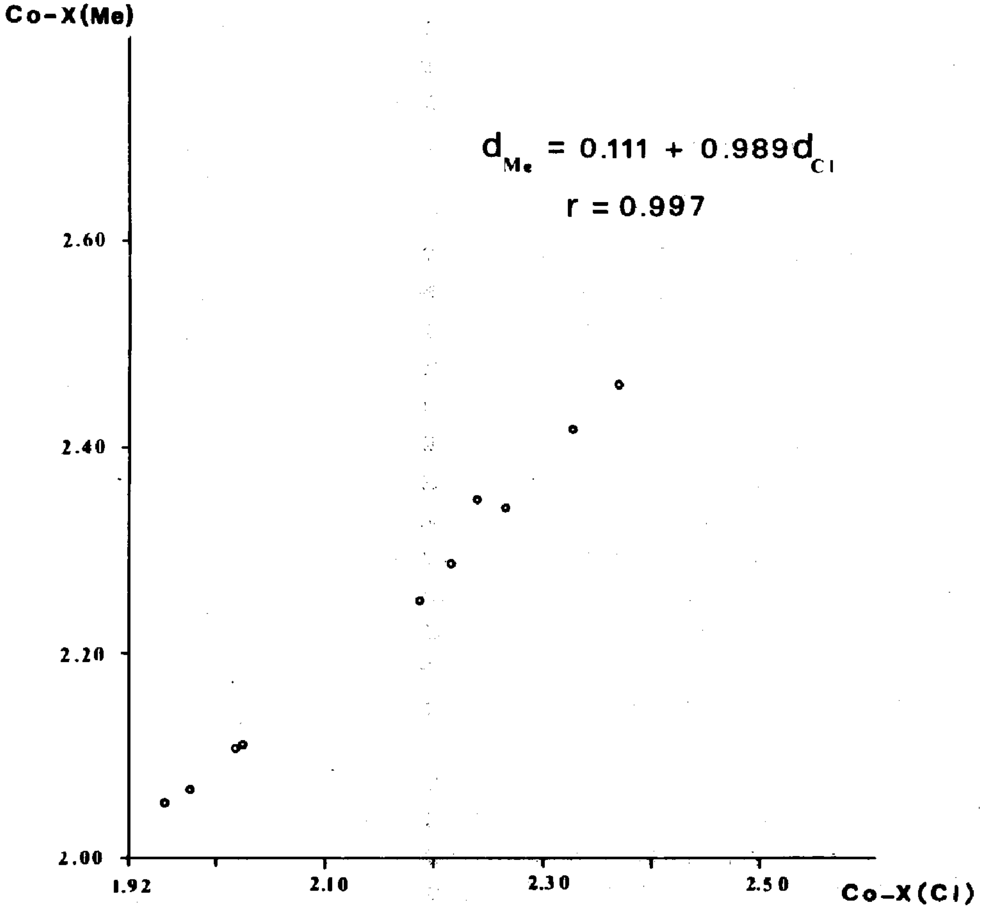

Fig. 8. Co–X (X = O, N, and P) bond lengths *trans* to Me (a strong *trans*-influence ligand) against the corresponding bond lengths *trans* to Cl (a weak *trans*-influence ligand).

Some additional points are worth noting. For similar *trans* ligands the Co–py bond lengths are longer than the Co–NH_3 distances, although the σ-covalent radius of N(sp^2) is expected to be shorter by ~ 0.05 Å than that of N(sp^3). This result suggests that the steric interaction of py with the DH units may be significant. Although not all the α and *d* values are available, these values do not exceed 7° and 0.05 Å, respectively, for N donors and they are significantly smaller than the values found for cobaloximes containing bulky P donors.

Co–O bonding

The Co–O axial bond lengths are given in Table 13. Unfortunately, there are too few values for a complete discussion to be given. However, data relative to the water derivatives indicate that the Co–O distances are also influenced by the nature of the *trans* ligand. In fact, an increase in the Co–O bond length from 1.955(4) Å for X = Br to 2.058(2) Å for X = Me is observed when L = H_2O. The increase of about 0.1 Å in the Co–O distance, when the *trans* ligand changes from a weak to a strong *trans*-influencing group, is similar to that found for the Co–P and Co–N distances for almost the same *trans* ligand, as illustrated graphically in Fig. 8. The results shown in Fig. 8 indicate that the same linear relationship probably holds for the Co–N, Co–P, and Co–O distances: $\text{Co–L}(X_1) = 0.989(\text{Co–L}(X_2)) + 0.111$, with $r = 0.997$, where X_1 is strong and X_2 a weak *trans*-influencing ligand. In other words, a mean increase in the Co–L bond (~ 0.1 Å) should be expected, independently of the nature of L [130].

Co–C bonding

The most interesting results have been found for organometallic derivatives. As demonstrated for numerous cases mentioned above, σ-bonded alkyl groups have a strong *trans* influence, although it is modulated by their σ-donating ability. Furthermore, evidence of some structural effects on the equatorial ligand compared with that of the non-organometallic axial ligands has been given.

The geometrical parameters which characterize the L–Co–CH_2R' fragment are given in Table 14. The Co–C bond length is significantly influenced by the hybridization of the donor carbon atom when R′ is not bulky. For similar L, the Co–C bond length is about 2.00 Å for sp^3, 1.96 Å for sp^2 and 1.90 Å for *sp* hybridized carbon atoms. For the CN complexes, the Co–C bond length varies from 1.903(9) to 1.914(7) Å.

A comparison of the data given in Table 14 with more recent studies [62] indicates that several kinds of structural change arise from changes in the electron-donating ability of R and from the interactions between the alkyl group, the equatorial moiety and the ligand L. The electronic nature of the R substituents influences the *trans* Co–N(py) bond length. If R contains an electron-withdrawing group, the Co–N(py) distance is shorter than that found for the methyl analogues. If R contains an electron-donating group, the distance is longer.

Distortions arising from the interaction of the axial CH_2R' group with the $(DH)_2$ ligand may be summarized as follows: (a) changes in the C–Co–N(eq) bond angles; (b) widening of the Co–CH_2–R′ angles and shortening of the CH_2R' bond lengths; (c) lengthening of the Co–C bond; and (d) deformation of the equatorial $Co(DH)_2$ unit. Point (a) is illustrated by data reported in Table 15 where the C–Co–N(eq) and L–Co–N(eq) coordination angles, the sum of which is very close to 360°, are reported for a series of $LCo(DH)_2CH_2R'$ complexes. One C–Co–N angle, (C–Co–N_a), is significantly larger than 90°, whereas this angle to the *trans* N, (C–Co–N_o) is smaller than 90°. The L–Co–N angles are close to 90°. The remaining C–Co–N(eq) angles are still very close to 90°. These data indicate that the Co–C bond bends in the plane defined by Co, N_a and N_o, and the L donor atom bends towards N_o and away from the R′ group. The CH_2R' group is often found almost directly above the Co–N_a coordination bond.

Result (b) is observed when R′ is sufficiently bulky. The Co–CH_2–R′ angle widens to values of up to 130° (Table 14), which is considerably larger than the angle expected for an sp^3 carbon atom and very near to that reported for the coenzyme of vitamin B_{12} [113]. The increase in this angle may lead to an increase in the *s* character of the hybrid orbital of C involved in the C–R′ bond. Indeed, a shortening is clearly apparent in the CH_2CF_3

TABLE 15

Coordination bond angles in cobaloximes containing CH_2R' axial groups

R′/L	∠C–Co–N_a	∠C–Co–N_o	∠L–Co–N_a	∠L–Co–N_o	Sum	∠L–Co–C
CN/$P(OMe)_3$	92.8	84.7	92.1	90.5	360.1	175.1
	92.5	84.0	92.0	93.5	362.0	177.5
CN/PPh_3	91.6	83.6	88.8	96.0	360.0	177.7
CN/$PChx_3$	87.8	85.5	92.8	94.0	360.1	178.7
NO_2/py	94.2	85.1	89.8	91.0	360.1	176.0
CF_3/$P(OMe)_3$	95.0	83.8	89.7	91.5	360.0	175.3
	95.9	84.5	90.9	88.8	360.1	172.8
CF_3/4-CN-py	94.5	85.8	90.6	89.1	360.0	174.6
CF_3/PPh_3	94.4	83.2	94.3	88.1	360.0	170.9
COOMe/py	94.9	84.6	89.7	90.7	359.9	–
CMe_3/H_2O	100.2	84.2	88.5	88.7	361.6	172.4
CMe_3/py	96.0	85.0	88.6	90.4	360.0	174.7
CMe_3/PPh_3	100.1	77.8	93.4	88.7	360.0	165.0
	101.1	76.5	90.2	92.2	360.0	168.2

derivatives. However, the strong deformation of the F–C–F angles, which could increase the *s* character of the hybrid orbital involved in the C–C bond, may enhance this shortening (see below). Analogously, for groups such as CH_2CN or CH_2Br, the C–C and C–Br distances of 1.424(5) and 1.84(1) Å, respectively, are significantly shorter than the expected values.

As far as point (c) is concerned, the data of Table 14 show that the Co–C bond length varies from values of about 2.00 Å with CH_2R' groups of small bulk such as Me and CH_2CN, to values of about 2.10 Å for groups of large bulk such as CH_2CMe_3. Point (d) has already been discussed in the previous section on P ligands.

All deformations in (a) and (d) may be attributed to steric effects arising from the interaction between axial and equatorial ligands. Since distortion (a) is also observed when the alkyl group is not particularly bulky and when distortions (b) and (c) are absent, and since distortion (c) is observed in i-C_3H_7 derivatives where the other distortions cannot take place, one can speculate that the above order should be indicative of the relative increase in energy needed to produce these structural changes. On this basis, the geometrical distortions found in these organometallic cobaloximes suggest that the steric bulk of CH_2R' groups increases in the order $CH_2NO_2 \sim CH_2CN < CH_2COOMe < CH_2CH_3 \sim CH_2CF_3 < CH_2Br < CH_2SiMe_3 < CH_3CMe_3$.

This trend shows that the effective bulk of the alkyl group may be significantly reduced if the alkyl group itself is distorted, as in the case of CH_2CF_3, which has "soft" C–F electron-bonding pairs. The effects of such a distortion of the CH_2CF_3 group are illustrated in Table 16, where the F–C–F angles and the C–C and C–F distances of the CH_2CF_3 grouping are reported for three cobaloximes. The calculated hybridization index (HI),

TABLE 16

Comparison of some bond lengths (Å) and angles (°) of the CH_2CF_3 group in some $LCo(DH)_2CH_2CF_3$ complexes

L	H_2C–CF_3	HI(C–C)	C–F	HI(C–F)	∠FCF
4-CN–py	1.469 (5)	1.7	1.368 (6); 1.363 (5)	4.1	104.2 (3); 104.9 (4)
			1.321 (5)	3.5	105.3 (3)
PPh_3	1.405 (5)	1.1	1.330 (7); 1.351 (8)	4.0	101.3 (4); 104.4 (4)
			1.429 (4)	6.9	99.9 (3)
$P(OMe)_3$ [a]	1.47 (1)	1.6	1.344 (7); 1.339 (9)	3.9	104.8 (6); 104.1 (6)
			1.362 (8)	3.8	105.7 (7)
	1.428 (8)	1.3	1.35 (1); 1.340 (9)	3.8	102.1 (6); 102.8 (5)
			1.388 (9)	5.6	105.4 (7)

[a] Data refer to two crystallographically independent molecules.

which is defined as the ratio of the sum of the squared coefficient of *p* AOs to the squared coefficient of the *s* AO of the hybrid orbital [131,132], is also given in Table 16. A mirror of symmetry was assumed for the C–CF_3 group since two C–F bonds were always equal within the limits of experimental error. The HI represents a qualitative measure of the *p* character of that particular hybrid orbital; HI is 3 for an sp^3 hybrid. The considerable shortening of the C–C bond to 1.405(5) Å, as well as the variation in the C–F distance from 1.330(7) to 1.429(4) Å, may be interpreted in terms of the *s* and *p* character of the hybrid orbitals involved in the formation of these bonds. In fact, shorter distances correspond to smaller values of the HI. Since the latter are calculated from bond angles around the carbon atom of CF_3, it appears that the observed variations in bond angle and bond length are qualitatively self-consistent. In addition, the opening up to 124° of the Co–CH_2–CF_3 angle will cause a further shortening of the C–CH_2 bond, as already noted.

The bulk of the ligand L may influence the size of the distortion of the Co–CH_2–R′ moiety. This effect is shown in Table 15, where the C–Co–N_o and C–Co–N_a angles generally decrease and increase, respectively, with increasing bulk of L. However, the most interesting result [62] is illustrated in Table 17, where it is shown that for the same alkyl group the increase in the bulk of L induces changes in *d* and *α* values from negative to positive,

TABLE 17

Variation of the Co–C bond lengths and of *d* and *α* parameters in the series $LCo(DH)_2X$ with increasing bulk of L and X

X	L	Co–C (Å)	*α* (°)	*d* (Å)	∠Co–CH_2–CMe_3 (°)
CH_2CMe_3	H_2O	2.044 (7)	−7	−0.04	126.9 (5)
	Py	2.060 (6)	−5	~0	130.3 (4)
	PMe_3	2.084 (3)	−5	~0	130.2 (2)
	PPh_3	2.118 (9)	+2	+0.04	129.2 (7)
Me	H_2O	1.990 (5)	−4	~0	
	Py	1.998 (5)	+3.2	+0.04	
	PMe_3	2.015 (3)	+4.0	+0.05	
	PPh_3	2.026 (6)	+14.0	+0.11	
					∠Co–CH_2–CF_3
CH_2CF_3	$P(OMe)_3$	2.032 (7)	−2.7	−0.01	124.5 (5)
	4-CN–py	2.010 (3)	−1.0	+0.01	122.6 (3)
	PPh_3	2.036 (3)	+1.7	+0.04	121.1 (3)
CH_2CH_3	4-N(H)=C(OMe)py	2.035 (5)	9.1[a]	+0.05	117.8 (4)
	PPh_3	2.045 (5)	+1.4	+0.06	126.2 (5)

[a] The two units are tilted.

accompanied by a lengthening of the Co–C bond. This lengthening is greater when the bulk of the alkyl group is large.

C. SOLUTION STUDIES

A large number of studies have been carried out on $Co(DH)_2$ compounds in solution. In this section, these studies will be divided into spectroscopic, kinetic, and equilibrium (thermodynamic) studies. It will not be possible to be comprehensive and to cite all relevant literature. Broader aspects of these topics have been reviewed [105]. Instead, emphasis will be placed on studies in which measurements have been made as axial ligand properties are systematically changed. Variations in equatorial ligands, which necessarily lead to a departure from the $Co(DH)_2$ models, will be mentioned where appropriate. However, many fewer studies have been made on the changes in properties of other B_{12} model systems which occur as the axial ligands are systematically changed.

(i) Equatorial ligands

Spectroscopic studies

The most extensive solution studies of the DH ligands have involved spectroscopic studies. These are best considered in conjunction with the section below on the spectroscopic changes which accompany changes in axial ligands. Changes in the electronic spectrum of cobaloximes as one of the O–H–O groups is deprotonated are discussed in the subsection on equilibrium studies and the ^1H NMR signal of this group is discussed under ^1H NMR of the axial ligand (see below).

Kinetic studies

The DH ligands do not readily undergo reaction. At high pH, the proton bridging the oxime O can be removed. The rate of deprotonation has been studied in a few cases (Table 18). K.L. Brown has suggested that the C=N bond is attacked by OH^- to give a carbinol amine [136]. In basic D_2O, in addition to the facile exchange of O $\cdots$ H $\cdots$ O with O $\cdots$ D $\cdots$ O, the protons of the oxime CH_3 groups will also undergo exchange [137–139]. Addition of strong base leads to cleavage of the Co–C bond [105,140]. The O–H–O group can be converted by BF_3 to O–BF_2–O [141], by Fe^{3+} to O–Fe–O [142,143], and by strong acid to O–H H–O [144] (Table 47). Extensive evaluations of the effects of axial ligand changes on these reactions have not been made, except for protonation [144].

TABLE 18

Rate constants and equilibrium quotients for the reactions of various complexes with OH^- [a]

Complex	$10^{-5}k_1$ (M^{-1} s^{-1})	$10^{-2}k_{-1}$ (s^{-1})	$10^{-2}K$ (M^{-1})
$Co(DH)_2(CN)_2^-$	1.90	1.35	1.18
$Co(DH)_2(NO_2)Br^-$	1.23	2.0	0.31
$Co(DH)_2(NO_2)_2^-$	1.18	0.80	1.29
$NH_3Co(DH)_2Cl$			1.1
$PyCo(DH)_2Cl$			5.0
$(NH_3)_2Co(DH)_2^+$	13.3	1.5	15.8

[a] From refs. 133, 134, and 135. See original papers for conditions and methods. Rate and equilibrium constants are defined as follows:

$$OH^- + LCo(DH_2)X \underset{k_{-1}}{\overset{k_1}{\rightleftharpoons}} [LCo(DH)(D)X]^- + H_2O;$$

$$K = [LCo(DH)(D)X^-]/[OH^-][LCo(DH)_2X].$$

Equilibrium studies

K.L. Brown [145,146] has reported values for the following equilibria (aqueous solution, 25°C)

$$pyCo(DH)_2R \xleftarrow{K'_{c-L}} pyCo(DH)(D)R^- + H^+$$

The values are given in Tables 19 and 42 and will not be discussed in detail here since they follow axial ligand trends as R changes. Thus, the pK'_{c-L} values decrease by about two log units when R is changed from isopropyl to cyanomethyl (13.9 to 11.8).

Studies of the base deprotonation of complexes of the type $H_2OCo(DH)_2X$ ($X \neq R$) have concluded that shifts of UV peaks from ~ 245–250 to 260 nm are caused by changes in the $\pi \rightarrow \pi^*$ transition of the equatorial ligand on dissociation of an equatorial proton [147–149]. Proton dissociation from the axial water is accompanied by spectral changes in the visible region. On this basis, K.L. Brown has assigned the first proton dissociation in $H_2OCo(DH)_2R$ complexes to the axial H_2O. When R is a weak electron donor (CH_2CN, CH_2CF_3), a second subsequent deprotonation is observed and is assigned to equatorial ligand deprotonation. For $pyCo(DH)_2R$, where no axial ligand can be readily deprotonated, there is a large increase in molar absorptivity in the 270–280 nm region.

The acidity constant of axial H_2O (K'_{c2}) is roughly an order of magnitude greater than the equatorial ligand acidity when $H_2OCo(DH)_2R$ and $pyCo(DH)_2R$ are compared for a given R (Table 19). The equatorial-ligand proton dissociation of $HOCo(DH)_2CH_2CN^-$ has a pK_a of ~ 14 (~ 2.2 log

TABLE 19

Rate and equilibrium data for py ligation in pyCo(DH)$_2$R[a]

R	σ^{*} [b]	k_{on} (M^{-1} s^{-1}) [c]	k_{off} (s^{-1})	k'_{off} (s^{-1})	k'_{on} (M^{-1} s^{-1})	K_f (M^{-1})	pK'_{c_2}	pK'_{c-L}	K'_f (M^{-1})	K_{cw}
i-C_3H_7	−0.19	1.49×10^4	3.31×10^1	1.14×10^2	$1.21\pm0.54\times10^4$	480	13.28	13.93	106 ±45	3.9
Et	−0.10	1.17×10^3	1.71	4.93	$4.77\pm1.60\times10^2$	785	12.97	13.88	96.8±30.4	3.0
Me	0	1.16×10^2	5.52×10^{-2}	1.63×10^{-1}	$4.11\pm0.90\times10^1$	2150	12.68	13.61	252 ±53	2.2
CH_2CH_2Ph	+0.08	1.22×10^3	8.83×10^{-1}	1.76	$4.00\pm1.31\times10^2$	1370	12.78	13.56	227 ±73	1.7
$(CH_2)_3CN$	+0.17	1.64×10^2	1.47×10^{-1}	4.11×10^{-1}	$3.41\pm0.80\times10^1$	1190	12.22	13.37	82.9±19.0	1.3
CH_2CH_2OMe	+0.19	1.65×10^2	1.20×10^{-1}			1420	12.19			1.2
CH=CHMe	+0.36	2.34×10^1	1.62×10^{-2}	4.88×10^{-2}	3.25 ± 0.66	1550	12.02	13.39	66.5±13.2	0.74
CH_2I	+0.85	4.20	1.57×10^{-3}			2640	11.72			0.17
CH_2CF_3	+0.92	4.56×10^{-1}	1.60×10^{-4}			2690	10.96	12.30	122 ± 7	0.14
CH_2Cl	+1.05	1.06×10^1	5.73×10^{-3}			2290	11.95			0.09
CH_2CN	+1.30	5.59×10^{-2}	9.92×10^{-6}			5090	10.56	11.77	311 ±14	0.04

---

[a] Aqueous solutions, 25°C. Rate and equilibrium constants are defined in the text. See ref. 145 for further details.

[b] Polar substituent constants (ref. 150).[c] Dreos Garlatti et al. [262] have measured k_{on} using thiourea in 1 M $NaNO_3$ (25°C). The following values of log k_{on} were obtained: Et, 3.31; $CH_2C_6H_5$, 3.16; Me, 2.12; CH_2Cl, 1.31; CH_2Br, 1.02; CH_2I, 0.95; CH_2CF_3, −0.04. These values, when comparable, are ~0.2 to ~0.3 log units greater than k_{on} in this Table. This probably reflects the different conditions.

units greater than $pyCo(DH)_2CH_2CN$), which is consistent with the negative charge on the complex [145].

(ii) Axial ligand variations

Most work on cobaloximes has involved the examination of changes in chemical and physical properties as axial ligands are changed. Of the three types of study reviewed here (spectroscopic, kinetic and equilibrium (thermodynamic)) the most extensive data are available on spectral properties, particularly NMR data. This information will be reviewed first.

Spectroscopic studies

NMR spectroscopic studies

In general, NMR spectral data should reflect the time-averaged ground state properties of the complex in solution. The preponderance of NMR data includes results for ^{1}H, ^{13}C, and ^{31}P. Other nuclei (^{19}F and ^{59}Co) have also been studied. A detailed discussion of the factors which influence NMR shifts and coupling constants is beyond the scope of this review. Furthermore, we will be concerned only with changes in shifts and coupling constants which accompany changes in axial ligation. Appleton et al. [151] have reviewed relevant aspects of the effects of ligands on spectroscopic trends in coordination compounds.

^{1}H NMR. Early studies on the ^{1}H NMR of cobaloximes [152] implied a relationship between ^{1}H NMR shifts and organic substituent constants for X. However, it was later shown that some of the compounds were incorrectly formulated and that there is no close relationship between ^{1}H NMR spectra and organic substituent constants [153]. ^{1}H NMR shifts are almost unique in comparison with shifts of heavier nuclei, in that the former are very sensitive to remote effects such as the proximity of anisotropic phenyl or carbonyl groups. Co is similarly anisotropic, and it has been concluded that the changes in ^{1}H NMR shifts in cobaloximes as a function of X primarily reflect changes in the anisotropy of Co as it undergoes small changes in hybridization as X is changed [153]. These changes in hybridization, although small, appear to be nearly independent of the metal ion [154] and therefore studies on cobaloximes have broader implications than for cobalt chemistry alone [154,155].

In Table 20, ^{1}H NMR shifts for a series of complexes of the type 4-tBut–$pyCo(DH)_2X$ are summarized. Two resonances are considered. First, the α-H resonance in the axial 4-tBut–py shifts to lower field as the X ligand is changed from a weakly electron-donating acido anion (e.g. NO_3^-) to a

TABLE 20

NMR spectroscopic data for $LCo(DH)_2X$ (L = pyridine and t-butylpyridine [a])

X	L = 4-tBut–py					L = py		
	^{13}C [b]			^1H [c,d]		^{13}C [e]		
	γ(4-tBut–py)	Oxime CH_3	Oxime N=C	Oxime CH_3	α(4-tBut–py)	γ (py)	Oxime CH_3	Oxime N=C
NCS	164.36	13.09	152.84	2.35	7.97			
NO_3	164.33	13.22	153.89	2.38	7.87			
SCN	164.03	13.35	152.80	2.33	8.09			
NCO	163.97	12.92	152.29					
CN	163.88	12.76	151.93	2.21	8.21			
Cl	163.85	13.08	152.44	2.33	8.01			
NO_2	163.81	12.79	152.43	2.27	8.07			
Br	163.72	13.09	152.83	2.33	7.98			
N_3	163.68	12.89	151.98	2.34	8.08	138.89	12.91	152.11
I	163.51	13.19	153.43		7.94			
$SCPh_2$					8.03			
p-$SO_2C_6H_4Me$	163.28	12.57	152.39		8.12			
SeCN					8.13			
$S_2CO(i\text{-}C_3H_7)$	163.09	12.85	152.10					
i-PrXan					8.15			
CH(CN)Br						138.64	12.92, 13.02	152.27, 152.42
$CH(CN)CH_2CN$						138.58	12.81, 12.95	152.55, 152.89
CH_2NO_2	163.09 [e]	12.67 [e]	151.42 [e]			138.46	12.65	151.56
CH_2CN						138.25	12.68	151.16
$CHBr_2$	162.87	12.69	151.46		8.24			
$P(O)(OMe)_2$	162.75	12.40	151.70		8.32			
S(t-But)	162.59	12.72	151.61		8.19			
SPh					8.20			

CH_2CF_3	162.50 [e]	12.25 [e]	150.67 [e]			138.03	12.22	149.94
CCl_3					8.28			
CH_2COOMe	162.45 [e]	12.41 [e]	150.67 [e]			137.97	12.38	150.79
$P(O)Ph_2$	162.39	12.03	151.22					
CH_2Br	162.37	12.32	150.07		8.33	137.96	12.31	150.34
CH_2I						137.98	12.54	150.25
DDT	162.26 [e]	12.11 [e]	149.96 [e]			137.79	12.10	150.12
p-C_6H_4Br	162.25	12.25	150.34		8.52			
$CH_2C_6H_4p$-CN	162.17	12.04	149.55		8.29			
C_6H_5	162.08	12.20	150.15		8.50			
p-C_6H_4OMe					8.52			
$CH{=}CH_2$	162.06 [e]	12.10 [e]	149.24 [e]			137.72	12.10	149.42
$CH_2C(Me)(COOEt)_2$						137.53		
Me	161.84	12.00	148.84	2.07	8.37	137.48	11.98	148.98
$CH_2C_6H_5$	161.73	11.88	149.17		8.30			
CH_2SiMe_3	161.67	12.12	149.03		8.35	137.42	12.10	149.59
$Sn(n$-$But)_3$					8.37			
CH_2CH_3	161.59	11.96	148.81		8.38	137.34	11.95	149.01
CH_2CHMe_2						137.32	12.01	149.89
c-C_5H_9						137.30	11.96	149.35
CH_2CMe_3	161.53 [e]	12.05 [e]	148.96 [e]			137.29	12.04	149.54
CH_2OMe [f]						137.24	11.88	150.00
i-C_3H_7	161.37 [e]	12.05 [e]	149.12 [e]		8.41	137.21	12.00	149.30
CH(Me)(Et)						137.17	12.04	149.41
c-C_6H_{11}						137.15	12.10	149.34
$CH(Et)_2$						137.10	12.02	149.73
CH(Me)(i-C_3H_7)						137.10	12.03	149.59
Adamantyl [f]						137.00	12.22	149.59

---

[a] In $CDCl_3$, oxime N=C tentative since αpyC resonance occurs at ~1–2 ppm away. [b] Ref. 156 unless otherwise noted. [c] Ref. 153. [d] Ref. 154. [e] Ref. 157. [f] Ref. 175.

more strongly electron-donating alkyl group (e.g. CH_2CH_3). This trend correlates very well with trends observed for other metal species, including trends in the NMR coupling constant between the metal nucleus and a ligand nucleus [154]. Since changes in such coupling constants primarily reflect changes in hybridization in the bonds between the ligand nucleus and the metal [151], it seems likely that a similar rehybridization is occurring for cobaloximes as X is varied [153].

The variation in hybridization could be transmitted to the α-H either via a through-bond electronic effect or via a through-space effect, since, as mentioned above, ^1H NMR shifts are very sensitive to through-space effects. If the Co is acting as an anisotropic group, then from the dipolar relationship, $((1 - 3\cos^2\theta)/R^3)$ [158], the changes in shifts of ^1H resonances in the equatorial ligand will be opposite to those of the axial L ligand as X is changed. From Table 20, this relationship may be observed for the ^1H resonances of the oxime CH_3 groups and the α-H of 4-tBut–py (Fig. 9).

Since ^1H NMR shifts in cobaloximes reflect the remote heavy-atom effect of Co which is primarily influenced by rehybridization of the cobalt by X, trends in oxime CH_3 shifts are essentially independent of L. For example, Table 21 contains ^1H NMR data for a series of 4-X–pyCo(DH)$_2$Me compounds. The oxime CH_3 resonance does not shift appreciably, whereas the axial CH_3 group shifts slightly. Using *N*-methylpyridinium salts as the basis data set, it was demonstrated that the Co(DH)$_2$ group transmits about two-thirds of the Hammett electronic substituent effect from pyridine to the *trans* methyl group [159]. Values of log K_f (K_f was determined in 50% DMSO–D_2O (v/v)) correlate linearly with the Hammett substituent parame-

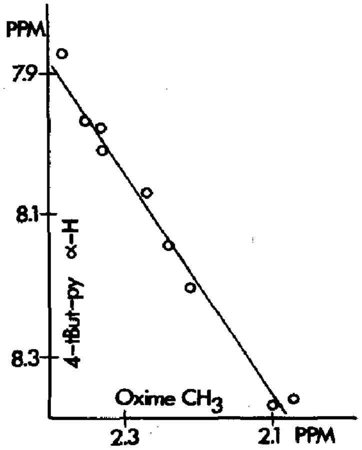

Fig. 9. ^1H NMR chemical shift for the α-H(4-tBut–py) versus ^1H NMR chemical shift for the oxime CH_3 of 4-tBut–pyCo(DH)$_2$X; X = (top to bottom) NO_3, NCS, Br, Cl, NO_2, isopropylxanthine, CN, Me, P(O)(OMe)$_2$, respectively [153].

TABLE 21

^{1}H NMR spectral data and formation constants for 4-X–pyCo(DH)$_2$CH$_3$ [a]

X	δ Co–CH$_3$	δ oxime CH$_3$	Log K_f
CN	0.78	2.08 [b]	–
H	0.68	2.07 [b]	–
Me	0.65	2.07 [b]	–
CN	0.63	2.11 [c]	2.03
H	0.55	2.10 [c]	3.16
Me	0.52	2.09 [c]	3.40
NH$_2$	0.40	2.09 [c]	4.14

[a] Ref. 159. [b] Solvent: CDCl$_3$. [c] Solvent: 50% (v/v) DMSO–d$_6$-D$_2$O.

ters (σ) for X, although this point was not noted by the authors [159]. The effect of L for O, C, S, N, As and P donors on the axial CH$_3$ shift has been reported for LCo(DH)$_2$CH$_3$ in NO$_2$Ph [160]. The resonances shift by ~ 0.5 ppm across the series.

Similarly, there is an evident relationship between the shifts of axial CH$_2$CH$_3$ ^{1}H NMR resonances and the basicity of L (Table 22). The CH$_3$ resonance shifts less than the CH$_2$ resonance, as might be expected. There is probably little change in anisotropy at Co across such a series and consequently the inductive effect appears to dominate the axial alkyl shift. For N donors, plots of $\Delta_{CH_2-CH_3}$ versus pK_b were linear and parallel for two groups of ligands consisting of aliphatic and aromatic N donor ligands, respectively.

TABLE 22

^{1}H NMR spectral data for LCo(DH)$_2$CH$_2$CH$_3$ and pK_b values for L [a]

L	δ_{CH_3}	δ_{CH_2}	$\Delta_{CH_2-CH_3}$	pK_b
PhNH$_2$	0.24	1.75	1.51	9.4
Morpholine	0.24	1.62	1.38	5.67
NH$_3$	0.29	1.64	1.35	4.75
PhCH$_2$NH$_2$	0.31	1.65	1.34	4.38
MeNH$_2$	0.29	1.59	1.30	3.34
Piperidine	0.23	1.53	1.30	2.88
3-CN–py	0.31	1.83	1.52	12.61
Py	0.33	1.73	1.40	8.79
Collidine	0.34	1.67	1.33	6.57
Imidazole	0.36	1.66	1.30	7.05
H$_2$O	0	1.60	1.60	14
Diethylmercaptan	0.26	1.84	1.63	19

[a] Ref. 161; $\Delta = \delta CH_2 - \delta CH_3$.

TABLE 23

^1H NMR chemical shifts (iPr-CH_3) for $LCo(DH)_2i\text{-}C_3H_7$ [a]

N donors								P donors		S donors	
NRR'R''				Five-membered rings		Six-membered rings					
NH_2	0.40	*Secondary amines*		1-Et-2-Me-benzimidazole	0.06	2-Me-py	0.10	$PChx_3$	0.16	SPh_2	0.17
Primary amines		$(n\text{-}C_3H_7)_2NH$	0.24	9-Me-adenine	0.28	Quinoline	0.14	$P(i\text{-}Pr)_3$ [b]	0.28	$S(CH_2Ph)_2$	0.40
$4\text{-}NO_2PhNH_2$	0.25	Et_2NH	0.27	2-iPr-imidazole	0.32	$2\text{-}NH_2\text{-}4,6\text{-}Me_2$-pyrimidine	0.20	PPh_3	0.41	SMe_2	0.44
t-But-NH_2	0.28	Piperidine	0.34	3-CM-adenine [c]	0.32	2-MeNH-py	0.23	$P(But)Ph_2$ [b]	0.50		
$3\text{-}NO_2PhNH_2$	0.30	Me_2NH	0.36	$1,2\text{-}Me_2$-imidazole	0.32	$2\text{-}NH_2$-3-Me-py	0.25	$P(Et)Ph_2$	0.57		
$4\text{-}BrPhNH_2$	0.35	Pyrrolidine	0.40	3-Benzyladenine	0.34	$2\text{-}NH_2$-pyrimidine	0.25	$P(CH_2CH_2CN)_3$	0.52		
$c\text{-}C_6H_{11}NH_2$	0.37	*Tertiary amines*		$1\text{-}Me\text{-}5\text{-}NO_2$-imidazole	0.44	$2\text{-}NH_2$-py	0.27	$P(OPh)_3$ [b]	0.53		
$i\text{-}C_3H_7NH_2$	0.37	Quinuclidine	0.21	Thiazole	0.48	$2\text{-}NH_2$-6-Me-py	0.30	$P(OMe)_3$	0.54		
$4\text{-}C_2H_5PhNH_2$	0.38	Me_3N	0.24	$5,6\text{-}Me_2$-benzimidazole	0.50	$PBu_3Co(DH)_2C_5H_4N$	0.42	$PBut_3$ [b]	0.54		
$4\text{-}Me_2NPhNH_2$	0.40			1-Me-imidazole	0.50	4-CN-py	0.42	$P(OCH_2CH_2Cl)_3$ [b]	0.54		
$EtNH_2$	0.41					Py	0.46	$P(OCH_2)_3CMe$	0.62		
$MeNH_2$	0.43					4-tBut-py	0.46	PMe_3	0.64		
						$4\text{-}Me_2N$-py	0.47				

[a] Refs. 49, 157. [b] Prepared in situ. [c] CM = carboxymethyl.

The apparent inductive effect of N donor ligands on the shift of the alkyl CH_3 resonance is relatively smaller for $LCo(DH)_2i\text{-}C_3H_7$ compounds (Table 23). For example, changing the N donor from 4-CN–py to $4\text{-}Me_2N$–py causes a shift of only ~ 0.05 ppm. However, the alkyl CH_3 shifts are much more sensitive to the steric bulk of the L ligand. The shift when L = 2-Me–py occurs about 0.3 ppm upfield relative to any complex where L is a sterically unhindered pyridine (i.e. lacking a 2-substituent). Likewise, for P donor ligands, the shifts are responding primarily to the bulk of L (Table 23). The relationship between the bulk of L and shift will be described and explained below. The lower sensitivity to inductive effects of the alkyl CH_3 shift in $i\text{-}C_3H_7$ compared with CH_2CH_3 compounds may reflect the shorter Co–C bond in the latter.

In general, non-alkyl cobaloximes have not exhibited any trends in ^1H NMR as a function of the electron donating properties of the axial ligands. However, as found above for $i\text{-}C_3H_7$ compounds, the ^1H NMR spectra of

TABLE 24

^1H NMR spectral data for $[LCo(DH)_2(MeOH)]^+$ and physical parameters for L[a]

RR'_2P	MeOH		Oxime CH_3		pK_a[b]	$\Sigma\chi$[c]	CCA	TCA
	δ (ppm)	^4J (Hz)	δ (ppm)	^5J (Hz)				
$PChx_3$	2.540	1.1	2.49	0.5	9.70	0.3	171	179
$P(i\text{-}C_3H_7)_3$	2.580	0.9	2.48	0.5	7.97	3.0	164	160
PPh_3	2.605	1.5	2.17	0.8	2.73	12.9	160	155
$P(But)Ph_2$	2.690	1.3	2.11	0.7		10.0	145	140
$P(Et)Ph_2$	2.690	1.3	2.10	0.7		10.4	145	141
$P(Me)Ph_2$	2.735	1.4	2.05	0.7	4.6	11.2	137	136
$P(CH_2Ph)_3$	2.745	1.3	2.29	0.6		10.1	136	165
$P(OMe)Ph_2$	2.750	1.6	2.10	0.7		16.3	134	132
$P(CH_2CH_2CN)_3$	2.755	1.5	2.53	0.8	1.36	21.9	134	130
$P(OC_6H_4\text{-}o\text{-}Me)_3$	2.760	2.7	2.10	0.6		28.2	133	133
$P(OC_6H_4\text{-}o\text{-}i\text{-}C_3H_7)_3$	2.760	2.7	2.11	0.6			132	148
$PBut_3$	2.770	1.2	2.44	0.8	8.43	4.2	131	130
$P(Me)_2Ph$	2.800	1.3	2.19	0.7	6.50	9.5	125	127
$P(OMe)_2Ph$	2.800	2.0	2.21	0.5		19.7	125	120
$P(O\text{-}i\text{-}C_3H_7)_3$	2.820	2.2	2.41	0.5	3.4	18.9	121	122
$P(OPh)_3$	2.830	2.8	2.22	0.5		29.1	119	121
PMe_3	2.855	1.0	2.41	0.6	8.65	7.8	<115	118
$P(OCH_2)_3CEt$	2.845	2.7	2.41	0.5		30.6	<115	101
$P(OMe)_3$	2.850	2.3	2.42	0.5		23.1	<115	107
$P(OEt)_3$	2.850	2.2	2.41	0.5		20.4	<115	109
$P(OCH_2CH_2Cl)_3$	2.850	2.6	2.44	0.4		27.9	<115	110

[a] See Ref. 162 for additional details. CCA and TCA are calculated and Tolman [129] cone angles, respectively. [b] See ref. 163. [c] See ref. 164.

non-organometallic cobaloximes also respond to changes in the bulk of L, particularly when L is a P donor ligand (Table 24). The data for $[LCo(DH)_2CH_3OH]^+$ complexes in Table 24 revealed no relationship between the shift of either equatorial or axial CH_3OH resonances and the electronic properties of L as measured by either pK_a of L or Tolman's $\Sigma\chi$. However, a good relationship was observed with ligand bulk as assessed using Tolman's cone angles. These data could be used to compile an experimentally determined cone angle (CCA) based on the spectroscopic data.

The relationship between L bulk and shift exhibits a characteristically dipolar relationship (opposite direction of shift for axial and equatorial ^1H resonances). The heavy-atom effect of cobalt is obviously responding and changing as L bulk is changed. The structural basis for this change may be a change in α bending or in the Co–donor atom distance, and this point is discussed later.

The importance of the Co heavy-atom effect on ^1H NMR of cobalt complexes is well known and the effect is often not important in diamagnetic complexes of other metals such as Rh(III) complexes [165]. The correlation of the effect with hybridization and changes in geometry was first made for cobaloximes [153,162], which have the advantage compared with other Co complexes of accommodating a large variety of axial ligands.

Care should be taken in utilizing ^1H NMR shifts as a measure of hybridization because any significant anisotropy in the axial ligand can also have an effect. Usually, the ^1H resonance of the oxime CH_3 group is affected. For example, this resonance for a given X in PPh_3 complexes is

TABLE 25

^1H NMR data for $LCo(DH)_2R$ and $LCo(DH)_2SO_2R$ (in $CDCl_3$) [a]

L	R	$LCo(DH)_2R$		$LCo(DH)_2SO_2R$	
		Oxime CH_3	Alkyl	Oxime CH_3	Alkyl
Py	Me	2.13	0.82	2.25	2.66
Isoquinoline	Me	2.08	0.83	2.25	2.69
PPh_3	Me	1.82 (8 Hz, ^5J)	1.18	1.97	2.57
$AsPh_3$	Me	1.90	1.30	2.00	2.62
SMe_2	Me	2.22	0.76	–	–
$AsPh_3$	Et	1.81	0.34(CH_3), 1.95(CH_2)	–	–
Py	$CH_2C_6H_5$	1.94	2.86(CH_2), 7.03(C_6H_5)	–	–
Isoquinone	$CH_2C_6H_5$	1.90	2.86(CH_2)	2.23	4.14(CH_2)
Py	i-C_3H_7	2.06	0.41(CH_3)	2.26	1.06(CH_3)
Py	2-octyl	2.07	0.39(β-CH_3)	–	–

[a] Ref. 166.

~ 0.3 ppm upfield to that in complexes where L anisotropy is low (Table 25). Other data in Table 25 further illustrate the sensitivity of the axial Co–CH_3 shift to L, particularly when the donor atom of L is changed. Once the CH_3 is removed from direct attachment to Co (in –SO_2CH_3 compounds) the shift dependence on L is greatly diminished.

An additional concern is the solvent; anisotropic solvents, typically aromatic, can also influence the shifts [167–169]. This phenomenon, aromatic solvent-induced shifts (ASIS), roughly reflects the dipole moment of the cobaloxime and is small for alkylcobaloximes and larger for $LCo(DH)_2X$ ($X \neq R$) complexes [167]. Such solvents should be avoided in any attempt to assess changes in hybridization at cobalt.

Some typical ASIS data for cobaloximes are given in Table 26. Comparing shifts in CH_2Cl_2 to those in C_6H_6, the oxime CH_3 resonance shifts about one-quarter of a ppm unit upfield for alkyl complexes. Shifts closer to one-half of a ppm unit are observed for related non-alkyl complexes [167]. The shift of the axial CH_3 is in the opposite direction, indicating a relatively electron-rich part of the molecule. The oxime O–H–O resonance (not given) shifts 0.5 to 1.0 ppm downfield (in alkyl complexes), as might be expected from the partial negative charge on the oxygens.

For benzene, the π system is electron rich and solvates the relatively electron-poor parts of the cobaloximes. Changing to a solvent such as C_6F_6 changes the direction of all the ASIS shifts. For this solvent, the electron-rich portion is the F-containing periphery [168,169].

The O–H–O resonance of cobaloximes is difficult to observe at ambient temperatures except for alkyl cobaloximes. This phenomenon, although known from some of the earliest ^1H NMR studies of cobaloximes [170], has not yet been investigated in detail. Relatively few such resonances have been

TABLE 26

ASIS effects on $LCo(DH)_2Me$ [a]

L	C_6H_6	C_6F_6	$C_6H_5NMe_2$
Δ, Oxime CH_3 (ppm)			
4-tBut-py	+0.24	−0.08	+0.24
$PBut_3$	+0.19	−0.12	+0.20
SMe_2	+0.26	−0.11	+0.34
Δ, Axial CH_3 (ppm)			
4-tBut-py	−0.62	+0.40	−0.39
$PBut_3$	−0.68	+0.30	–
SMe_2	−0.53	+0.37	−0.19

[a] Measurements made at 100 MHz; $\Delta = \tau(X) - \tau(CH_2Cl_2)$ (ref. 167).

TABLE 27

NMR spectroscopic data for $P(OMe)_3Co(DH)_2X$ [a]

X	^{13}C NMR δ			^{31}P NMR δ	^2J (Hz) P–C	^5J (Hz) P–H	^{1}H NMR δ Oxime CH_3
	OCH_3	Oxime CH_3	Oxime N=C				
NO_3	55.70	12.82	153.41	89.0	9.2	0.7	2.35
CN	54.45	12.55	151.25	102.9	8.6	2.3	2.28
Cl	55.19	12.77	151.70	97.3	8.7	1.4	2.31
NO_2	54.57	12.65	152.37	103.2	8.4	1.7	2.28
Br	55.07	12.86	152.03	100.9	9.0	1.35	2.30
N_3	54.64	12.67	151.11		8.2	1.3	2.33
I	54.93	12.94	152.60	101.8	8.7	1.7	2.28
p-SO_2PhMe	54.13	12.41	151.88		8.0		
CH_2NO_2	53.75	12.61	150.46		7.8		
$Co(DBF_2)_2Me$ [b]	53.48	13.09	155.40		7.9		
$CHCl_2$	53.41	12.37	150.56	122.4	7.9	3.2	2.22
CH_2CN	53.40	12.55	150.11	122.2	7.6	3.1	2.24
$CHBr_2$	53.62	12.54	150.80	110.1	7.8	3.0	2.23
$P(O)(OMe)_2$	53.29	12.24	150.90	121.0	6.8	3.4	2.20
CH_2CF_3	53.19	12.11	149.85	121.9	7.4	3.6	2.18
CH_2COOMe	53.15	12.30	149.63		7.3		
$P(O)Ph_2$	53.13	11.84	150.08		6.7		
CH_2Cl	52.77	12.10	149.23	126.5	6.8	3.5	2.17
CH_2Br	52.87	12.26	149.27	126.3	6.7	3.4	2.18
CH_2I	52.95	12.53	149.18	119.1	6.8	3.4	2.22
DDT [c]	52.83	12.01	149.22		7.0		
p-C_6H_4Br	52.82	12.11			7.2		
C_6H_5	52.67	12.09	149.21	127.3	6.9	3.9	2.05
$(CH_2)_3CN$	52.51	12.04	148.56	129.4	6.6	3.95	2.18
$CH{=}CH_2$	52.41	12.06	148.49		6.0		
Me	52.24	11.96	147.96	128.2	5.9	3.7	2.14
$CH_2C_6H_5$	52.46	11.81	148.13		6.5		
$(CH_2)_2C_6H_5$	52.32	11.98	148.27	130.3	6.0	4.0	2.15
CH_2SiMe_3	52.54	12.05	148.50		7.0		
n-C_3H_7	52.20	11.93	148.11	130.5	5.3		
CH_2CH_3	52.16	11.89	147.87	131.1	5.6	4.1	2.16
c-C_3H_5	52.37	12.01	148.08		6.5		
c-C_5H_9	52.26	11.92	148.24		6.2		
c-C_7H_{13}	52.21	12.06	148.25		6.0		
CH_2CMe_3	52.36	11.94	148.86		5.4		
CH_2CHMe_2	52.25	11.95	148.06		6.5		
i-C_3H_7	52.18	11.97	148.11	131.9	6.4		
CH(Me)(Et)	52.16	11.98	148.13		6.3		
c-C_6H_{11}	52.20	12.03	148.16		6.6		
$CH(Et)_2$	52.22	12.02	148.21		5.5		

[a] In $CDCl_3$; see refs. 156, 157, 162, 173 and 174. See also ref. 204. [b] The equatorial OHO protons are replaced with BF_2^+. [c] $C(Cl) = C(C_6H_4\text{-}p\text{-}Cl)_2$.

recorded [160,170] and they are found in the region of ~ 18 ppm (except in ref. 171). The solvent and the presence of H_2O also seem to influence this signal. Dynamic ^1H NMR data for the O–H–O signals of cobaloxime dimers have been studied at low temperatures [226].

As mentioned above, the best NMR criterion for hybridization is direct coupling between the metal nucleus and a ligand nucleus [151]. Coupling can only be transmitted by *s* orbitals, which have non-zero electron density at the nucleus. Unfortunately, ^{59}Co has a spin of 7/2 and coupling is difficult to resolve. Coupling via many bonds is inherently more difficult to interpret. However, the five-bond coupling between coordinated ^{31}P and the oxime CH_3 [170] is readily measured in the ^1H NMR spectrum of cobaloximes with P donor ligands (Tables 24, 27 and 28). The coupling, which increases as electron donation by X increases, follows trends found for chemical shifts and therefore also correlates with trends in hybridization observed for other metal species [153,154].

In principle, the five-bond coupling will increase as the *s* character of the Co–P bond increases. The P donor orbital will have higher *s* character if the substituents on P are electronegative. Thus the $^5J_{PH}$ coupling constants for cobaloximes are largest for phosphite complexes and smallest for trialkylphosphine complexes. This effect is small, however.

The coupling constant is also dependent on X. In theory, the *s* character of the Co–P bond could increase or decrease as X becomes a better electron donor. If X uses more metal *s* character in its bonding, the *s* character of the Co–P bond would be decreased. Alternatively, the $XCo(DH)_2$ group is a poorer electron acceptor and the P ligand would use more *s* character in its electron donation to cobalt. Similarly, the degree of *s* character in the Co–N(oxime) bonds would change as the *s* character in the axial bonds changes. Finally, the Co–P bond length increase (as X donor ability increases) should decrease coupling. These conflicting effects are difficult to evaluate without a quantitative theoretical treatment. However, the observation that the $^5J_{PH}$ coupling trend is consistent with changes observed for other metals is evidence that metal rehybridization is occurring [153,154].

^{13}C NMR. In contrast to trends in ^1H NMR, shifts of ^{13}C resonances are influenced relatively little by the heavy Co atom. For C atoms close to cobalt (such as C-1 in $PBut_3$ and the α-C in N–py compounds) evidence has been presented that remote effects can be detected [156]. However, in most cases, such remote effects are small compared with the relatively large range of shifts in ^{13}C and ^{31}P NMR and are likely to show parallel trends with the major factor influencing the shifts, i.e. the local heavy-atom effect of the heavier C nucleus. Thus, in general, ^1H NMR shifts of non-alkyl ligands as X is changed can be viewed as an indirect probe of changes at the Co atom,

TABLE 28

NMR spectroscopic data for $LCo(DH)_2X$ ($L = PBut_3, PPh_3$)[a]

X	$PBut_3$							PPh_3[e]		
	^{13}C NMR δ			^1J (Hz)[b] P–C	^{31}P NMR[c] δ	^1H NMR δ[d] Oxime CH_3	^5J (Hz)[d] P–H	^{31}P NMR δ	^5J P–H	^1H NMR δ Oxime CH_3
	Oxime CH_3	Oxime C=N	C_1, $PBut_3$							
NCS	12.74	152.01	20.37	24.6	24.0	2.37	1.4			
NO_3	12.84	153.48			35.6	2.37	0.8			
SCN	13.05	151.66			29.8	2.37	1.4			
CN	12.52	150.37	18.98	21.8	34.6	2.29	2.1			
Cl	12.77	151.66	20.44	23.6	30.9	2.33	1.3	25.6	1.51	2.02
NO_2	12.61	152.31	20.47	22.0	22.3	2.34	1.4	21.5	1.76	1.99
$C_5H_4N_5$[g]	12.65	152.53	20.22	23.4						
$C_5H_3N_4O$[h]	12.65	152.49	20.20	23.4						
Br	12.86	151.99	20.08	23.2	33.9	2.34	1.2	30.4	1.47	2.03
N_3	12.62	150.89	20.79	23.2	25.8	2.36	1.4			
I	12.95	152.44	19.22	22.4	33.8	2.29[f]	1.5[f]	32.5	2.05	1.99
$SCPh_2$						2.04[f]	1.6[f]			
$SnPh_3$					24.9					

p-$SO_2C_6H_4Me$	12.35	151.56	20.13	20.0	19.0	2.06 ^{f}	2.1 ^{f}			
$P(O)(OMe)_2$	12.17	150.15	18.82	17.6						
CH_2CN								23.0	2.78	1.92
S(t-But)						2.23 ^{f}	2.6 ^{f}			
$CHBr_2$					9.5	2.20 ^{f}	2.5 ^{f}			
CCl_3						2.16 ^{f}	3.0 ^{f}			
CH_2CF_3								21.2	2.98	1.85
C_6H_4Br	11.99	148.43	19.49	15.8						
CH_2Br	12.16	148.45	19.78	17.2	5.5	2.21 ^{f}	3.1 ^{f}	20.0	2.88	1.87
$CH_2C_6H_5$						1.94 ^{f}	3.3 ^{f}			
C_6H_5	11.99	148.24	19.51	15.4	3.2	2.04 ^{f}	3.5 ^{f}			
C_6H_4OMe	12.00	148.19	19.45	15.6						
Me	11.81	146.87	19.50	15.0	1.9	2.16	3.3	20.4	3.13	1.84
$CH_2C(Me)(COOEt)_2$								20.0	3.23	1.75
n-C_3H_7					1.9					
CH_2CH_3					2.3		3.4 ^{f}	20.9	3.32	1.82
CH_2CMe_3								17.2	3.47	1.78
i-C_3H_7					3.1		3.7 ^{f}	22.7	3.52	1.82
CH(Me)(Et)								21.4	3.56	1.82

---

[a] $CDCl_3$ solvent. Data from ref. 156 unless otherwise noted. [b] Ref. 156. [c] Ref. 174. [d] Ref. 153, unless otherwise noted. [e] Ref. 157, 174 and 175. [f] Ref. 167. [g] Adeninato. [h] Hypoxanthinato.

whereas ^{13}C shifts of ligand nuclei remote from Co are more reflective of changes in bonding occurring within the ligands [156]. Two other points should be noted. First, since the remote effect of the Co is best viewed as a small change in field (δH) observed by the resonating nucleus, the size of the effect can be calculated from (a) the dipolar relationship, (b) the geometry of the complex, and (c) the effects measured on ^{1}H NMR shifts. This type of calculation [156] confirms that the remote effect of Co will be small ($\ll 1$ ppm for remote atoms) compared with the range of shifts observed for such remote nuclei as the γ-C of pyridine ligands (~ 3 ppm). Secondly, there is no a priori reason for the ^{13}C shifts of axial and equatorial ligands to change in opposite directions as X electron-donating ability changes. Indeed, it has been found that the resonances change in the same direction and move upfield as the electron-donating ability of X is increased (Tables 20, 27 and 28).

Because the interpretation of ^{13}C shifts (or shifts of other heavy nuclei, e.g. ^{31}P) is not simply related to the electron density, the direction of a change in shift does not in itself give an indication of the nature of the change in electron density. However, it is well known that alkyl groups are better electron donors than acido groups. Consequently, the ordering of the ^{13}C resonances reflects trends in electron donation.

Typical ^{13}C NMR trends are observed for complexes of $P(OMe)_3$ (Table 27). For complexes with this ligand, $^{2}J_{PC}$ decreases by ~ 50% in going from hard, poorly electron-donating X (NO_3) to good electron-donating alkyl groups (CH_2CH_3). Likewise, in $PBut_3$ complexes, $^{1}J_{PC}$ decreases with increasing electron-donating ability of the X ligand. As mentioned above, the trend in C-1 for this latter series may be complicated by other effects.

One last type of comparison should be noted. On complex formation, the shifts of the L ligand, particularly ^{13}C and ^{31}P, are changed. For most ligands, this shift is downfield. For example, shifts on complex formation for some $PhNH_2$ compounds are given in Table 29. For 4-tBut–py complexes the shifts of the α, β, and γ ^{13}C resonances are shifted ~ 1.3 ppm, 2.5 ppm, and ~ 4.5 ppm, respectively, downfield on complexation to form the NO_3 complex. The corresponding shifts on forming the CH_2CH_3 complexes are ~ 0 ppm, ~ 1.8 ppm and ~ 2 ppm. Thus, for ^{13}C shifts, these approach the free ligand value as the electron-donating ability of X increases. This is in keeping with the weaker bonding between Co and L as X electron-donating ability increases.

For $P(OMe)_3$, the ^{13}C shift is 49.14 ppm [156 supplementary] and $^{2}J_{PC}$ is 10.6 Hz. Thus, the downfield shift on coordination follows the above trend but the coupling constant for weakly electron-donating X is most similar to the free ligand value. However, a change in sign of the coupling constant cannot be ruled out. The situation for $PBut_3$ complexes is complicated owing

TABLE 29

^{13}C NMR spectral data for $PhNH_2Co(DH)_2X$ [a]

X	Δ (C_4) [b]	X	Δ (C_4) [b]
Me	3.9	CH=CH_2	5.1
CH_2CH_3	3.9	PhC=CH_2	5.2
n-C_3H_7	4.0	MeC=CHCOOEt	5.3
$CH_2C_6H_5$	4.4		

[a] Ref. 176. [b] $\Delta = \delta$(complexed) − δ(free) for the C_4 carbon of $PhNH_2$.

to the large number of ligand resonances and coupling constants. Tentative assignments of resonances have been made for both shifts and coupling constants [156 supplementary].

^{31}P NMR. Most of the published data on this topic can be found in one paper [174] (however, see ref. 177). Since ^{31}P shifts are influenced by electron density and electron distribution at P, many of the factors discussed for ^{13}C apply to ^{31}P NMR. ^{31}P NMR shifts are also influenced by changes in bond angles at P [178]. Additionally, P is directly bonded to Co and this proximity can increase the importance of heavy-atom effects of Co on ^{31}P shifts relative to most ^{13}C shifts.

The conclusions of the most extensive study on ^{31}P NMR were as follows:

For variation in X:

(1) The ^{31}P shift varies over a wide range as X is changed (up to 40 ppm for L = $PBut_3$).

(2) As the *trans* influence of X is increased, the ^{31}P shifts of coordinated phosphines shift upfield, whereas those of coordinated phosphites shift downfield.

(3) However, the order in X is similar for both phosphines and phosphites (Tables 27 and 28).

(4) This trend is the typical *trans* effect/influence series found in most rate, spectroscopic, and structural studies.

For variation in L:

(5) Phosphine coordination chemical shifts appear to be considerably influenced by phosphine steric size.

(6) Phosphite coordination chemical shifts appear to be more influenced by the electronic nature of phosphite substituents.

(7) The relative shifts of coordinated phosphines and phosphites are the same for both X = Cl and X = CH_3, although the Co–P bond is longer for X = CH_3 (Table 30).

In general:

(8) Since the ^{31}P NMR shifts follow well-defined empirical trends, these

values will be useful in structural characterization and in the assessment of the *trans* influence of X.

(9) Since so many factors appear to influence ^{31}P shifts, and since both electronic and steric effects are important, detailed evaluation of the nature of the Co–P bond is not possible from ^{31}P NMR shifts.

For PPh_3 complexes (Table 28) the complications arising from steric effects have eliminated any close relationship of ^{31}P NMR shifts to the *trans* influence of X [175]. Therefore, point (8) should probably be qualified and appears to hold for small cone angle ligands only.

TABLE 30

^{31}P NMR chemical shifts for $LCo(DH)_2X$ [a]

L	X = Cl		X = Me	
	^{31}P NMR δ	Δ	^{31}P NMR δ	Δ
$P(i\text{-}C_3H_7)_3$	35.0	14.2	–	–
$PChx_3$	23.9	9.9	3.3	−10.7
PPh_3	24.9	30.1	19.8	25.0
$P(Et)Ph_2$	34.8	46.2	19.8	31.2
$P(But)Ph_2$	32.3	48.3	16.6	32.6
PEt_3	36.0	44.6	5.7	24.3
$P(Me)Ph_2$	21.4	48.2	8.0	34.8
$PBut_3$	30.9	61.8	1.9	32.8
PMe_3	26.8	87.7	–	–
$P(OMe)Ph_2$	124.3	8.7	126.4	10.8
$P(OMe)_2Ph$	140.3	−18.7	158.3	−0.7
$P(OPh)_3$	81.6	−46.4	112.1	−12.9
$P(OCH_2CCl_3)_3$	101.5	−36.1	–	–
$P(OCH_2CH_2Cl)_3$	96.7	−41.9	127.3	−11.3
$P(OBut)_3$	92.0	−47.1	127.5	−11.6
$P(O\text{-}i\text{-}C_3H_7)_3$	86.1	−53.2	118.2	−19.9
$P(OEt)_3$	90.9	−48.3	–	–
$P(Oallyl)_3$	94.5	−44.8	124.2	−15.1
$P(OMe)_3$	97.3	−43.7	128.2	−12.8

[a] Ref. 174; $\Delta = \delta(\text{complexed}) - \delta(\text{free})$.

^{19}F NMR. The cobalt-containing moiety can be viewed as a substituent just like numerous other substituents used in physical organic studies. ^{19}F NMR substituent chemical shifts (SCS) were determined for a series of complexes of the type $LCo(DH)_2CH_2C_6H_4F$ (Table 31). For all compounds where L are neutral ligands, changes in L cause only minor changes in the SCS values in CH_2Cl_2. SCS values obtained in DMF may represent population averaging due to L exchange with DMF. A large increase in the SCS

TABLE 31

^{19}F NMR chemical shifts for $LCo(DH)_2CH_2C_6H_4F$ [a]

L	^{19}F δ(*para*) [b]		^{19}F δ(*meta*) [c]
	CH_2Cl_2	DMF	CH_2Cl_2
DMSO	4.67	–	–
SMe_2	4.71	5.02	2.77
MeCN	4.79	–	–
NMe_3	4.80	5.12	–
Py	d	d	2.91
DMF	4.98	5.44	–
PPh_3	4.97	4.92	2.97
$P(OMe)_3$	5.24	5.19	3.42
CN^-	8.05	8.50	4.12

[a] Shifts are referenced to internal fluorobenzene. See ref. 179 for details. [b] The alkyl is *p*-fluorobenzyl. [c] The alkyl is *m*-fluorobenzyl.

was observed when the neutral ligands were replaced by CN^-, possibly indicating a large increase in the electron-donating ability of the $-CH_2Co(DH)_2CN^-$ group. These effects have been attributed to hyperconjugation in a manner similar to those observed for main group substituents [179].

^{19}F NMR SCS values were determined for a series of $[XCo(DH)_2p\text{-}CH_2C_6H_4F]^-$ complexes where X is a monoanionic two-electron-donating ligand [180]. The electron-donating capacity of $-CH_2Co(DH)_2X^-$ depends markedly on the nature of X, and also on the nature of the counter ion (Table 32). Consistently higher SCS values were observed for $AsPh_4^+$ salts compared with salts of NEt_4^+, possibly due to differences in ion pairing for the cations. The order of SCS values for the complexes roughly parallels the basicity of X.

TABLE 32

^{19}F NMR chemical shifts (ppm) for $LCo(DH)_2(p\text{-}CH_2C_6H_4F)$ [a]

L	Counterion		L	Counterion	
	$AsPh_4^+$	Et_4N^+		$AsPh_4^+$	Et_4N^+
CN^-	8.49	8.08	Cl^-	7.04	–
NO_2^-	7.80	–	Br^-	6.72	–
N_3^-	7.60	7.12	NCS^-	6.78	6.38
NCO^-	7.50	–	I^-	6.52	–

[a] Chemical shifts are referenced to internal fluorobenzene. See ref. 180 for details.

TABLE 33

^{19}F NMR chemical shifts and formation constants for $LCo(DH)_2C_6H_4F$ [a]

L	pK_a (L)	*meta*		*para*		σ_1	σ_R^0
		K_f (M^{-1})	δ	K_f (M^{-1})	δ		
Measurements made in DMSO							
4-CN–py	2.24	$5.44 \pm 1.8 \times 10$	1.430	$5.52 \pm 1.2 \times 10$	9.483	−0.305	−0.228
4-Carboxamido–py	3.77	$3.47 \pm 0.6 \times 10^2$	1.550	$3.59 \pm 0.4 \times 10^2$	9.560	−0.328	−0.225
Py	5.56	$7.24 \pm 0.58 \times 10^2$	1.660	$5.90 \pm 0.28 \times 10^2$	8.750	−0.346	−0.193
4-Me–py	6.36	$1.69 \pm 0.09 \times 10^3$	1.745	$1.24 \pm 0.06 \times 10^3$	–	–	–
4-NH_2–py	9.40	$3.89 \pm 0.47 \times 10^4$	2.051	$1.01 \pm 0.13 \times 10^4$	9.976	−0.424	−0.212
DMSO	–	–	1.860	–	10.270	−0.389	−0.231
Measurements made in MeOH							
4-Carboxamido–py	3.77	–	1.115	–	9.702	−0.201	−0.252
MeOH	–	–	0.980	–	9.750	−0.178	−0.260
Glycine ethyl ester	7.86	$2.02 \pm 0.24 \times 10^3$	1.583	$2.05 \pm 0.16 \times 10^3$	9.660	−0.283	−0.227
2,2-Dimethoxyethylamine	8.86	$2.35 \pm 0.18 \times 10^3$	1.626	$1.99 \pm 0.19 \times 10^3$	9.638	−0.291	−0.224
2-Methoxyethylamine	9.68	$3.64 \pm 0.30 \times 10^3$	1.690	$2.35 \pm 0.35 \times 10^3$	9.738	−0.302	−0.224
n-Propylamine	10.80	$4.03 \pm 0.41 \times 10^3$	1.754	$2.76 \pm 0.23 \times 10^3$	9.793	−0.313	−0.222
S-Methyl-2-mercaptoethanol	–	6.78 ± 0.46	0.813	8.37 ± 0.17	9.044	−0.148	−0.245
Methyl-*S*-methylmercaptoacetate	–	0.92 ± 0.08	0.731	0.74 ± 0.17	9.154	−0.134	−0.253
PPh_3 [b]	–	$3.21 \pm 0.41 \times 10^2$	0.608	$5.10 \pm 0.08 \times 10^2$	9.653	−0.125	−0.289
Methyl mercaptoacetate	7.83	$1.72 \pm 0.3 \times 10^3$	2.510	$1.49 \pm 0.40 \times 10^3$	10.333	−0.445	−0.202
Methyl mercaptopropionate	9.27	$1.86 \pm 0.26 \times 10^3$	2.553	$2.11 \pm 0.54 \times 10^3$	10.457	−0.453	−0.204
2-Mercaptoethanol	9.51	$2.02 \pm 0.32 \times 10^3$	2.603	$2.24 \pm 0.30 \times 10^3$	10.496	−0.462	−0.203
CN^-	9.00	$> 7.5 \times 10^4$	2.549	$> 6.7 \times 10^4$	9.949	−0.452	−0.188
SCN^-	0.85	–	1.590	–	9.714	−0.284	−0.228
NCS^-	0.85	–	1.928	–	9.894	−0.343	−0.217

[a] Ref. 181. [b] The solvent is $CHCl_3$.

In an extensive study, ^{19}F NMR chemical shifts of L(or X)Co(DH)$_2$C$_6$H$_4$F (*meta* and *para*; Table 33) have been correlated with chemical shifts of other monosubstituted fluorobenzenes via the Taft dual-substituent parameter equation [181]. The inductive and delocalization substituent parameters, σ_I and σ_R^0, respectively (Table 33), were felt to provide a measure of the susceptibility of the cobalt center to inductive and resonance effects. It was suggested that the results indicate that π-electron donation occurs from cobalt to the covalently bound alkyl group. It was also concluded that the amount of π donation varies substantially with the nature of L or X. Values of σ_I correlate linearly with pK_a values of L or X for ligands in the following three categories: RNH$_2$, 4-X–py, RS$^-$. Values of σ_R appear insensitive to all L where L are N donor ligands. Complexes with *trans* π-accepting ligands such as CN$^-$ were believed to have the least resonance-donating potential. Several other studies utilizing both cobaloximes and other Co species are referenced in a recent review [105].

^{59}Co NMR and NQR. ^{59}Co NMR and NQR data have been obtained for a series of LCo(DH)$_2$X compounds ([182]; see also ref. 183). These data have been interpreted [182] in terms of the relative partial field-gradient contributions of the axial ([X]) and equatorial ([*N*]) ligands. Values of chemical shift,

TABLE 34

^{59}Co NMR and NQR data for LCo(DH)$_2$X [a]

L	^{59}Co NMR δ (ppm)		$e^2q_{zz}Q/h$ (MHz)		$[N]/[X]$	
	X = Me	X = Cl	X = Me	X = Cl	X = Me	X = Cl
MeOH	4040	–	−41.62	–	1.8	–
NMe$_3$	4360	–	−33.27	–	1.4	–
Py	4490	2980	−29.52	+64.82	1.10	3.1
3-Me–py	4490	–	–	–	–	–
4-Me–py	4490	–	–	–	–	–
1-(2-Trifluoromethyl-phenyl)imidazole	4560	–	−31.34	–	1.35	–
SMe$_2$ [b]	4960	–	+30.30	–	0.68	–
AsPh$_3$	5200	–	+32.02	–	0.67	–
P(C$_6$H$_4$-*p*-OMe)$_3$	5340	–	–	–	–	–
PPh$_3$	5350	3360	+28.12	+60.45	0.73	2.8
MeCN	5470	–	–	–	–	–
PBut$_3$	5530	4020	−46.20	−43.64	0.54	1.9
P(OMe)$_3$	6570	4550	−43.33	–	0.56	–

[a] Chemical shifts are referenced to external aqueous [Co(NH$_3$)$_6$]Cl$_3$; see ref. 182 for details. See also ref. 183 for additional ^{59}Co NMR data.

[b] For R = CHCl$_2$, values for ^{59}Co NMR δ, $e^2q_{zz}Q/h$, and $[N]/[X]$ are 4560 ppm, −36.93 MHz, and 1.6, respectively.

$e^2q_{zz}Q/h$, and $[N]/[X]$ are given in Table 34; values of $[N]/[X]$ are believed to represent the relative interaction between the axial and equatorial ligands and Co.

A plot of ^{59}Co NMR chemical shift against $[N]/[X]$ is fairly linear. This series appears to reflect the electron donating ability of the axial ligands and, when comparison is possible, the data are consistent with information generally available by other spectroscopic techniques. The strong dependence of the ^{59}Co NMR chemical shifts on a neutral ligand is not characteristic of other spectroscopic techniques. It is unfortunate that so little ^{59}Co NMR data is available. The NQR data set, when it was published, was the most extensive data set of its type ever assembled [182].

Other references to ^{59}Co NMR of related compounds may be found in a recent review [105].

Electron spectra

Spectrophotometric data have been obtained for a series of $LCo(DH)_2R$ complexes where L is an N, O, P, As, or Sb donor ligand (Table 35) [184]. Low-energy absorptions between 400 and 500 nm for organocobaloximes were designated as the Co–C charge transfer (CT) ($\sigma_2 + \sigma_3$) transitions based on extended, self-consistent HMO calculations. The energies of these transitions are sensitive to the nature of L and to the amount of C 2*s* character. The Co–C CT transition energy is greater for an *sp* hybridized alkyl than for one with sp^3 hybridization. The transition energies for the Co–CH_3 compounds increase in the order: $L = H_2O \leqslant SbPh_3 \leqslant AsPh_3 < PPh_3 <$ py $<$ benzimidazole $\simeq$ RCN $< NH_3 <$ imidazole. The transition energies were

TABLE 35

Co–C CT transition energies for $LCo(DH)_2R$ in alcohol–water [a]

L	R = Me		R = CH_2CH_3		R = n-C_3H_7	
	λ_{max}(nm)	ϵ	λ_{max}(nm)	ϵ	λ_{max}(nm)	ϵ
Imidazole	410	1.95×10^3	405	8.3×10^2	–	–
NH_3	412.5	1.09×10^3	412	1.26×10^3	–	–
Benzimidazole	425	1.2×10^3	420	1.15×10^3	414	1.41×10^3
$PBut_3$	–	–	428	8.3×10	–	–
$C_6H_{11}CN$	425	3.18×10^2	–	–	406	4.2×10^2
Py	438	1.48×10^3	448	1.40×10^3	454	5.5×10^2
PPh_3	446	1.37×10^3	440	4.6×10^2	454	1.07×10^3
$AsPh_3$	446	8.14×10^2	456	1.14×10^3	455	1.45×10^3
$SbPh_3$	447.5	2.48×10^3	458	1.06×10^3	455	1.51×10^3
H_2O	448	1.53×10^3	456	1.38×10^3	455	1.68×10^3
2-Me–py	450	2.07×10^3	–	–	–	–

[a] See ref. 184 for further details.

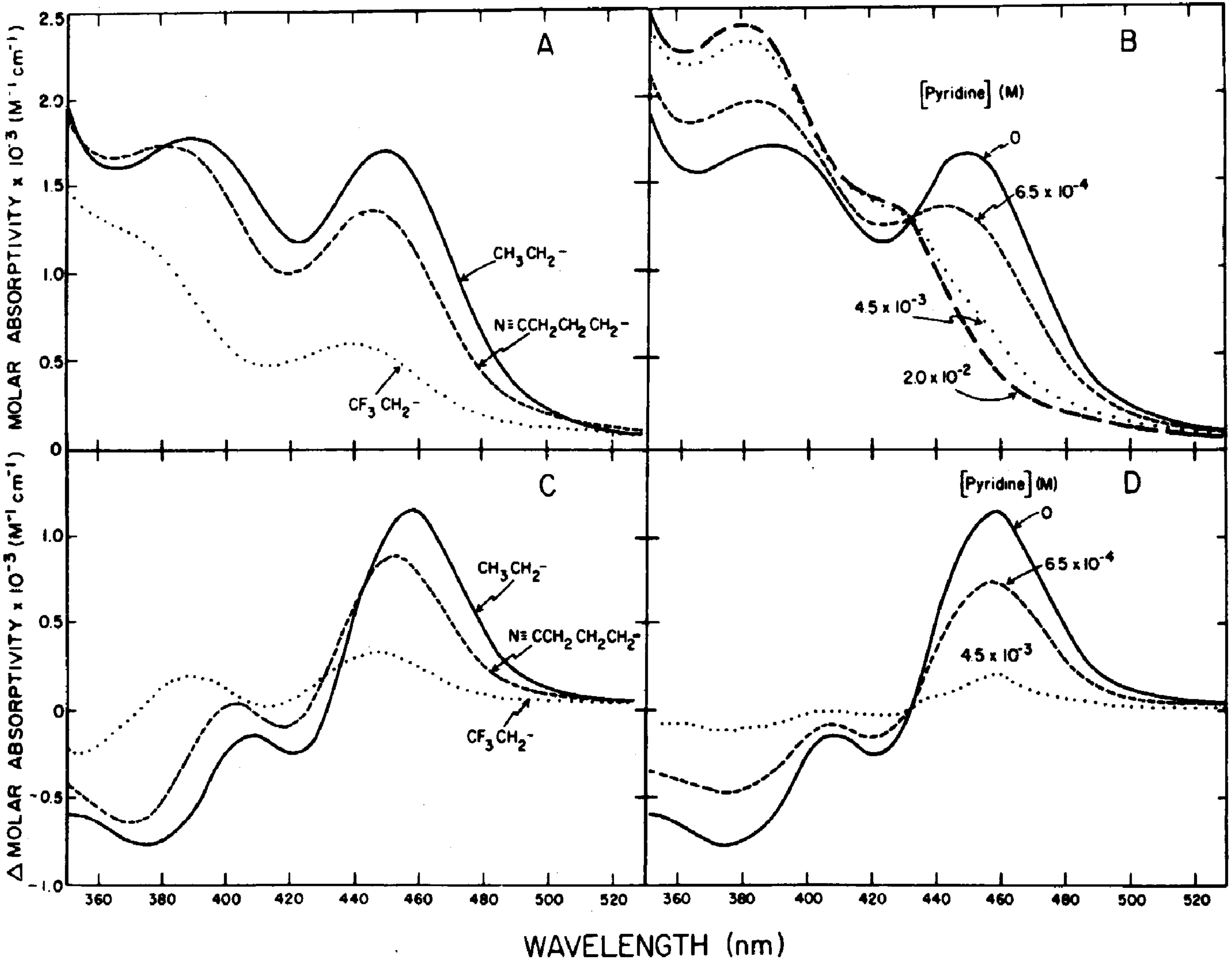

Fig. 10. Visible spectra of $H_2OCo(DH)_2R$ and $pyCo(DH)_2R$, pH = 6.5 (A) $H_2OCo(DH)_2R$, R = $CH_2CH_2CH_2CN$ (------), CH_2CF_3 (······). (B) $H_2OCo(DH)_2CH_2CH_3$ with added py: [py] = O (——), 6.5×10^{-4} M (------), 4.5×10^{-3} M (······), 0.02 M (-- --). (C) Difference spectra for $H_2OCo(DH)_2R$ and $pyCo(DH)_2R$; R = CH_2CH_3 (——), $CH_2CH_2CH_2CN$ (------), CH_2CF_3 (······). (D) Difference spectra for $H_2OCo(DH)_2CH_2CH_3 + [py]_x - pyCo(DH)_2CH_2CH_3$; [py] as in part B. From ref. 145.

found to correlate with the rate of photolysis and, although sufficient data are not available for complete analysis, we note here that the trends in Co–C CT transition energies also seem to correlate with the leaving ability of L (Table 40).

As the electron donating ability of the axial alkyl ligand increases, the Co–C CT band generally moves to longer wavelengths. However, there are some irregularities in the trends.

A more empirical study of the electronic spectra of organocobaloximes in the 550–350 nm region was reported by K.L. Brown et al. [145]. These investigators felt that the electronic transitions were not particularly sensitive to L, especially when R contained an electron-withdrawing substituent. These workers examined the effects of ligands such as py in the spectra of $H_2OCo(DH)_2R$ in aqueous solution. The greatest change in spectra occurred when R was a good electron donor (Fig. 10). They hypothesized that, in aqueous solution, a solvated pentacoordinate species "$Co(DH)_2R$" was present and that it was converted to a six-coordinate species by added L. This change in coordination number accounted for spectral changes, particularly a decrease in intensity of the larger energy transition (Tables 36 and 37). When R contained electron-withdrawing constituents, the percentage of the "$Co(DH)_2R$" form was small and hence spectral changes on adding pyridine were smaller.

These workers also observed small shifts and intensity changes in the spectra of $H_2OCo(DH)_2R$ with clearly defined isosbestic points as a function of temperature (Fig. 11). Such changes are consistent with a $6 \rightleftarrows 5$

TABLE 36

Electronic absorption spectral properties for $H_2OCo(DH)_2R$ [a]

	σ^* [b]	λ_1 (nm)	$\epsilon_1 \times 10^{-3}$ ($M^{-1} cm^{-1}$)	λ_2 (nm)	$\epsilon_2 \times 10^{-3}$ ($M^{-1} cm^{-1}$)	λ_3 (nm)	$\epsilon_3 \times 10^{-4}$ ($M^{-1} cm^{-1}$)
i-C_3H_7	−0.19	462.5	1.43	390	1.94	231	2.76
CH_2CH_3	−0.10	451	1.69	390	1.76	224	2.83
Me	0	440	1.43	384.5	1.69	223.5	2.18
$CH_2CH_2C_6H_5$	+0.08	448.5	1.48	384	1.80	233	3.28
$(CH_2)_3CN$	+0.17	446	1.35	382	1.74	227	2.62
CH_2CH_2OMe	+0.19	444	1.18	378	1.65	228	2.44
CH=CHMe	+0.36	442	0.964	380	1.16	220	2.32
CH_2I	+0.85	441	0.825	–	–	236	2.49
CH_2CF_3	+0.92	439	0.587	365	1.29	234.5	2.31
CH_2Cl	+1.05	435	0.875	365	1.67	233	2.52
CH_2CN	+1.30	447.5	0.469	370	1.04	235.5	2.26

[a] Aqueous solution, pH 6.5; see ref. 145 for further details. [b] Ref. 150.

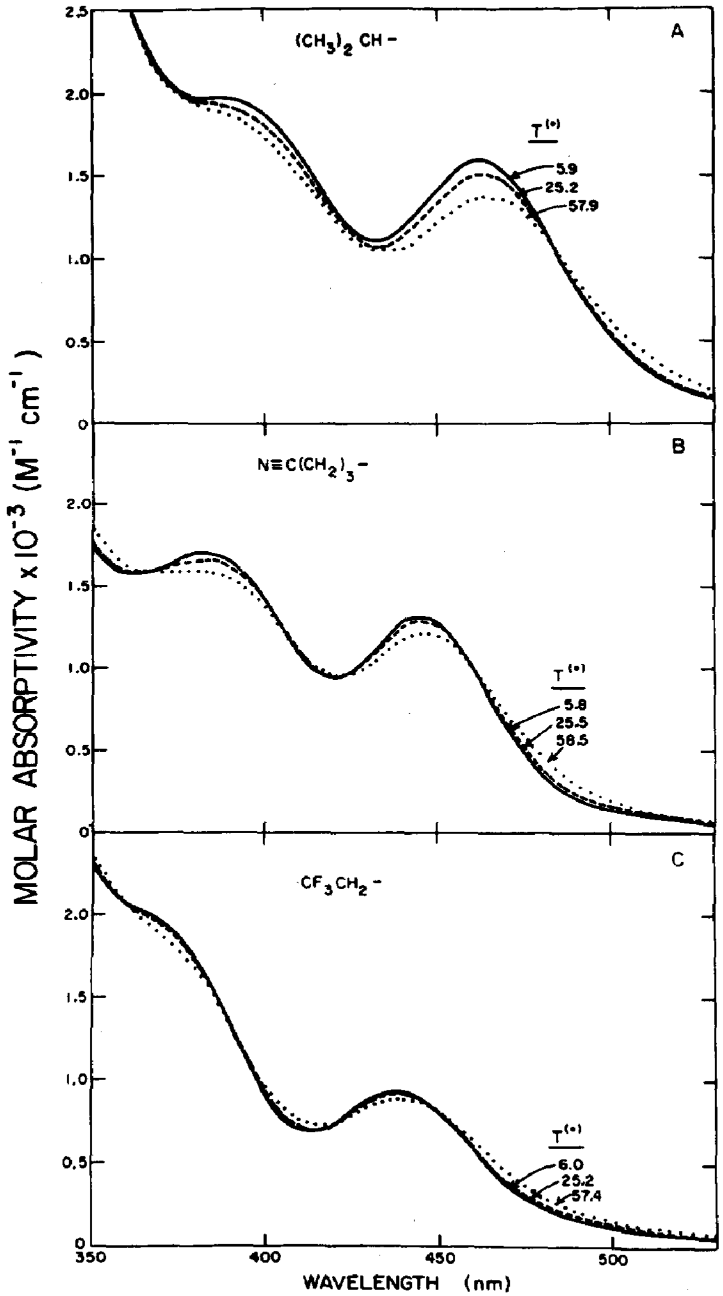

Fig. 11. Temperature dependence of the visible spectra of $H_2OCo(DH)_2R$, pH = 6.5: (A) i-C_3H_7, 5.9° (———), 25.2° (------), 57.9° (······); (B) $CH_2CH_2CH_2CN$, 5.8° (———), 25.5° (------), 58.5° (······); (C) CH_2CF_3, 6.0° (———), 25.2° (------), 57.4° (······). From ref. 145.

coordinate equilibrium since the changes were largest when R was a good electron donor. Attempts to measure the reaction rate by T-jump (temperature-jump) methods were not successful. A lower limit for $k = k_1 + k_{-1}$ of

TABLE 37

Electronic absorption spectral properties for $pyCo(DH)_2R$ [a]

R	σ^* [b]	λ_1 (nm)	$\epsilon_1 \times 10^{-3}$ ($M^{-1} cm^{-1}$)	λ_2 (nm)	$\epsilon_2 \times 10^{-3}$ ($M^{-1} cm^{-1}$)
$i\text{-}C_3H_7$	−0.19	430	1.48	375	3.06
CH_2CH_3	−0.10	420	1.42	379	2.42
Me	0	415	1.12	375	2.16
$(CH_2)_3CN$	+0.17	417	1.10	372.5	2.32
CH_2CH_2OMe	+0.19	415	0.910	368	2.14
CH=CHMe	+0.36	411	0.882	365	1.61
CH_2I	+0.85	419	0.700	–	–
CH_2CF_3	+0.92	415	0.434	355	1.63
CH_2Cl	+1.05	410	0.670	352	2.24
CH_2CN	+1.30	420	0.360	370	1.03

[a] Aqueous solution; ref. 145. [b] Ref. 150.

~ 2×10^5 s^{-1} was suggested. In this same study, electronic spectra were used to assign the deprotonation site of $H_2OCo(DH)_2R$ to the axial H_2O.

Ingraham and co-workers carried out an interesting and informative study of the effects of temperature on the electronic spectra of alkyl cobaloximes in benzene [185]. The spectrum of $pyCo(DH)_2CH_3$ is T dependent but is not influenced significantly by solutions containing as much as 70% pyridine. Thus a $6 \rightleftarrows 5$ coordinate equilibrium (or dimer formation) is clearly ruled out as a basis for the spectral changes in this solvent.

After considering several explanations, these workers suggested that long bond-length isomers existed, in which the length of the Co–N(py) bond was the principal difference between the isomers. The T dependence of $H_2OCo(DH)_2CH_3$ in water was also attributed to the existence of bond-length isomers. Movement of the Co out of the 4-N plane of the $(DH)_2$ groups was excluded by considering the effects of changing R to CH_2CH_3 and $i\text{-}C_3H_7$, when no trends were observed. Based on arguments too complex to reproduce here, the percentage of the long-bond isomer of $pyCo(DH)_2CH_3$ was estimated to be ~ 1% at 25°C in benzene.

IR spectra

Much less work has been done with IR spectroscopy. In one study [186] (Table 38) the cyanide stretching frequencies were reported for a series of complexes of the type $AsPh_4[RCo(DH)_2CN]$. The stretching frequency increases with the electronegativity of the α-carbon of R. Some related data are available for Co corrins [187].

TABLE 38

Cyanide stretching frequencies (cm^{-1}) of $[RCo(DH)_2CN]AsPh_4$ [a]

R	$\nu(\pm 1\ cm^{-1})$	R	$\nu(\pm 1\ cm^{-1})$
n-C_8H_{17}	2109	$CH_2{=}CH$	2118
2-C_8H_{17}	2110	*trans*-PhCH=CH	2119
c-C_6H_{11}	2109	*cis*-PhCH=CH	2119
Me	2112	$CH_2{=}CPh$	2120
$PhCH_2$	2112	PhC≡C	2130
3-$MeOC_6H_4CH_2$	2114	NC	2130
$CH_2{=}CMe$	2117	Me(CO)NC	2134

[a] See ref. 186 for further details.

Kinetic studies

Rate and mechanistic studies on cobaloximes have been very extensive. It will not be possible to review all such studies in depth. This review will focus on substitution reactions of organometallic compounds in non-coordinating solvents. Since extensive information is available on organometallic compounds in coordinating solvents, much of this work, which is largely due to K.L. Brown [145,146,188], will be reviewed to some extent. However, we will try to be complete in our discussion of studies which have employed non-coordinating solvents. We will also review in less detail rate studies of other types of reactions where extensive series have been examined.

Substitution reactions

Non-organometallic compounds. Aspects of this subject have been reviewed recently in this journal [110]. Coordinating solvents are usually employed. Complexes of some good *trans* effect ligands, SO_2R and $R_2P(O)$, have been studied in non-coordinating solvents but are included below in discussions of organometallic compounds since the behavior of such compounds is similar to the complexes with X = R.

A detailed study of the aquation of $pyCo(DH)_2Cl$ and $NH_3Co(DH)_2Cl$ has appeared [134]. These compounds aquate via three processes which are zero, first, and second order with respect to $[OH^-]$. The zero-order process is normal aquation. The first-order process is the hydrolysis of the monoanion $LCo(DH)(D)Cl^-$. The nature of the second-order process is less clear but most likely involves $LCo(D)_2Cl^{2-}$. Pyridine is also lost at very high pH. This recently reported study covers an extensive pH range and earlier studies [189,190] employing smaller pH ranges were discussed [134].

Halpern and co-workers [133] have investigated the first-order OH^--catalyzed reactions of $Co(DH)_2XY^-$ ($X = $ or $\neq Y$) and could not distinguish between several possible mechanisms. No competition for a five-coordinate species could be detected when the competitor NO_2^- was present. Using T-jump methods, the rates of O–H–O deprotonation by $OH^-(k_1)$ and subsequent reprotonation by H_2O (k_{-1}) were measured (Table 18) for several anionic complexes and the cation, $Co(DH)_2(NH_3)_2^+$. The values of k_1, k_{-1}, and hence $K=(k_1/k_{-1})$ changed in the expected direction with change in charge.

Hague and Halpern have studied anation reactions of $H_2OCo(DH)_2X$ (X = I, NO_2) by various anions [191]. They found the *trans* effect of the coordinated anions to be small, whereas Wilmarth has reported a large *trans* effect for SO_3 in $H_2OCo(DH)_2SO_3^-$ [192]. More recent work by Deutsch [193,194] has allowed a correlation of the relative *trans* effect for various X ligands in studies using either CH_3OH [193,194] or H_2O [146,191,195,196] as the solvent. Although differences in conditions and the failure of the weak *trans* labilizers to yield limiting first-order conditions complicate an extensive comparison, the order of *trans* labilizing ability appears to be $CH_3(900) > C_6H_5(300) > SO_3(100) > (CH_3O)_2PO(50) \gg CH_3C_6H_4SO_2(1) \gg I \sim NO_2$ [193,194].

In a typical non-coordinating solvent, such as CH_2Cl_2 and C_6H_6, complexes where X is Cl, Br, SCN, etc., readily undergo ligand exchange. The net overall reaction appears to be a substitution process but it is inhibited by strong oxidizing agents ($BrCCl_3$) and accelerated by $LCo(II)(DH)_2$ complexes [197]. An investigation [197] of the reaction revealed that it proceeds by inner-sphere electron transfer according to the following mechanism ($(DH)_2$ assumed):

$$\begin{array}{l} L' + LCo(II) \rightarrow L'Co(II) + L \\ \underline{L'Co(II) + XCo(III)L \rightarrow L'Co(III)X + LCo(II)} \\ \qquad L' + XCo(III)L \rightarrow L'Co(III)X + L \end{array}$$

The reaction is the major pathway for substitution when X is a good bridging ligand, since trace amounts of Co(II) are usually present in most preparations. Failure to recognize the potential role of Co(II) in cobaloxime chemistry has often led to incorrectly interpreted or irreproducible results [198]. When X is SCN, the electron-transfer pathway is responsible for N to S bonded SCN equilibration [198–200]. It has been shown that $LCo(DH)_2SCN$ can form either $L'Co(DH)_2SCN$ or $L'Co(DH)_2NCS$, depending on whether the Co(II) catalyst attacks the S (adjacent attack) or the N (remote attack) of the SCN bridging ligand [199]. The rates of bridging electron-transfer reactions have not been studied in detail, however.

In general, except where the Co(II)-catalyzed pathway is favorable, substitution processes of $LCo(DH)_2X$ complexes where X is a weak *trans* labilizer involve loss of X unless L is a weak ligand such as H_2O or CH_3OH.

The *trans* effect of L on X solvolysis in DMSO varies by ~100 on comparing L = NH_3 (~ 6 × 10^{-6} s^{-1}) with L = the S donor $NH_2C(S)NHNH_2$ (~ 5 × 10^{-4} s^{-1}) [110]. Costa and co-workers [201] have compared the *trans* labilizing effect of R_3P with $PhNH_2$ derivatives. The P donors are about ten times more labilizing, and the labilizing effect increases with both R_3P basicity and steric size when promoting the solvolysis of a *trans* Cl in a CH_3OH/30% H_2O solution.

Organometallic compounds:

Non-coordinating solvents. There is some controversy surrounding the ligand exchange reactions of organometallic cobaloximes. Although initial studies involved coordinating solvents such as H_2O, we will begin our discussion with non-coordinating solvents, where less controversy exists. In almost all cases, the consensus of investigators has been that the ligand exchange process is dissociative, with the following primary mechanism in effect ($(DH)_2$ assumed):

$$\mathrm{LCoR} \underset{k_{-1}}{\overset{k_1}{\rightleftharpoons}} \mathrm{CoR} + \mathrm{L}$$

$$\mathrm{CoR} + \mathrm{L}' \xrightarrow{k_2} \mathrm{L'CoR}$$

$$\overline{\mathrm{LCoR} + \mathrm{L}' \rightarrow \mathrm{L'CoR} + \mathrm{L}}$$

The rate-determining step is the dissociative first step indicated by k_1 in the mechanism, and $k_{obs} = k_1$. The five-coordinate CoR intermediate then reacts with excess L′ to produce the final product.

Evidence for this mechanism in non-coordinating solvents came initially from dynamic NMR studies by T.L. Brown [160,202–204] and later from stopped-flow spectrophotometric studies in the laboratories of one of the present authors [61,81,205,206]. The dynamic NMR studies demonstrated that ligand exchange reaction rates in non-coordinating solvents were independent of non-coordinated (hence entering) ligand concentration. However, dynamic NMR studies are usually limited to cases where the resonances of a group in the ligand can be resolved for free and coordinated ligand environments and then merged by changes in temperature. This method is time consuming, is limited to a case where the leaving and entering ligand are identical, and usually leads to rates obtained with different solvents and at different temperatures.

Consequently, the most extensive data have been obtained by conventional spectrophotometric methods, often with a stopped-flow instrument [61,81,205,206]. These methods have the additional advantage over dynamic NMR methods that the entering and leaving ligand are not identical.

Therefore, mass-law rate retardation studies, in which excess leaving ligand is added, are possible. Analysis of this situation leads to a rate expression such that

$$\frac{1}{k_{\mathrm{obs}}} = \frac{k_{-1}[\mathrm{L}]}{k_1 k_2[\mathrm{L}']} + \frac{1}{k_1}$$

From this experiment, the ratio k_{-1}/k_2 can be obtained. This competition ratio in effect gives the relative reactivity of the five-coordinate species towards L and L′.

An additional advantage of being able to vary the entering ligand is that a true S_N1 LIM reaction should be independent of both the nature and concentration of the entering ligand; this was indeed found. For non-bulky ligands, which lack H-bonding functionalities such as $-NH_2$ groups, the value obtained for k_{-1}/k_2 is essentially unity for a very wide variety of ligands [207]. This finding requires that the five-coordinate intermediate be very reactive for cobaloximes, in contrast with the analysis of ligand exchange processes in water, where evidence has been presented that a solvated five-coordinate species is stable [145,188]. It has been suggested that solvent H_2O must interact with cobaloximes in such a way as to stabilize the five-coordinate species while not binding directly to Co.

The ligand exchange rates, k_{obs}, for many different X ligands and for a variety of leaving ligands are given in Tables 39, 40 and 41. In general, as R or X electron-donating ability increases, the rate of ligand dissociation also increases [211]. As the basicity of the leaving ligand decreases, the rates of dissociation increase. As the steric bulk of the leaving ligand increases, the rate of dissociation increases. These trends are as expected and will be quantitatively treated in a later section. It should be noted that there is no apparent deviation in the relative leaving ability of a given ligand with changes in the *trans*-effect X ligand. Thus, for any given two L leaving ligands, a plot of k_{obs} vs. k_{obs} for many different X tends to be linear. Studies of complexes where the bulk of L or R has been systematically changed have not been reported.

Thus, just as spectroscopic trends for $\mathrm{LCo(DH)_2X}$ series do not appear to depend on L in most cases, the relative *trans* effect of X does not seem to depend on L. Cross-comparison of kinetic or spectroscopic and structural data will be found in section C.

Organometallic compounds:

Coordinating solvents. Kallen and K.L. Brown have carried out extensive studies of kinetic and equilibrium processes involving alkylcobaloximes in aqueous solutions [146,195]. The work has been extended by K.L. Brown [145,188]. In contrast to the studies in non-coordinating solvents, studies in

TABLE 39

Kinetic parameters for dissociation of L from $LCo(DH)_2Me$ [a]

L	T (°C)	Solvent	k (s^{-1})	E_a (kcal mol^{-1})	$\Delta H^{\neq}$ (kcal mol^{-1})	$\Delta G^{\neq}$ (kcal mol^{-1})	$\Delta S^{\neq}$ (cal mol^{-1} K^{-1})
$P(OMe)_3$	100	C_6H_5Br [b]	20.4 ± 3	22.9 ± 3	22.1 ± 3	19.8 ± 0.1	6.3 ± 3
$P(OMe)_3$	100	$C_6H_5NO_2$ [b]	11.9 ± 2	24.0 ± 3	23.3 ± 3	20.2 ± 0.1	8.4 ± 4
3-Fluoropyridine	130	$C_6H_5NO_2$	874 ± 400	23.0 ± 3	22.2 ± 3	18.4 ± 0.4	9.3 ± 8
1-(1-Trifluoromethylphenyl)-imidazole	130	$C_6H_5NO_2$	26.1 ± 5	27.9 ± 3	27.1 ± 3	21.2 ± 0.1	14.6 ± 7

[a] See ref. 202 for further details. [b] See ref. 204 for additional solvents.

TABLE 40

Pseudo first-order rate constants (s^{-1}) for the dissociation of L from $LCo(DH)_2X$ by $PBut_3$, X = Me, $i\text{-}C_3H_7$ [a]

L	Me	$i\text{-}C_3H_7$
2-Me–py	$1.5\pm0.2\times10^{2}$ [b]	–
$2\text{-}NH_2\text{-}py$	3.5 ± 0.1 [b]	–
$P(OC_6H_5)_3$	2.3 ± 0.3	–
9-Methyladenine	1.6 ± 0.1	7.9×10^{2} [e]
Aniline	1.5 ± 0.1 [c]	–
$P(OC_6H_4\text{-}p\text{-}Me)_3$ [e]	9.0×10^{-1}	–
$P(C_6H_{11})_3$	$3.8\pm0.3\times10^{-1}$	–
3-Benzyladenine	$2.6\pm0.2\times10^{-1}$	$3.1\pm0.3\times10^{1}$
$P(i\text{-}C_3H_7)_3$	$1.6\pm0.1\times10^{-1}$	–
$PBut_3Co(DH)_2C_5H_4N$ [e]	1.4×10^{-1}	–
$P(OCH_2CH_2Cl)_3$	$5.2\pm0.4\times10^{-2}$	–
$P(OCH_2)_3CMe$	$5.0\pm0.4\times10^{-2}$	–
PPh_3	$4.5\pm0.1\times10^{-2}$ [c]	$3.9\pm0.2\times10^{1}$ [c]
4-CN–py	$4.1\pm0.3\times10^{-2}$ [b]	$2.7\pm0.3\times10^{1}$ [c]
3-Ethoxycarbonyl-methyladenine	$3.7\pm0.4\times10^{-2}$	$2.5\pm0.2\times10^{1}$
Thiazole	$3.5\pm0.1\times10^{-2}$	$3.1\pm0.4\times10^{1}$
Quinuclidine	$1.6\pm0.1\times10^{-2}$	$1.8\pm0.2\times10^{1}$
$1,2\text{-}Me_2\text{-imidazole}$	$1.1\pm0.1\times10^{-2}$	$1.1\pm0.1\times10^{1}$
Py	$8.0\pm0.8\times10^{-3}$	3.0 ± 0.2
$P(OMe)_3$	$4.1\pm0.2\times10^{-3}$	3.3 ± 0.3
$P(CH_2CH_2CN)_3$	$2.8\pm0.1\times10^{-3}$	–
4-tBut–py	$1.3\pm0.1\times10^{-3}$ [d]	$8.6\pm0.5\times10^{-1}$
$PPh_2(OMe)$	$7.7\pm0.5\times10^{-4}$	–
$4\text{-}(CH_3)_2N\text{-}py$	$4.4\pm0.3\times10^{-4}$	$1.6\pm0.1\times10^{-1}$
1-Me–imidazole	$2.5\pm0.2\times10^{-4}$	$1.2\pm0.1\times10^{-1}$
PPh_2Et	$1.1\pm0.1\times10^{-4}$	$7.3\pm0.4\times10^{-2}$

[a] CH_2Cl_2, 25°C; ref. 209, unless otherwise noted. [b] Ref. 81. [c] Ref. 175. [d] Ref. 206. [e] Ref. 210.

aqueous solutions are complicated both by the intermediacy of the solvated species and by acid–base equilibria. The deprotonation of the equatorial $(DH)_2$ system of cobaloximes has been discussed above. The existence of such equilibria can provide an opportunity to assess the effect of charge on rates and equilibrium constants.

After an initial study of the ligation of $H_2OCo(DH)_2CH_3$ with thiols [195], K.L. Brown et al. examined the ligation by primary amines, 4-substituted pyridines (Table 42) and thiolate anions. The reactions are second order, in contrast to the simpler first-order process that occurs in non-coordinating solvents. The ranges of rate constants for ligation (k_{on}) were 4.3–7.5 (RNH_2), 12.8–27.3 (RS), 49.6–55.2 (RSH), and 92–200 M^{-1} s^{-1} (4-X–py). The dependence of the ligation rates on ligand and ligand concentration undoubtedly arises from the solvation of the ligand by water and competition of the incoming ligand and water for the five-coordinate intermediate formed in the dissociation step. The data for 4-X–py are given in Table 42. Also given in this Table are rate constants for ligand dissociation (k_{off}), the formation constant (K_{f}), $-\log$ acid dissociation constant ($\mathrm{p}K'_{\mathrm{c-L}}$), some relevant constants for the deprotonated complex, and the acid dissociation constant for 4-X–pyH$^+$($\mathrm{p}K'_{\mathrm{L}}$). The deprotonated complex undergoes exchange reactions about an order of magnitude more rapidly than the neutral complex, whereas $K_{\mathrm{f}} > K'_{\mathrm{f}}$. The formation constants increase with ligand basicity and the O–H–O functionality becomes less acidic.

In later studies, the series pyCo(DH)$_2$R (Table 19) and DEACo(DH)$_2$R (Table 43) (DEA = dimethoxyethylamine) were examined to ascertain the influence of changing R [145,188]. The constants given in Tables 19 and 43 are those defined above, and $\mathrm{p}K'_{\mathrm{c2}}$ is the $-\log$ of the axial H_2O acid dissociation constant for $H_2OCo(DH)_2R$ (but see below) and K_{cw} is defined in eqn. (1).

$$H_2OCo(DH)_2R \overset{K_{cw}}{\rightleftarrows} \text{“}Co(DH)_2R\text{”} \qquad (1)$$

The postulated existence of the “Co(DH)$_2$R” species which is suggested by K.L. Brown et al. to be a solvated five-coordinate species is currently somewhat controversial. We will discuss some of the other data in Tables 19 and 43 in the following section on equilibrium data. In general, the rates of ligand dissociation from LCo(DH)$_2$R where L is an N donor or H_2O in coordinating solvents increases with the electron-donating ability of R, as found in the less complicated situation in non-coordinating solvents.

An additional complication of studies using coordinating solvents is the observation by Espenson [212] that substitution of $H_2OCo(DH)_2CH_2CH_3$ by $M(CN)_6^{n-}$ involves prior association. More recently [213], prior association was found for substitution of $H_2OCo(DH)_2R$ (R = Me, CH_2Cl, CH_2CF_3) by NH_3 as well as for other amines but not SCN^- when R is CH_2Cl. The solvated “Co(DH)$_2$R” species was ruled out as an explanation of the results. However, no very good electron-donating R ligands were employed.

The authors [213] supported a previous suggestion by Darensbourg [214] that the equilibrium species consists of a Lewis base, hydrogen-bonded to one of the oxime O–H–O protons. However, since all the entering ligands exhibiting a prior equilibrium are H bond donors, it is also possible that the interaction may involve H donation from the entering ligand to one of the oxime oxygens as was observed in the solid state for complexes containing L = 2-NH$_2$–py [81]. More recently [215], the same group reported the substitution of water in $H_2OCo(DH)_2R$ by NH_3 as a function of pH in aqueous solution and found that the rate of substitution (k'_{on}) is similar to

TABLE 41

Pseudo first-order rate constants (s^{-1}) for the dissociation of L from $LCo(DH)_2X$ (CH_2Cl_2, 25°C) [a]

X	4-CN–py [b]	PPh_3 [c]	$P(OMe)_3$ [b]	1-N-Me-- imidazole [b]	$P(Et)Ph_2$ [b]	$2\text{-}NH_2\text{–py}$ [e]	4-tBu–py [d]
CH_2CN	$3.0\pm0.3\times10^{-5}$ [f]	$2.4\pm0.3\times10^{-5}$	–	–	–	–	–
$p\text{-}SO_2C_6H_4CH_3$	$2.0\pm0.4\times10^{-4}$ [d]	–	–	–	–	–	–
$CHBr_2$	$5.2\pm0.3\times10^{-4}$ [d]	–	$6.1\pm0.6\times10^{-5}$	–	–	–	–
$CHCl_2$	–	–	$1.7\pm0.3\times10^{-4}$	–	–	–	–
$SCPh_3$	–	$7.6\pm0.7\times10^{-4}$ [d]	–	–	–	–	–
CH_2CF_3	$2.7\pm0.2\times10^{-4}$ [e]	$8.3\pm0.3\times10^{-4}$	–	–	–	$2.4\pm0.1\times10^{-2}$	–
CH_2I	$1.6\pm0.3\times10^{-3}$	–	–	–	–	–	–
CH_2Br	$2.6\pm0.1\times10^{-3}$ [e]	$3.8\pm0.1\times10^{-3}$	$2.3\pm0.4\times10^{-4}$	$6.5\pm0.4\times10^{-6}$	$2.9\pm0.2\times10^{-6}$	$1.5\pm0.1\times10^{-1}$	–
CH_2Cl	$3.1\pm0.1\times10^{-3}$	–	$2.2\pm0.3\times10^{-4}$	–	–	–	–
$p\text{-}C_6H_4Br$	$1.0\pm0.1\times10^{-2}$ [d]	–	–	–	–	–	–
$P(O)(OMe)_2$	$1.0\pm0.1\times10^{-2}$ [d]	$2.6\pm0.3\times10^{-2}$ [d]	–	–	–	–	2.7×10^{-4}
$p\text{-}C_6H_4OCH_3$	$1.6\pm0.3\times10^{-2}$ [d]	–	–	–	–	–	–
$CH{=}CH_2$	$1.7\pm0.1\times10^{-2}$	–	–	$8.1\pm0.6\times10^{-5}$	$3.6\pm0.2\times10^{-5}$	–	–
C_6H_5	$2.9\pm0.6\times10^{-2}$ [d]	$7.4\pm0.4\times10^{-2}$ [d]	–	–	–	–	–
$(CH_2)_3CN$	$3.1\pm0.3\times10^{-2}$	–	$9.0\pm0.8\times10^{-3}$	–	–	–	–
Me	$4.1\pm0.3\times10^{-2}$ [e]	$4.5\pm0.2\times10^{-2}$	$4.1\pm0.2\times10^{-3}$	$2.5\pm0.2\times10^{-4}$	$1.1\pm0.1\times10^{-4}$	3.5 ± 0.1	$1.3\pm0.1\times10^{-3}$
$P(O)(OMe)\text{-}(C_6H_5)$	–	–	–	–	–	–	3.3×10^{-3}

$P(O)(C_6H_5)_2$	–	–	–	–	–	–	3.6×10^{-3}
$CH_2C_6H_4$- *p*-CN	$4.5\pm0.3\times10^{-2}$ [d]	–	–	–	–	–	–
CH_2SiMe_3	$4.3\pm0.6\times10^{-1}$	–	$2.4\pm0.3\times10^{-2}$	$1.1\pm0.1\times10^{-3}$	$6.6\pm0.4\times10^{-4}$	–	–
$CH_2C_6H_5$	$3.3\pm0.7\times10^{-1}$	–	$8.9\pm0.4\times10^{-3}$	–	–	–	–
CH_2CH_3	$9.6\pm0.1\times10^{-1}$ [e]	1.4 ± 0.1	$8.6\pm0.7\times10^{-2}$	$6.3\pm0.5\times10^{-3}$	$2.1\pm0.1\times10^{-3}$	$5.8\pm0.3\times10^{1}$	$4.0\pm0.2\times10^{-2}$
$CH_2CH_2CH_3$	1.2 ± 0.1	–	–	–	–	–	–
$CH_2C(Me)$- $(COOEt)_2$	$3.4\pm0.1\times10^{-1}$ [f]	1.5 ± 0.1	–	–	–	$2.7\pm0.1\times10^{1}$ [f]	–
CH_2CHMe_2	1.4 ± 0.1 [e]	–	$1.9\pm0.3\times10^{-1}$	$1.0\pm0.1\times10^{-2}$	–	$1.0\pm0.1\times10^{2}$	–
CH_2CMe_3	$1.1\pm0.1\times10^{1}$ [f]	$3.4\pm0.1\times10^{1}$	–	$5.3\pm0.4\times10^{-2}$	$4.0\pm0.3\times10^{-2}$	–	–
$c\text{-}C_5H_9$	$1.4\pm0.1\times10^{1}$	–	–	–	–	–	–
$i\text{-}C_3H_7$	$2.7\pm0.3\times10^{1}$ [f]	$6.1\pm0.6\times10^{1}$	2.3 ± 0.3	$1.6\pm0.1\times10^{-1}$	$6.6\pm0.3\times10^{-2}$	–	–
$c\text{-}C_6H_{11}$	$3.9\pm0.4\times10^{1}$	–	–	–	–	–	–
CH(Me)(Et)	$4.0\pm0.2\times10^{1}$	–	–	$1.9\pm0.2\times10^{-1}$	$9.8\pm0.3\times10^{-2}$	–	–
CH(Me)- $(n\text{-}C_3H_7)$	$4.4\pm0.1\times10^{1}$	–	–	–	–	–	–
CH(Me)- $(i\text{-}C_3H_7)$	$8.3\pm0.1\times10^{1}$	–	–	–	–	–	–
$CHEt_2$	$1.0\pm0.1\times10^{2}$	–	–	–	–	–	–

---

[a] Entering ligands (except as otherwise noted): PBu_3 for L = 4-CNpy, PPh_3, 1-MeIMID; Ph_2EtP, Thiazole; 1-MeIMID for L = $P(OMe)_3$.
[b] Ref. 209, except as noted. [c] Ref. 175, except as noted. [d] Ref. 206. [e] Ref. 81. [f] Ref. 175.

TABLE 42

Rate and equilibrium data for 4-x-py ligation in 4-x-pyCo(DH)$_2$Me [a]

x	k_{on} (M^{-1} s^{-1})	k_{off} (s^{-1})	k'_{off} (s^{-1})	k'_{on} (M^{-1} s^{-1})	K_f (M^{-1})	pK'_{c-L}	K'_f (M^{-1})	pK'_L
CN	9.21×10	2.91×10^{-1}			3.29×10^2			2.24
CONH$_2$	1.17×10^2	1.56×10^{-1}			8.03×10^2			3.77
H	1.14×10^2	5.52×10^{-2}	1.63×10^{-1}	3.90×10^2	2.04×10^3	13.61	2.39×10^2	5.51
Me	1.28×10^2	4.04×10^{-2}	1.26×10^{-1}	4.46×10^1	3.25×10^3	13.65	3.54×10^2	6.36
NH$_2$	1.96×10^2	1.94×10^{-2}	1.26×10^{-1}	5.83×10^1	1.11×10^4	14.06	4.63×10^2	9.40

[a] Aqueous solution, 25°C. See text and list of abbreviations for definition of constants and ref. 146 for further details. See ref. 195 for ligation by S ligands.

TABLE 43

Rate and equilibrium data for dimethoxyethylamine (DEA) ligation in DEACo(DH)$_2$R [a]

R	σ^* [b]	K_f (M^{-1})	pK'_{c2}	K_{cw}	k_{on} (M^{-1} s^{-1})	k_{off} (s^{-1})
CHEt$_2$	−0.225	257 ± 16	13.38 ± 0.02	2.8	–	–
i-C$_3$H$_7$	−0.19	331 ± 15	13.28 ± 0.02	2.0	–	–
Et	−0.10	608 ± 42	12.97 ± 0.02	7.7×10^{-1}	$8.09 \pm 0.64 \times 10$	$1.33 \pm 0.05 \times 10^{-1}$
CH$_2$CH$_2$Ph	−0.06	714 ± 19	12.78 ± 0.02	5.1×10^{-1}	$5.11 \pm 0.17 \times 10$	$7.15 \pm 0.14 \times 10^{-2}$
Me	0.00	861 ± 20	12.68 ± 0.02	2.8×10^{-1}	5.09 ± 0.17	$5.91 \pm 0.14 \times 10^{-3}$
(CH$_2$)$_3$CN	+0.17	1060 ± 60	12.22 ± 0.02	4.8×10^{-2}	$1.30 \pm 0.08 \times 10$	$1.23 \pm 0.02 \times 10^{-2}$
CH$_2$CH$_2$OMe	+0.19	1060 ± 50	12.19 ± 0.02	3.9×10^{-2}	9.40 ± 0.59	$8.87 \pm 0.37 \times 10^{-3}$
CH$_2$CH$_2$OPh	+0.31	1130 ± 40	12.02 ± 0.08	1.1×10^{-2}	7.24 ± 0.10	$8.00 \pm 0.20 \times 10^{-3}$
CH=CHMe	+0.36	1070 ± 40	12.02 ± 0.01	6.8×10^{-3}	1.38 ± 0.02	$1.33 \pm 0.04 \times 10^{-3}$
CH$_2$CH$_2$COOMe	+0.38	1040 ± 30	11.78 ± 0.05	5.5×10^{-3}	$1.15 \pm 0.03 \times 10$	$1.21 \pm 0.05 \times 10^{-2}$
C$_6$H$_5$	+0.60	1390 ± 30	11.72 ± 0.03	5.7×10^{-4}	$6.21 \pm 0.15 \times 10^{-1}$	$4.54 \pm 0.13 \times 10^{-4}$
CH$_2$CF$_3$	+0.92	~ 2840	–	–	$2.69 \pm 0.09 \times 10^{-2}$	$9.49 \pm 0.13 \times 10^{-6}$
CH$_2$COOMe	+1.06	~ 6000	–	–	$2.71 \pm 0.10 \times 10^{-2}$	$4.57 \pm 0.03 \times 10^{-6}$

[a] Aqueous solution, pH = 8.6–10.7, 25°C. See ref. 188 for further details. [b] Polar substituent constants (ref. 150).

that reported earlier (Table 43) and they conclude that the reactions apparently proceed via an S_NCB mechanism. They suggest that in alkaline media, two counteracting effects influence substitution rates as follows: (1) substitution rates are decreased due to formation of a hydroxo species which is generally thought to be substitution inert and (2) substitution rates are increased due to formation of the conjugate base, $H_2OCo(DH)(D)R^-$. Effect (1) appears to dominate [215].

Non-substitution reactions

Co(III). Cobaloximes containing P–OMe groupings readily undergo nucleophilic attack by N donors such as pyridine or by $X^-(Br^-)$ to give a $P{=}O^-$ and methylated nucleophile [173,205,216] (Table 44). The reaction in Table 44 appears to follow the typical *trans* influence effect of X, although no $P(OMe)_3$ ligand dissociation takes place. Evidence has been presented that the reaction involves an S_N2 attack at the OMe C [216]. The increase in electron density at this C via decreased electron acceptance by $Co(DH)_2X$ as X becomes a better electron donor explains the observed trend. There is excellent correlation between the ^{13}C chemical shift of the OMe C (Table 27) and log k for the data in Table 44.

One of the most interesting sets of studies on the effects of axial ligands on rate processes has been conducted by Halpern and co-workers [217,218]. The data are summarized in Table 45. The second column in Table 45 gives the value of the equilibrium constant for the following process:

$$LCo(DH)_2CH(Me)Ph \rightleftarrows LCo(II)(DH)_2 + PhCH{=}CH_2 + 1/2H_2 \tag{2}$$

TABLE 44

Rate constants for the reaction [a] $P(OMe)_3Co(DH)_2X + (PPh_3Me)Br \rightarrow P(O)(OMe)_2Co(DH)_2X^- + MeBr + PPh_3Me^+$

X	k_{obsd} (s^{-1})	X	k_{obsd} (s^{-1})
NO_3	$2.16 \pm 0.06 \times 10^{-2}$	$CHCl_2$	$1.80 \pm 0.13 \times 10^{-5}$
Cl	$5.73 \pm 0.25 \times 10^{-3}$	CH_2CN	$1.80 \pm 0.07 \times 10^{-5}$
Br	$5.67 \pm 0.20 \times 10^{-3}$	$P(O)(OMe)_2$	$1.81 \pm 0.13 \times 10^{-5}$
I	$3.98 \pm 0.31 \times 10^{-3}$	CH_2Br	$4.16 \pm 0.21 \times 10^{-6}$
N_3	$1.89 \pm 0.09 \times 10^{-3}$	C_6H_5	$1.77 \pm 0.09 \times 10^{-6}$
NO_2	$2.50 \pm 0.13 \times 10^{-3}$	Me	$4.75 \pm 0.66 \times 10^{-7}$
CN	$6.98 \pm 0.39 \times 10^{-4}$	i-C_3H_7	$5.63 \pm 0.61 \times 10^{-7}$
SO_2PhMe	$4.89 \pm 0.30 \times 10^{-4}$	CH_2CH_3	$2.20 \pm 0.11 \times 10^{-7}$
$CHBr_2$	$4.55 \pm 0.23 \times 10^{-5}$		

[a] At 31.5±0.5°C, CH_2Cl_2, 0.6 M $(PPh_3Me)Br$, and [Co] = 0.05 M. See ref. 173 for further details.

TABLE 45

Summary of equilibrium and kinetic data for the thermal decomposition of $LCo(DH)_2CH(Me)Ph$[a]

L	10^6K_1 (25°C)($M^{3/2}$)	ΔH^0 (kcal mol^{-1})	ΔS^0 (cal mol^{-1} K^{-1})	D_{Co-R} (kcal mol^{-1})	10^4k_1 (25°C)(s^{-1})	$\Delta H_1^{\neq}$ (kcal mol^{-1})	$\Delta S_1^{\neq}$ (cal mol^{-1} K^{-1})
4-NH_2-py	5.5	23.4	54.3	21.2	4.0	23.1	3.8
4-Me-py	13.6	22.3	52.5	20.1	6.0	21.8	0.9
Py	19.5	21.7	52.1	19.5	7.3	21.6	−0.2
4-CN-py	47.2	20.1	47.5	17.9	13.1	20.1	−3.9
Imidazole	4.0	23.0	52.5	20.8	1.7	23.0	1.9
$P(Me)_2Ph$	–	–	–	24.0	1	25.9	10.5
$PBut_3$	–	–	–	21.0	12	22.8	5.1
$P(Me)Ph_2$	–	–	–	–	14	–	–
$P(CH_2CH_2CN)_3$	–	–	–	20.0	31	22.1	4.5
$P(Et)Ph_2$	–	–	–	19.0	33	21.3	1.9
PPh_3	–	–	–	17.0	192	19.3	−1.4
$PChx_3$	–	–	–	–	4800[b]	–	–

[a] In acetone. See refs. 217, 218 for details. [b] Estimated value.

The next two columns give the thermodynamic parameters for this process. The fifth column gives the calculated Co–C bond dissociation energy for reaction (3) for N donor ligands calculated from a thermodynamic cycle.

$$LCo(DH)_2CH(Me)Ph \rightarrow LCo(II)(DH)_2 + CH(Me)Ph \qquad (3)$$

For P donor ligand complexes in Table 45, the D_{Co-R} were estimated from the T dependence of the forward rate constant for reaction (2). The rate constant and kinetic activation parameters for both N and P donor ligand complexes are given in the last three columns of Table 45. The values of D_{Co-R} for N donor ligand complexes estimated by the kinetic method (not shown) agree well with the values obtained using the thermodynamic method.

It is of some interest that, for N donors, the strength of the Co–C bond increases with increasing electron donation by L. This effect is opposite to that found for halogen abstraction reactions (8), which are discussed below, and is consistent with stabilization of the Co(III) oxidation state in preference to the Co(II) oxidation state by good electron donors. The relationship of D_{Co-R} to the properties of L is apparently different for P donor ligands. Here, the electron donating ability of L is secondary to steric size. Bulky L ligands promote Co–C bond cleavage. It is interesting that Co–C bond lengths for complexes with *trans* P donor ligands are longer than those for complexes with N donor ligands (Tables 11 and 12). This point will be considered in further detail below. There is some electronic effect of P donor ligands since D_{Co-R} is estimated to be somewhat higher for the $PBut_3$ complex than for the complex with the sterically similar but more weakly electron-donating phosphine $P(CH_2CH_2CN)_3$.

Schrauzer and co-workers have found that the rate constant for photodealkylation of alkylcobaloximes depends on the energy and intensity of the electronic transition assigned to Co–C charge transfer [184] (Table 46).

TABLE 46

Pseudo first-order rate constants and quantum yields for aerobic photolysis of $LCo(DH)_2R$ in water [a]

L	R = Me k (s^{-1})	R = CH_2CH_3 k_1 (s^{-1})
CN^-	2.3×10^{-4}	1.22×10^{-3}
Imidazole	2.3×10^{-4}	1.0×10^{-3}
NH_3	4.7×10^{-4}	7.2×10^{-4}
Py	1.67×10^{-3}	3.5×10^{-3}
Benzimidazole	1.72×10^{-3}	4.4×10^{-3}
H_2O	2.1×10^{-3}	5.8×10^{-3}

[a] Ref. 184.

These spectral characteristics in turn appear to reflect the strength of the L to Co bond. The CH_2CH_3 derivative is photolyzed more readily than the Me derivative.

Adin and Espenson [219] examined the alkylation of Hg^{2+} by $H_2OCo(DH)_2R$ under aqueous acidic conditions, thus:

$$H_2OCo(DH)_2R + Hg^{2+} + H_2O \xrightarrow{k_1} RHg^{+} + H_2OCo(DH)_2H_2O^{+} \qquad (4)$$

The reactive complex is actually $H_2OCo(DH)(DH_2)R^+$ where one of the –O–H–O– groups has been protonated to –OH HO–. A concurrent study by Halpern's group, reported later, confirmed the alkylation studies and extended them to arylation and benzylation of Hg^{2+}. This more extensive data is given in Table 47 along with K_B as defined by

$$K_B = \frac{[H_2OCo(DH)(DH_2)R^+]}{[H_2OCo(DH)_2R][H^+]} \qquad (5)$$

K_B increases with the expected trends of electron donation by the R group. For R = aryl and benzyl, k_1 and K_B increase on going from electron-withdrawing to electron-donating substituents. K_B increases with electron donation by the alkyl group in alkyl complexes but k_1 decreases. This latter trend was felt to be consistent with that expected for an S_E2 mechanism. The reaction of $H_2OCo(DH)_2CH_2CF_3$ is immeasurably slow and this finding is also consistent with such a mechanism.

Co(II). Halpern's group has extensively investigated the reaction between $LCo(II)(DH)_2$ compounds and RX [220,221]. The mechanism and stoichiometry of the reaction are given in eqns. (6)–(8) ($(DH)_2$ assumed).

$$LCo(II) + RX \rightarrow LCo(III) + R \qquad (6)$$

$$\underline{R + LCo(II) \rightarrow LCo(III)R} \qquad (7)$$

TABLE 47

Kinetic data for the reaction of $H_2OCo(DH)_2R$ with Hg^{2+} at 25°C ($\mu = 1.0$) [a]

R	k_1 (M^{-1} s^{-1})	K_B (M^{-1})	R	k_1 (M^{-1} s^{-1})	K_B (M^{-1})
Me	54	3.5	p-$CH_3C_6H_4CH_2$	9.0×10^{-2}	1.9
CH_2CH_3	1.2×10^{-1}	3.9	p-$CH_3OC_6H_4CH_2$	11.3×10^{-2}	2.6
n-C_3H_7	9.4×10^{-2}	4.7	C_6H_5	4.0×10^{2}	1.0
$C_6H_5CH_2$	7.5×10^{-2}	2.4	p-FC_6H_4	2.5×10^{2}	1.4
p-$NO_2C_6H_4CH_2$	6.5×10^{-3}	1.1	p-$CH_3C_6H_4$	4.5×10^{3}	0.8
p-$FC_6H_4CH_2$	2.8×10^{-2}	1.7	p-$CH_2OC_6H_4$	3.0×10^{4}	2.4

[a] See ref. 144 for details.

TABLE 48

Kinetic data for the reactions of $LCo(II)(DH)_2$ with benzyl bromide [a]

L	pK_a (L)	k ($M^{-1}\,s^{-1}$)	L	pK_a (L)	k ($M^{-1}\,s^{-1}$)
Py	5.2	1.5×10^{-1}	$P(C_6H_4\text{-}p\text{-}Me)_3$		3.4×10^{-2}
4-Me–py	6.1	2.1×10^{-1}	$P(C_6H_4\text{-}p\text{-}OMe)_3$	4.46	4.8×10^{-2}
1-N-Me–imidazole	7.0	5.5×10^{-1}	$PBut_3$	8.43	1.6
Piperidine	11.1	1.0×10^{-1}	PMe_3	8.65	7.1
$P(OMe)_3$		1.5×10^{-1}	PEt_3	8.69	1.1
$P(C_6H_4\text{-}p\text{-}Cl)_3$		9.7×10^{-3}	$PChx_3$	9.7	$\sim 2\times10^{-3}$ [b]
PPh_3	2.73	2.1×10^{-2}			

[a] In benzene solution, 25°C. See ref. 220 for further details. [b] Estimated by the present authors from related data in ref. 220.

$$2\ LCo(II) + RX \rightarrow LCo(III)X + LCo(III)R \qquad (8)$$

The slow step in the reaction is the halogen abstraction step (6). For small N donor ligands, increasing ligand basicity leads to an increased rate of halogen abstraction (Table 48). As for Co–C bond cleavage, steric factors also seem important where L are P donor ligands. For small P donor ligands, the rate increases with basicity (compare $P(OMe)_3$ with PMe_3) but, at similar basicity, decreases markedly with size (compare PEt_3 with $PChx_3$).

Co(I). Good evidence exists that $LCo(I)(DH)_2$ compounds and RX form $LCo(DH)_2R$ via an S_N2 displacement reaction at C or via electron-transfer reactions [105]. We will not review this evidence but will be concerned with the effects of L on the reaction rate. The most extensive data on this topic was collected by Schrauzer and Deutsch [141]. The assessment of the effects of L on the rate was confounded by the existence of the following equilibrium

$$L + H_2OCo(I)(DH)_2 \rightleftharpoons LCo(I)(DH)_2 + H_2O \qquad (9)$$

which was not particularly favorable and the fact that $H_2OCo(I)(DH)_2$ appeared to be more reactive than most L complexes investigated. The values in Table 49 are therefore often approximate. It appears that with a given class of L (N, P donors, etc.), the reaction rate increases with increasing basicity, whereas possible π acceptor ligands decrease the reaction rate.

Equilibrium studies

Extensive information on equilibria involving cobaloximes is available on several types of processes. We have discussed equilibria involving O–H–O protonation and deprotonation above (Tables 19, 43 and 47). The acid

TABLE 49

Effect of axial bases on the reaction of LCo(I)(DH)$_2$ with EtBr [a]

L	k_{obsd} (M^{-1} s^{-1})	L	k_{obsd} (M^{-1} s^{-1})
H_2O	11	PPh_3	0.3
Py	6	$AsPh_3$	1.3
2-Me–py	6	$SbPh_3$	1.9
2,6-Me_2–py	5	$PBut_3$	1.6
$PhNH_2$	6	Me_2S	3
$C_6H_{11}NH_2$	10	$C_6H_{11}NC$	0.5
4-CN–py	5		

[a] 25°C, 0.1 N NaOH. See ref. 141 for further details.

dissociation for axial H_2O was also discussed (Tables 19 and 43). We have also considered the equilibrium involving Co–C bond homolysis in LCo(DH)$_2$CH(Me)Ph (Table 45). Two remaining classes of equilibrium processes need to be considered here. These are equilibria involving the formation of complexes from solvato species and protonation or deprotonation of axial R ligands. Some miscellaneous equilibrium studies will be described last.

Formation constants

Non-aqueous solvents. Toscano has utilized ^1H NMR to determine the relative abundance of each cobaloxime in DMSO-d$_6$ as described by eqn. (10) [157]. Although a wide range of X ligands was employed, there was very little change in log K_f when L = 4-CN–py (Table 50). Two temperatures were employed in the study because complexes with relatively good electron-donating R ligands were in rapid exchange on the NMR time scale at 32°C.

In contrast to the results just described, a similar set of measurements on the process in eqn. (10), where L is varied and X = Me, thus

$$L + DMSO\text{-}d_6Co(DH)_2X \rightleftharpoons LCo(DH)_2X + DMSO\text{-}d_6 \qquad (10)$$

gave a difference of about two log units in log K_f (Table 50). For pyridine ligands, K_f increased with increasing ligand pK_a. Sterically hindered N donor ligands had the lowest formation constants, whereas phosphite ligands had K_f in the same range as py ligands.

These two trends, small dependence on X when L is constant and large dependence on L when R is constant, are readily understood. As X changes, the dissociation rates of DMSO-d$_6$ and 4-CN–py both increase in a nearly parallel fashion, leading to almost no dependence on X. However, if X is

TABLE 50

$\log_{10}$ of the formation constants for DMSO–d_6Co(DH)$_2$R + L ⇌ LCo(DH)$_2$R + DMSO–d_6 [a]

L = 4-CN–py			R = Me	
R	log K_f ($T = 32°C$) [b]	log K_f ($T = 20°C$) [c]	L	log K_f (32°C) [c]
P(O)(OMe)$_2$	1.26	–	NMe$_3$	1.24
C_6H_5	1.35	1.63	3-CM–adenine [f]	1.41
i-C_3H_7	[d]	1.68	3-Me–adenine	1.42
CH$_2$SiMe$_3$	1.51	–	3-Benzyladenine	1.47 [e]
n-C_3H_7	1.66	1.68	PPh$_3$	1.56
CH$_2$CHMe$_2$	1.69	1.92	4-CN–py	1.73
Et	1.71	1.94	Thiazole	2.12
Me	1.73	1.99	P(OCH$_2$)$_3$CMe	2.13
c-C_3H_5	1.73	–	1-Me-2-NO$_2$–imidazole	2.17
CH$_2$CMe$_3$	[d]	1.73	Quinuclidine	2.25
c-C_5H_9	[d]	1.76	P(OMe)$_3$	2.57
(CH$_2$)$_3$CN	1.73	2.05	P(O-i-C_3H_7)$_3$	2.59
p-SO$_2$PhMe	1.73	–	1,2-Me$_2$–imidazole	2.86
CH=CH$_2$	1.74	1.97	Py	2.96
CH$_2$C$_6$H$_5$	1.75	2.05	4-tBut–py	3.13
CN	1.78	–	P(OMe)Ph$_2$	3.45
CH$_2$Cl	1.79	2.06		
CH$_2$Br	1.80	2.07		
CH$_2$I	1.82	–		
NO$_2$	1.85	–		
CH$_2$CF$_3$	1.86	2.11		
CH$_2$CN	1.88	2.19		
CHBr$_2$	1.88	–		
CH$_2$NO$_2$	1.96	–		

[a] Ref. 157. [b] Average of three values obtained at $[Co(DH)_2R]_{tot} = 0.02$, 0.03, and 0.04 M. [c] Average of two values obtained at $[Co(DH)_2R]_{tot} = 0.02$ and 0.04 M. [d] Fast-exchange NMR spectra were obtained. [e] Log K_f values for other compounds with L = 3-benzyladenine: P(O)(OCH$_3$)$_2$ 1.01; CH$_2$CH$_3$ 1.19; Me 1.47; CH$_2$Br 1.58. [f] CM = CH$_2$COOEt.

constant, the rate of L dissociation will influence K_f. Since ligand dissociation rates vary considerably as discussed above, the variation in K_f can easily be explained.

Aqueous solution. K.L. Brown et al. measured K_f values for py (Table 19) and DEA (Table 43) as a function of R. A plot of log K_f vs. σ^* was linear with a small positive slope for R with $\sigma^* > 0.2$ but was steeper and curved at values of σ^* below this value. This curvature was attributed to the presence of significant amounts of "Co(DH)$_2$R" when R is highly electron donating [145,188].

*p*K*$_a$s of axial groups.* The pK_as of the conjugate acids of *m*- and *p*-isomers of $LCo(DH)_2C_6H_4NMe_2$ [222] have been correlated with those of *N*,*N*-dimethylanilinium ions with non-cobalt substituents via a dual-substituent parameter equation. The results show that resonance interactions of the anilinium type (p-$Me_2N^+C_6H_4Co^-(DH)_2L$) are negligible. Values of σ_I (inductive substituent parameter) compare favorably with those determined from the pK_as of carboxyethylcobaloximes [223,224] but do not agree well with values determined using ^{19}F NMR chemical shifts where a different solvent (MeOH) was employed. Differences in σ_I values are ascribed to solvent effects. Values of σ_R (resonance substituent parameter) are insensitive to solvent effects, and differences between values derived from ^{19}F NMR data and pK_a data were attributed to resonance interactions involving the metal *d* orbitals. This study also contained some formation constant data.

Brown's group also measured acid dissociation constants for R groups containing a $-CO_2H$ function either β (carboxymethyl, 1-carboxyethyl) or γ (α-carboxyethyl) to cobalt. Some of the data obtained are given in Table 51. The pK_a values for the carboxymethyl compounds illustrate that these are very weak acids. The magnitude of this "β effect" can be appreciated by comparison of the data for a given L (when possible) with that for the analogous α-carboxyethyl derivative, also given in Table 51. The substituent constants derived from LFER are also given in the Table. Finally, the K_f for the acid and conjugate base complexes, K_f^{AH} and $K_f^{A^-}$, are also given. The formation constants for the neutral complexes are generally higher than those for the anionic species.

Crumbliss and Morgan [232] have obtained pK_a data for proton dissociation from the axial H_2O ligand in $[X\text{-}pyCo(DH)_2H_2O]ClO_4$ (Table 54). An extremely good correlation was obtained between values of pK_a for the complex and values of pK_a for $X\text{-}pyH^+$. This demonstrates that as the base strength of L increases, the acidity of the coordinated H_2O decreases. This effect is mediated by coordination to Co as indicated by the obtained slope of ~ 0.2.

Miscellaneous studies. Marzilli and co-workers [199] have examined the effects of L on the ambidentate isomerization equilibrium constant for SCN (Table 52). The less basic ligand L formed S or N bonds in series involving (a) substituted pyridines, (b) phosphines, and (c) phosphites. However, no cross-correlations between the three series were possible.

Drago and co-workers [225] examined the enthalpy changes accompanying the reaction (11) in several solvents, including CH_2Cl_2. The enthalpy changes,

$$[Co(DH)_2CH_3]_2 + 2\ L \rightleftharpoons 2\ LCo(DH)_2CH_3 \qquad (11)$$

TABLE 51

Equilibrium constants for L ligation and R deprotonation in $LCo(DH)_2R$ [a]

L	pK_L	K_f^{AH} (M^{-1})	$K_f^{A^-}$ (M^{-1})	pK_a^L	σ_I	L	pK_L	K_f^{AH} (M^{-1})	$K_f^{A^-}$ (M^{-1})	pK_a^L	σ_I
R = carboxymethyl						*R = 2-carboxyethyl*					
H_2O				6.30	−0.445	*S*-Methyl-2-mercapto-ethanol		2.95×10^1	4.46×10^1	4.71	−0.045
(2-Methylthio)-ethanol		4.55×10	5.52×10	6.22	−0.425						
Methyl(methylthio)-acetate		5.54	7.31	6.18	−0.415	*S*-Methyl methylmercapto-acetate		4.48	6.31	4.74	−0.065
4-CN–py	2.24	3.86×10^2	3.35×10^2	6.36	−0.460	Methylmercapto-acetate	7.83	1.55×10^5	1.06×10^5	5.06	−0.271
4-carboxamido–py	3.77	1.34×10^3	1.03×10^3	6.41	−0.473	Methylmercapto-propionate	9.27	3.62×10^5	2.31×10^5	5.09	−0.291
Py	5.56	6.33×10^3	3.65×10^3	6.54	−0.505	2-Mercaptoethanol	9.51	4.27×10^5	2.59×10^5	5.11	−0.304
4-Me–py	6.36	1.34×10^4	7.37×10^3	6.56	−0.510	4-CN–py	2.24	1.45×10^2	1.61×10^2	4.84	−0.132
4-NH_2–py	9.40	6.09×10^4	2.41×10^4	6.70	−0.546	4-Carboxamido–py	3.77	4.06×10^2	4.20×10^2	4.88	−0.155
2,2,2-Trifluoroethyl-amine	5.68	1.17×10^2	7.31×10	6.50	−0.495	Py	5.56	1.51×10^3	1.20×10^3	4.99	−0.226
Glycine ethyl ester	7.86	2.59×10^3	1.15×10^3	6.65	−0.533	4-Me–py	6.36	2.75×10^3	1.99×10^3	5.03	−0.252
2,2-Dimethoxyethyl-amine	8.86	6.92×10^3	2.90×10^3	6.68	−0.540	4-NH_2–py	9.40	9.53×10^3	5.88×10^3	5.10	−0.297
2-Methoxyethyl-amine	9.68	1.45×10^4	5.40×10^3	6.73	−0.553	2,2,2-Trifluoro-ethylamine	5.68	2.34×10	3.04×10	4.78	−0.090
n-Propylamine	10.80	4.60×10^4	1.48×10^4	6.79	−0.568	Glycine ethyl ester	7.86	3.22×10^2	4.02×10^2	4.79	−0.097
Methyl thioacetate	7.83	7.87×10^6	8.68×10^5	7.26	−0.686	2,2-Dimethoxy-ethylamine	8.86	5.85×10^2	6.75×10^2	4.83	−0.123
Methyl thiopropi-onate	9.27	2.57×10^7	1.79×10^6	7.46	−0.736	2-Methoxy-ethylamine	9.68	1.10×10^3	1.23×10^3	4.85	−0.136
2-Thioethanol	9.51	2.42×10^7	1.68×10^6	7.46	−0.736	n-Propylamine	10.80	2.96×10^3	3.08×10^3	4.87	−0.149

[a] Refs. 223 and 224; see text for definition of constants.

TABLE 52

Equilibrium constants for the reaction $LCo(DH)_2NCS \rightleftharpoons LCo(DH)_2SCN$ [a]

L	$\Sigma\chi$	K(S/N)	L	$\Sigma\chi$	K(S/N)
4-CN-py		1.44	$P(Me)Ph_2$	11.2	1.71
Py		1.35	$PBut_3$	4.2	1.18
t-But-py		0.90	$P(OPh)_3$	29.1	1.06
$4\text{-}NH_2\text{-}py$		0.63	$P(OCH_2)_3CEt$	~ 30	0.93
PPh_3	12.9	2.47	$P(OMe)_3$	23.1	0.79
$P(But)Ph_2$	10.0	1.91	$P(O\text{-}i\text{-}C_3H_7)_3$	18.9	0.65

[a] In nitrobenzene, 33°C. See ref. 199 for further details. For studies of the solvent dependence of K(S/N), see ref. 210.

TABLE 53

Solvation-minimized corrected enthalpies (kcal mol^{-1}) for methylcobaloxime-donor systems [a]

L	$-\Delta H$
Dimethylcyanamide	12.7
Py	20.8
1-Me-imidazole	22.1
Tetrahydrothiophene	15.3
Trimethylolpropanephosphine ester	19.7
$P(OMe)_3$	19.2
Tetrahydrofuran	15.8

[a] Ref. 225, CH_2Cl_2 solvent.

corrected for L solvation and for the dimerization enthalpy, are given in Table 53. In this study, values of E and C for methylcobaloxime were calculated to be 9.14 and 1.53, respectively. The E/C ratio places the complex as a borderline hard/soft acid. The relatively low affinity of $Co(DH)_2Me$ for oxygen donors was attributed to an entropy effect possibly arising from steric interactions with the equatorial ligand system.

Herlinger and T.L. Brown [226] report the ^1H NMR and dynamic NMR on $[Co(DH)_2R]_2$ where R is CH_3, CHF_2, and CH_2Cl. The spectra exchange broaden with coalescence, T increasing in the order indicated for R, but a large dependence on R was not observed. The process is complex and the interested reader is referred to the original article.

Electrochemistry

Electrochemical reduction. The electrochemical reduction of cobaloximes has received relatively little attention compared to Schiff-base B_{12} models and the data available for organocobaloximes are somewhat contradictory. Thus more work to clarify this area is certainly warranted.

In early work with non-organocobaloximes, Costa et al. demonstrated that (1) axial ligands have a marked effect on the Co(III)/Co(II) reduction potential, and (2) the nature of the equatorial ligand governs the Co(II)/Co(I) reduction [227,228]. They also showed that, for the compounds studied, results may be complicated by O–H–O proton dissociation and/or reactions involving the Co(II) species subsequent to reduction [228].

Finke, Elliot and co-workers have studied the electrochemical behavior of some alkyl- and non-alkyl-cobaloximes in an attempt to compare their redox properties with those of (DO)(DOH)pn models, cobalamins, and cobinamides [229,230]. They found that, whereas the B_{12} derivatives and the (DO)(DOH)pn models undergo reversible electrochemical reduction, the cobaloxime reduction is irreversible under all conditions of added L, solvent, temperature, and scan rates employed. However, Le Hoang et al. found the electrochemical reduction of organocobaloximes to be reversible for most cases in DMSO [231]. Using cyclic voltammetry and polarography, two reduction steps were observed: $Co(III)(DH)_2R/Co(II)(DH)_2R$ and $Co(II)(DH)_2R/Co(I)(DH)_2R$. Cyclic voltammetry indicated that Co–C bond cleavage occurred upon reduction. Upon reoxidation, the Co–C bond reformed and starting materials were recovered in yields of 60–95%. For the optically active compounds where R is 2-octyl, complete retention of configuration was observed. The authors suggested that the alkyl group may be reversibly trapped by the equatorial ligand during the reduction process [231].

Crumbliss and Morgan [232] have obtained a rather extensive set of data

TABLE 54

Peak potential (E_p) for Co(III/II), pK_a of axial H_2O, reduction rates of [X-pyCo$(DH)_2H_2O$]ClO_4 (k_1) by Fe^{2+} and reduction rates of [X-pyCo$(DH)_2$OH] (k_2) by Fe^{2+}[a]

X–py	E_p (V) [b]	X-pyH$^+$ pK_a [c]	Complex pK_a [d]	10^3k_1 (M^{-1} s^{-1}) [e]	$10^{-3}k_2$ (M^{-1} s^{-1}) [e]
4-Me–py	−0.42	6.03	6.42	1.17	1.66
3-Me–py	−0.42	5.67	6.36	2.38	2.17
H–py	−0.39	5.21	6.25	2.83	2.91
4-Cl–py	−0.38	3.83	6.05	12.7	3.62
3-Cl–py	−0.35	2.81	5.84	32.0	7.13
4-CN–py	−0.34	1.86	5.73	23.5	6.38
3-CN–py	−0.32	1.35	5.65	–	–

[a] Ref. 232. [b] Co(III/II) peak potentials in CH_3CN (0.1 M TEAP) relative to Ag/AgCl electrode. [c] Ref. 263. [d] 25.0°C; 2.0 M $NaNO_3$. [e] 25.0°C; $[ClO_4^-]_T = 2.0$ M.

TABLE 55

Peak potential (E_p) (Co III/II) and reduction rates (k_x) by Fe^{2+} for $[X\text{-}pyCo(DH)_2N_3]$ [a]

X–py	E_p [b] (V)	10^2k_x (M^{-1} s^{-1}) [c]	X–py	E_p [b] (V)	10^2k_x (M^{-1} s^{-1}) [c]
3-NO_2–py	−0.54	5.85	3-CH_3–py	−0.66	0.544
3-CN–py	−0.53	7.44	4-CH_3–py	−0.68	0.356
4-CN–py	−0.57	3.52	3-OH–py	−0.61	
3-Br–py	−0.57		4-OH–py	−0.66	
4-Br–py	−0.65		3-NH_2–py	−0.66	
3-Cl–py	−0.58	3.18	4-NH_2–py	−0.88	
4-Cl–py	−0.61	1.42	4-$N(CH_3)_2$–py	−0.90	
Py	−0.64	0.848			

[a] Ref. 232. [b] Peak potentials relative to Ag/AgCl obtained by cyclic voltammetry in CH_3CN containing 0.1 M TEAP. [c] 25°C; $[ClO_4^-]_T = 2.0$ M.

on the electrochemical and chemical one-electron reduction of cobaloximes with substituted pyridines (Tables 54 and 55). For all complexes studied, values of E_p (peak potential) were found to decrease with increasing pyridine ligand basicity. For aquo complexes, values of E_p correlate linearly with values of pK_a for the pyridinium species. Also, for N_3 complexes (Table 55) values of E_p correlate separately with pK_a values where L are 4-substituted pyridines and with pK_a values where L are 3-substituted pyridines. For the three series of cobaloximes containing *trans* OH, H_2O and N_3, the log of the rate constants for chemical reduction by Fe^{2+} were found to correlate linearly with X substituent $\bar{\sigma}$ parameters. This demonstrates that as the basicity of L increases, the reduction by Fe^{2+} proceeds at a slower rate.

These data show that as the basicity of L increases, it becomes more difficult to reduce the cobaloxime, either electrochemically or chemically.

Electrochemical oxidation. Organocobaloximes can be oxidized electrochemically [233,234,237,240–242] and chemically [233,235,239]. EPR data suggest that the oxidized species contains Co(IV) [233,236,238]. Halpern et al. have estimated that the unpaired electron resides in a hybrid molecular orbital consisting primarily of 3*d* character with about a 30% contribution from the 4*p* orbital [236]. The oxidized complexes are unstable at room temperature and undergo solvent-assisted dissociation at low scan rates [241]. In the presence of Cl^-, decomposition of 1-methylheptylbis(dimethylglyoximato)Co(IV) occurs via nucleophilic attack at the ligating C, yielding Co(II) and R–X with inversion of configuration [239].

Vol'pin et al. have also shown that pyridine reacts with "$[RCo(DH)_2]^+$" via an S_N2 pathway similar to reactions with Cl^- [240]. Rate constants for

TABLE 56

Electrochemical data for the redox couple $RCo(DH)_2/[RCo(DH)_2]^+$ and rate constants for the reaction of $[RCo(DH)_2]^+$ with pyridine[a]

R	$E_{1/2}$ (V)	$k \times 10^{-2}$ ($M^{-1}\,s^{-1}$)
p-$CH_2C_6H_4Me$	0.784	0.83
$CH_2C_6H_5$	0.800	1.01
p-$CH_2C_6H_4F$	0.814	2.09
p-$CH_2C_6H_4Cl$	0.830	2.66
p-$CH_2C_6H_4CO_2Et$	0.852	5.83
p-$CH_2C_6H_4NO_2$	0.885	13.80

[a] Ref. 240.

this reaction (Table 56) were found to correlate well with Hammett substituent constants [240].

The one-electron electrochemical oxidation of $H_2OCo(DH)_2R$ to $[H_2OCo(DH)_2R]^+$ has been systematically studied by Chum et al. [241]. Half-wave potentials for complexes with a variety of R groups including R = *para*-substituted benzyl were found to correlate well with the Taft σ^* parameter for R and the pK_a for RH.

In recent work by Costa et al., rate and thermodynamic data (Table 57) were obtained as a function of R for the reversible, one-electron oxidation of $H_2OCo(DH)_2R$ in CH_3CN [242]. Plots of log k_s (k_s = apparent rate constant) vs. $E_{1/2}$ were linear, indicating that α_{app} (apparent transfer coefficient) is independent of potential. A linear relationship between $E_{1/2}$ for $H_2OCo(DH)_2R$ and the Co–C bond length of $pyCo(DH)_2R$ with R = Me, CH_2CH_3, CH_2CMe_3, and $CHMe_2$ reflects the importance of steric interactions on oxidation potentials.

TABLE 57

Electrochemical and thermodynamic data for the reaction[a] $H_2OCo(DH)_2R \rightleftharpoons e^- + [H_2OCo(DH)_2R]^+$

R	$E^r_{1/2}$ (V)[b]	$-\log k_s$	R	$E^r_{1/2}$ (V)[b]	$-\log k_s$
CH_2CF_3	0.902	1.97	CH_2CH_3	0.753	1.47
C_6H_5	0.861	1.95	n-C_4H_9	0.751	1.52
$CH_2C_6H_4$-p-NO_2	0.833	1.70	n-C_3H_7	0.750	1.50
$(CH_2)_3CN$	0.810	1.95	$CH_2C_6H_4$-p-Me	0.740	1.52
Me	0.785	1.55	CH_2CMe_3	0.732	1.63
$CH_2C_6H_4$-p-Cl	0.780	1.56	c-C_5H_9	0.720	1.72
$CH_2C_6H_5$	0.758	1.54	i-C_3H_7	0.708	1.65
CH_2CHMe_2	0.754	1.66	$CHEt_2$	0.677	1.88

[a] Ref. 242. [b] Versus SCE.

D. COMPARISON OF SOLUTION AND STRUCTURAL DATA

(i) Equatorial ligands

Spectroscopic studies

Since there is very little variation in the structure of the equatorial ligand, spectra generally depend on changes in axial ligands and will be discussed as appropriate in other subsections.

Kinetic studies

Guschl and Brown [160] found that the rate of proton exchange for the O–H–O group is probably a function of the O–O distance, since the (DO)(DOH)pn compounds, which have shorter O–O distance (~ 2.39 Å [243]), exhibit slower proton exchange than cobaloximes, where the average O–O distances are 2.482 Å and 2.497 Å for organometallic and non-organometallic compounds, respectively. Exchange in the organometallic compounds is slower than in the non-organometallic compounds, which is consistent with these average distances. The evidence for the more rapid exchange in the non-organometallic compounds is the difficulty of observing this resonance in the ^{1}H NMR spectrum of such compounds [170].

The ^{1}H NMR shift of the O–H–O resonance should also reflect O–O distances. However, the range of shifts is rather small as L is changed [160]. As X is changed [152], the O–H–O in CH_2Cl_2 at −54°C varies from 18.51 ppm (NO_2) to 18.81 ppm (Me) for $pyCo(DH)_2X$ compounds.

Equilibrium studies

A plot (not shown) of pK'_{c-L} (Table 19) for L = py and R = CH_2CF_3 (L = CNpy for Co–N), $CHCH_2$ (CH = CHMe for pK'_{c-L}), Me, CH_2CH_3, i-C_3H_7 vs. Co–N(py) distance indicates that a reasonable relationship exists with both values increasing as R becomes more electron donating. However, the O–O distance varies little and does not fit the trend.

For $H_2OCo(DH)_2X$, the pK_a is a much more sensitive function of X electron-donating ability. In this case, the deprotonation site has been assigned to the axial H_2O [145,146] and the pK_a is designated pK'_{c2}. The difference, $pK'_{c-L} - pK'_{c2}$, increases from ~ 0.7 ± 0.1 for a good electron-donating R to ~ 1.2 for a poorly electron-donating R (Tables 18 and 43). From Table 18, we calculate pK'_{c-L} for X = Cl to be 11.3. Palade [244] has found a value of pK'_{c2} of 6.30 for $H_2OCo(DH)_2Cl$. The difference is thus ~ 5 for acido ligands. Values of pK'_{c2} for other $H_2OCo(DH)_2X$ include 6.44 (Br), 7.66 (NO_2) and 8.05 (OH) [244]. Other workers have reported values of 6.87 (I) and 7.28 (NO_2) [148]. Relatively few Co–OH_2 bond distances are available, but these lengths (1.955 Å (Br), 1.980 Å (NO_2), 2.055 Å (CH_3))

reflect the decreasing acidity of the axial H_2O (Table 13). Since Co–N and Co–O bond lengths should be parallel, as mentioned above, we plotted (not shown) pK'_{c2} vs Co–N distance and obtained the same trend as for pK'_{c-L}. For both plots the data are somewhat scattered and possibly suggest that the pK values become less sensitive to X electron-donating ability as X becomes a good electron donor (CH_2CH_3, i-C_3H_7).

There is relatively little information on the influence of L on pK'_{c-L} (Table 42). Clearly, as L becomes a better electron donor, pK'_{c-L} increases in value. However, the relationship between Co–N (axial) or Co–C bond lengths and electron-donating ability of ligands such as 4-X–py is not known. As readers of this review will discover, the absence of this type of data is serious since many types of studies have employed 4-X–py complexes.

(ii) Axial ligand variations

Spectroscopic studies

NMR spectroscopic studies

^1H NMR. Unfortunately, insufficient NMR data exist on $LCo(DH)_2X$ (where L is py or a substituted py) to allow a meaningful comparison of axial py ligand shifts vs structure as X is varied. However, it is known that ^1H NMR shifts in py complexes closely parallel ^{13}C NMR shifts where data are available (see below) [156].

For the complexes of the type $LCo(DH)_2CH_3$, the axial CH_3 ^1H NMR shifts appear to be a somewhat sensitive function of the electronic properties of L (Tables 21 and 25). However, there appears to be no strong correlation between the Co–C bond length and the reported shifts in these Tables and in ref. 160.

For two series, $LCo(DH)_2$i-C_3H_7 (Table 23) and $LCo(DH)_2(CH_3OH)^+$ (Table 24), the ^1H NMR parameters of the axial ligands seem to be sensitive to steric and not to electronic effects of L. For the first series, the axial CH_3 resonance moves upfield by ~ 0.2 ppm as the bulk of L is increased from py to 2-NH_2–py or from $P(OCH_2)_3CMe$ to PPh_3. For both pairs, the Co–L, Co–C, *d* and α values all increase (Tables 11 and 12).

For the series $[LCo(DH)_2CH_3OH]^+$, the ^1H NMR chemical shift of the methanol CH_3 resonance appears to reflect the bulk of L, where L is a P donor [162] or an N donor (W.C. Trogler, unpublished results). These relationships were attributed to the change in anisotropy at cobalt resulting from the distortion of the $Co(DH)_2$ moiety (increasing α values) as bulk increased. However, subsequent crystallographic work, while corroborating the importance of steric factors, has not led to a clear relationship between either α or *d* and shift. Nevertheless, there is a good correlation between

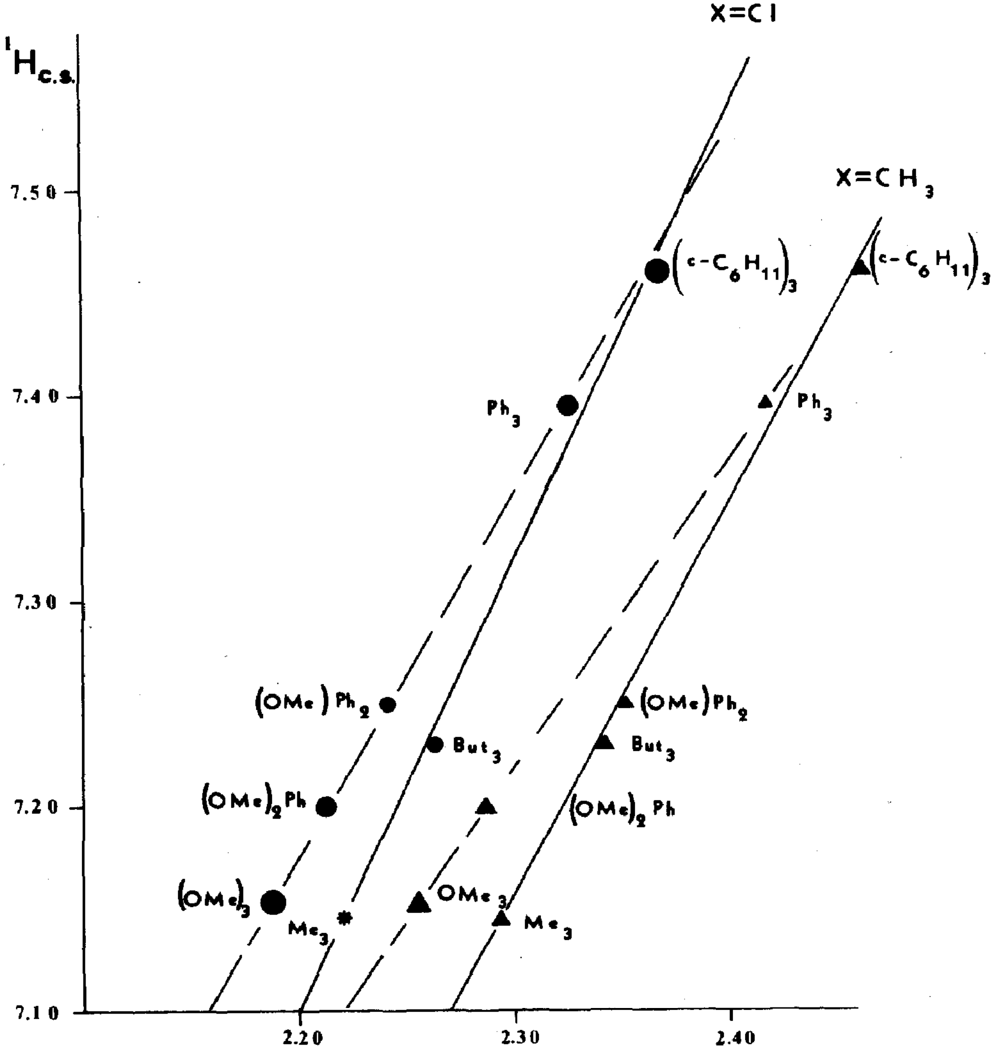

Fig. 12. ^{1}H NMR chemical shift of the Me group of methanol in $[PR_3Co(DH)_2O(H)Me]^+$ cations (Table 24) against Co–P bond lengths in $PR_3Co(DH)_2X$ with X = Cl, Me (Table 11). Circles refer to X = Cl and triangles to X = Me.

shift and Co–P distance (Fig. 12). With the exception of $P(OMe)Ph_2Co(DH)_2Me$, phosphite *trans* ligands appear to follow a slightly different trend than phosphine compounds [71]. This difference, however, is most pronounced for small L, where the CH_3 shift is no longer a sensitive function of L ligand size. More structural data on complexes with ligands of slightly larger than average bulk, such as $P(i\text{-}C_3H_7)_3$, could help to clarify the relationships between shift and structural parameters since, with this type of L, the shift is a very sensitive function of bulk.

There is no relationship between either $^4J_{PH}$ or $^5J_{PH}$ and structure. The coupling constants primarily reflect the orbital character of the Co–P bond [162], which is probably only slightly, if at all, influenced by the length of the Co–P bond.

For $PPh_3Co(DH)_2X$ complexes, there is a clear relationship between the shift of the equatorial oxime CH_3 ^1H NMR signal and Co–P distance (Fig. 13). This relationship holds because the anisotropy of the Ph groups is not large enough to influence the shifts, in agreement with a semi-quantitative calculation [79]. In relationships of the type shown in Fig. 13, it is not clear whether both are caused by the same factor, most likely the rehybridization of the Co as the orbital character of the Co–X bond changes, or whether the variation in Co–P distance leads to a variation in Co anisotropy.

^{13}C NMR. As stated in section C, ^{13}C NMR shifts appear to reflect the expected bonding trends quite well, particularly if nuclei remote from Co are examined. Probably the best correlation which currently exists is that between the γ ^{13}C NMR shift of 4-tBut-py and the Co–N bond length of the related py complex (Fig. 14). The excellent linear correlation implies that ^{13}C NMR shifts of this type can be a good indirect measure of the *trans* influence of X for complexes in solution. The γ ^{13}C NMR shift approaches that of the free ligand when X has a strong *trans* influence, and such a relationship is consistent with the properties of the coordinated ligand approaching those of the free ligand.

Similarly, a plot (not shown) of ^{13}C shifts of $P(OMe)_3$ in $P(OMe)_3Co(DH)_2X$ compounds against Co–P distance gives a reasonable linear relationship. However, the best electron donor X in the series is Me.

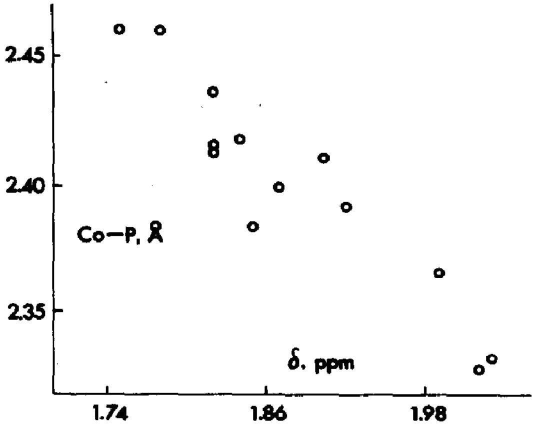

Fig. 13. Co–P distance (from ref. 79) versus ^1H NMR chemical shift of the oxime CH_3 group for $PPh_3Co(DH)_2X$; X = (top to bottom) $CH_2C(CH_3)(CO_2C_2H_5)_2$ and neo-C_5H_{11} (left to right, respectively), CH_2CHMe_2, Me, CH_2CH_3, i-C_3H_7, $CH(CH_3)CN$, CH_2Br, CH_2CN, CH_2CF_3, NO_2, Br, Cl, respectively.

Therefore, this relationship must be considered tentative, particularly because the relationship between ${}^{2}J_{CP}$ and the Co–P distance is not linear (the J value does, however, generally increase as Co–P bond length increases). An indication that py and phosphite ligands may not respond in the same manner to ligands with a large *trans* influence results from a comparison of Co–N bond lengths for pyridine complexes and ${}^{13}C$ NMR shifts of $P(OMe)_3$ complexes (Fig. 15). This relationship is linear up to ~ CH_3, but, for better electron-donating R, Co–N bond lengths increase, whereas ${}^{13}C$ shifts remain within a narrow range.

${}^{31}P$ NMR. Extensive ${}^{31}P$ NMR data on series of the type $LCo(DH)_2X$ are available only where L is PPh_3 or $P(OMe)_3$. If L is PPh_3, no worthwhile correlation exists [79]. This has been attributed to the confounding influence of several, sometimes opposing, factors on the ${}^{31}P$ shifts of complexes where

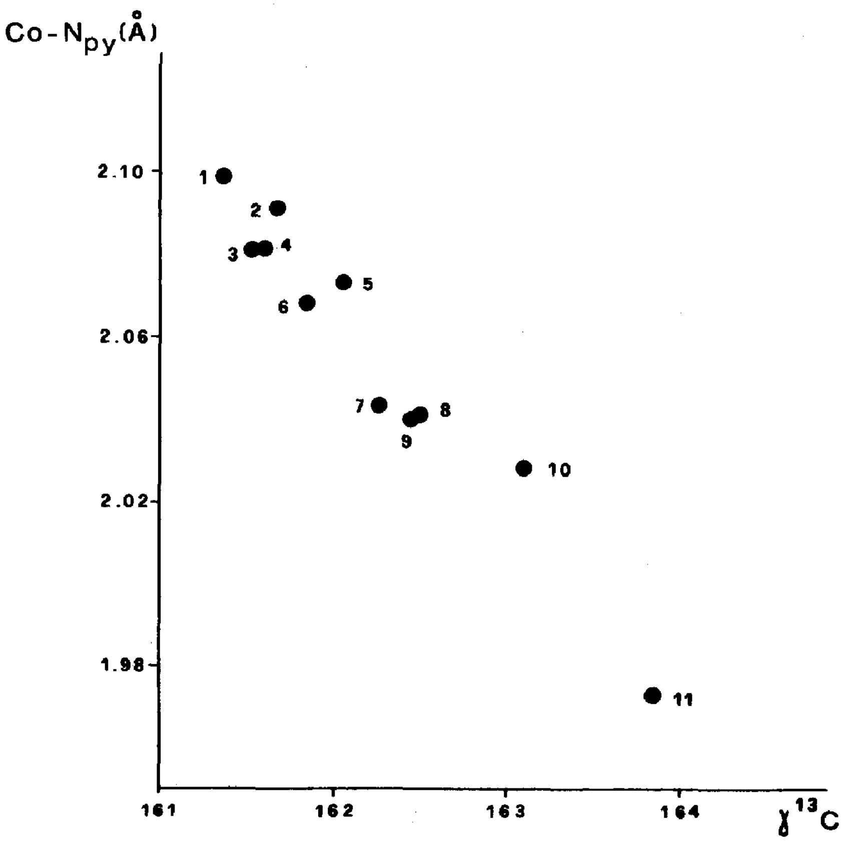

Fig. 14. Linear relationship between the Co–N(py) bond lengths in $pyCo(DH)_2X$ complexes and the γ ${}^{13}C$ chemical shift of 4-tBut–py analogues. 1 = i-C_3H_7; 2 = CH_2SiMe_3; 3 = CH_2CMe_3; 4 = CH_2CH_3; 5 = Me; 6 = $CH{=}CH_2$; 7 = $C(Cl){=}C(C_6H_4\text{-}p\text{-}Cl)_2$; 8 = CH_2COOMe; 9 = CH_2CF_3; 10 = CH_2NO_2; 11 = N_3.

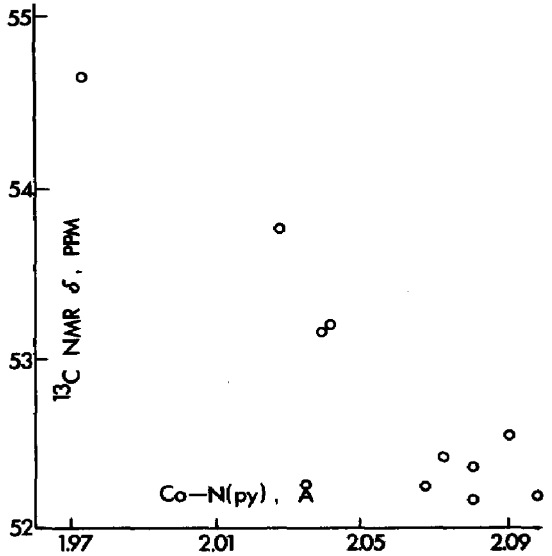

Fig. 15. ^{13}C NMR chemical shift of the $P(OMe)_3$ group for $P(OMe)_3Co(DH)_2X$ (Table 27) versus Co–N(py) distance for $pyCo(DH)_2X$ (Table 12). X = (top to bottom) N_3; CH_2NO_2; CH_2CF_3; CH_2COOMe; CH_2SiMe_3; $CH{=}CH_2$; CH_2CMe_3; Me; i-C_3H_7; CH_2CH_3.

L is a bulky P donor. A better relationship between the shift, the *trans* influence of X, and Co–P distance is found in the series with the non-bulky $P(OMe)_3$ ligand. Again, only a few cobaloximes with $P(OMe)_3$ as an axial ligand have been structurally characterized, and this ligand tends to be disordered in cobaloximes.

^{19}F NMR. Generally, ^{19}F NMR shifts have been measured in studies aimed at evaluating Co compounds as ring substituents (Tables 31–33). The shifts must be responding to electronic effects. In general, the F substituent is attached to Co via a Co–C bond, the length of which has relatively little dependence on L electronic properties. Therefore, there is no evident relationship between shift and any structural parameters. Such F compounds, in any case, have never been structurally characterized.

^{59}Co NMR. The trends in Table 34 generally follow those for Co–C bond lengths with L = O, N or P donors, in that order. The NQR parameter, $[N]/[X]$, generally follows this order also.

Electronic spectra

Where comparisons are possible, the electronic spectra in Tables 35–37 appear to reflect the ease of displacement of the L ligand. Complexes with more weakly bound L ligands have higher extinction coefficients (Table 35).

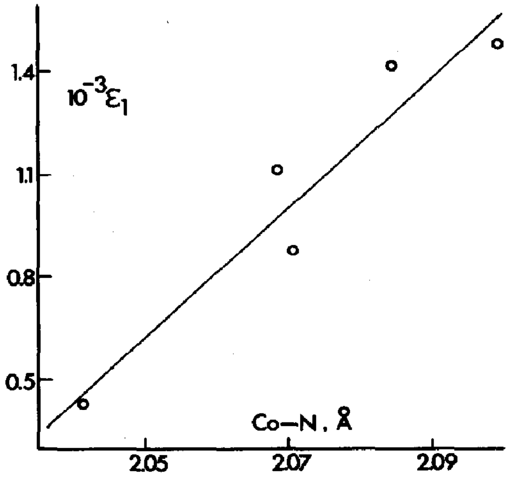

Fig. 16. Extinction coefficient (ϵ_1, Table 37) for $pyCo(DH)_2X$ versus Co–N(py) distance (Table 12). X = (left to right) CH_2CF_3; Me; $CH{=}CH_2$ and $CH{=}CHMe$ for Co–N and ϵ_1, respectively; CH_2CH_3; i-C_3H_7.

If L is held constant with $L = H_2O$ (Table 36) or L = py (Table 37), the intensities increase with the *trans* effect or influence of R. A good correlation is found between Co–N bond lengths and extinction coefficient (Fig. 16). There is no evidence that pyridine is dissociated in any of these complexes and, therefore, the relationship does not seem to reflect the formation of five-coordinate species.

IR spectra

Insufficient overlap exists between the ligands employed in Table 38 and in X-ray studies for any meaningful comparisons.

Kinetic studies

Substitution reactions

Non-organometallic compounds. There are no extensive systematic structural studies of non-organometallic cobaloximes which allow comparisons of neutral ligand exchange, since most L employed in crystallographic studies are poor leaving groups and X usually is substituted in displacement reactions. However, the structure of $H_2OCo(DH)_2NO_2$ gives a Co–O bond length of 1.980 Å [46]. This value is less than the 2.055 Å in $H_2OCo(DH)_2CH_3$. This relationship is consistent with the much greater *trans* effect of CH_3 over NO_2 [194].

Bond lengths of Co–Cl *trans* to PR_3 are slightly larger than those *trans* to N donors (Tables 11 and 12). In turn, $PR_3Co(DH)_2Cl$ complexes solvolyze somewhat faster than chlorocobaloximes with N donor ligands [201]. However, the observation that the rates increase with PR_3 bulk [201] does not have a parallel in Co–Cl bond lengths (Table 11), where the values for $L = PBut_3$ are essentially identical to those for $L = PChx_3$. The greater reactivity of the $PChx_3$ complex may be a transition state effect since steric strain may be released as the Co–Cl bond breaks.

Organometallic compounds: non-coordinating solvents. Systematic studies have been carried out in which either L or R is held constant and R or L is varied. As stated above, there is no convincing evidence that the relative L leaving ability is a function of R or that the *trans* effect of R is a sensitive function of L. There are reasons to suspect that such interdependence of ligand effects should occur. The STI of a bulky L could decrease the R ligand donor ability by lengthening the Co–C bond. The *trans* effect of R should then decrease. Alternatively, as the *trans* influence of R decreases, the bond between Co and the ligating atom of L will decrease and, consequently, repulsive interactions between L and the dioxime ligands could be important. This repulsive interaction in the ground state could be released in the transition state, and the *trans* effect of weakly electron-donating R would be enhanced relative to the magnitude of this effect expected from the electronic effect of R. However, these two possibilities would work in opposition and, if the effects are not large to begin with, no clear relationship between the reactivity of $LCo(DH)_2R$ and the bulk of L or R would exist.

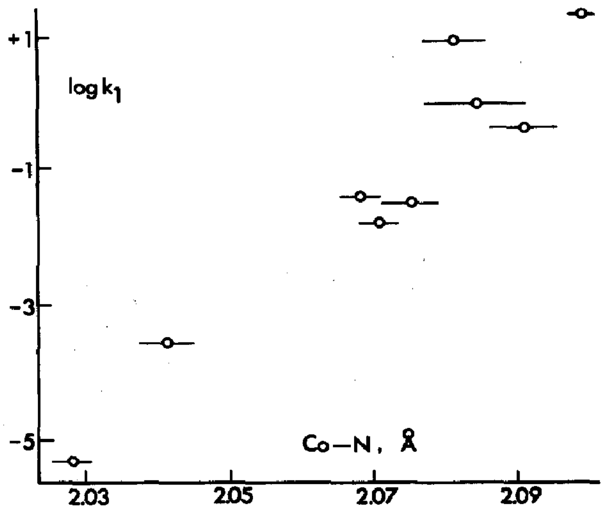

Fig. 17. Log k_1 for 4-CN-pyCo(DH)_2R versus Co–N(py) for $pyCo(DH)_2R$; R = (left to right) CH_2NO_2, CH_2CF_3, Me, $CH{=}CH_2$, $CH_2C(CH_3)(COOEt)_2$, CH_2CMe_3, CH_2CH_3, CH_2SiMe_3, $i\text{-}C_3H_7$.

For series in which R is held constant, ligand exchange rates have been found to be a function of X′ in 4-X′–py complexes (Tables 40, 42). As stated above, there is currently no structural data for comparison. For PR_3 ligands of similar basicity, the leaving rates increase with PR_3 bulk. Thus, the Co–P bond length in $PChx_3$ complexes is relatively large (Table 11) and this ligand is a relatively good leaving ligand (Table 40). Alternatively, PMe_3 forms complexes with relatively short Co–P bonds and it is such a poor leaving ligand that its dissociation rate probably cannot be measured under conditions normally used.

For series in which L is held constant, ligand exchange rates have been found to be a sensitive function of R (Tables 41 and 43). A plot of log k_1 for L = 4-CN–py vs Co–N(py) bond lengths (Fig. 17) is fairly linear and the *trans* effect and *trans* influence are therefore closely related. A similar plot of PPh_3 leaving rates vs Co–P distance (not shown) gives the same relationship, but with much more scatter.

Organometallic compounds: coordinating solvents. Unfortunately, relatively few of the organometallic complexes studied in aqueous solution (Tables 19 and 43) have R groups which are in complexes with known structures. No worthwhile comparisons are possible.

Other reactions

Co(III). Rates of nucleophilic attack on the C of coordinated $P(OMe)_3$ (Table 44) cannot be correlated with the O–C bond length owing to the generally low accuracy of these particular distances, which result from $P(OMe)_3$ disorder. However, there is a correlation (not shown) between Co–P bond length and reactivity. Increased electron donation from $P(OMe)_3$ to Co(III) should both decrease the Co–P bond length and increase the electrophilicity of the C in $P(OMe)_3$, and this relationship is found.

The dependence of D_{Co-R} in Table 45 on L is quite interesting. Again, 4-X–py complexes have not been structurally characterized in any systematic way. However, bulky P donor ligands generally increase Co–C bond lengths and this lengthening is reflected in weaker Co–C bonds for complexes with such bulky ligands.

The relationship between the “strength” of binding of L to Co and photodealkylation (Table 46) was mentioned in section B. The Co–C bond lengths appear to increase very slightly across the following series: H_2O, py, 3-N–Me–imidazole. The photodealkylation rates decrease in this same order.

It is not possible to correlate structural data with alkylation rates of Hg^{2+} by $H_2OCo(DH)_2R$ (Table 47). The steric bulk of the R group must influence the approach of Hg^{2+} and this steric effect dominates the rates in comparison with any electronic or steric intramolecular interaction. If anything, there is a reverse correlation between expected Co–C bond length and reactivity.

Recently, Bakac and Espenson [245] have examined the reversible alkyl group transfer between $(H_2O)_xCo(DBF_2)_2$ and Cr^{2+} in H_2O, pH 1.3, 25°C. For eqn. (12), where Co designates the $Co(DBF_2)_2$ unit

$$Cr^{2+} + CoR \overset{K}{\rightleftharpoons} CrR^{2+} + Co \qquad (12)$$

the value of K was found to be 6.43×10^{-2}, 3.70×10^{-3}, 2.80×10^{-3} and $\leqslant 10^{-5}$ for R = Me, C_2H_5, Bz, and CH_2OCH_3, respectively. It was felt that the dependence of K on R, except for the Bz reaction, reflects the lengthening of the *trans* Co–OH_2 bond as R *trans* influence increases and that this dependence provides good evidence for an S_H2 mechanism. Since the $H_2OCo(DBF_2)_2Bz$ complex undergoes unimolecular homolysis with a rate constant of 7.58×10^{-6} s^{-1} at 25°C, these workers were able to calculate k for the reverse reaction (8.8×10^7 M^{-1} s^{-1}) and to estimate the Co–C bond dissociation enthalpy as ca. 24 ± 3 kcal mol^{-1}.

Co(II). No five-coordinate $LCo(DH)_2$ complexes have been structurally characterized. However, the rates of halogen abstraction (Table 48) for complexes where L is a P donor ligand appear to depend on steric bulk [220]. Assessment of steric bulk by an X-ray method [71] or by an NMR method [162] for $PR_3Co(DH)_2X$ complexes leads to a close linear relationship. This dependence is illustrated in Fig. 18. Undoubtedly, the longer Co–P bond of bulky L destabilizes the Co(III) oxidation state relative to Co(II) [220].

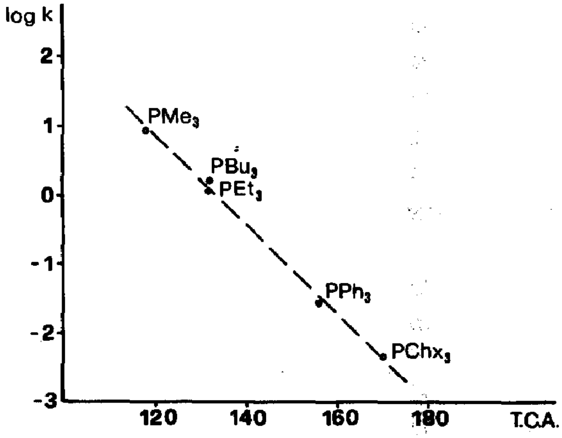

Fig. 18. Log k for halogen abstraction (Table 48, ref. 220) versus the Tolman cone angle, obtained by an X-ray method [71].

Co(I). No Co(I)$(DH)_2$ complexes have been studied crystallographically. No clear relationship exists between the data in Table 49 and structural data on cobaloximes.

Equilibrium studies

Formation constants (Tables 19, 43 and 50) are relatively independent of R, since both the forward and reverse rates are influenced similarly. Nevertheless, log K_f in DMSO (Table 50) vs. Co–N bond lengths in pyCo$(DH)_2$R are somewhat linearly related (plot not shown) and log K_f decreases with increasing bond distance.

As for other types of studies, correlation of structural and equilibrium data with changes in L is not fruitful since L usually changes in both electronic and steric properties. This would not be the case for 4-X–py compounds (Tables 42, 45, 51 and 52), where steric properties remain constant, but the structural data for comparisons are not available.

Electrochemical studies

Many of the studies involve L variation, and structural comparisons are difficult. Additionally, many studies involve substituted aryl or benzyl derivatives which have not been extensively studied by X-ray structural methods. However, Costa et al. [242] have found a very interesting relationship between $E_{1/2}$ for electrochemical oxidation of $H_2OCo(DH)_2R$ and the Co–C bond length of pyCo$(DH)_2$R (Fig. 19). However, the relationship is restricted to R groups which have no electronegative substituents. No appreciable Co–C bond shortening is expected for such compounds, but $E_{1/2}$ changes substantially. In Fig. 19, we have included an estimated value for $E_{1/2}$ based on the Co–C bond length in 3-N–Me–imidazole-Co$(DH)_2$adamantyl [246]. It would be interesting to know whether the

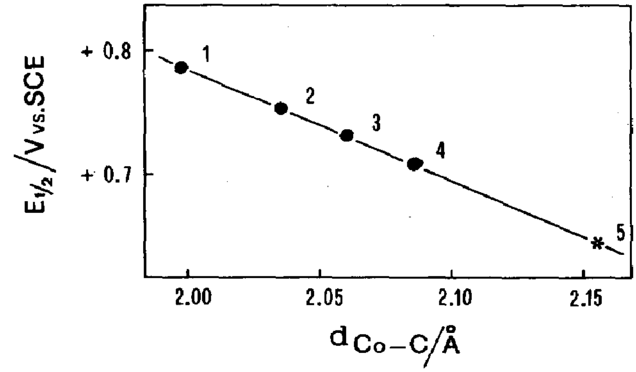

Fig. 19. $E_{1/2}$ for the electrochemical oxidation reaction of $H_2OCo(DH)_2R$ [246] versus Co–N(py) distance for pyCo$(DH)_2$R. R = 1, Me; 2, CH_2CH_3; 3, CH_2CMe_3; 4, i-C_3H_7; 5, adamantyl (estimated value of $E_{1/2}$).

actual $E_{1/2}$ will correspond to the estimated value. The effects of 3-N–Me–imidazole and py on Co–C bond length should be similar. The adamantyl compound was recently structurally characterized [246] and has the largest Co–C bond length accurately determined to date. It is also the first compound with a Co–C(tertiary) bond which has been structurally characterized.

(iii) Some final conclusions

We have identified a number of relationships between the solution and structural properties of cobaloximes. More recent solution studies have focused on compounds with R or L groups which have been well characterized by X-ray methods. Earlier studies, particularly the extensive studies of K.L. Brown, have involved many R groups for which structural data are absent. Since the major contributions to the structural and spectroscopic characterization and a considerable amount of the kinetic and equilibrium properties of cobaloximes have come from our laboratories, the most extensive correlations come from systematic variations in L when it is a P donor or in X when L is a pyridine ligand, the subjects of particular interest to workers in these laboratories. This emphasis should not be taken to imply that other types of systematic studies are not interesting or important. Recently, our interest has expanded to include joint studies with other equatorial ligand systems, particularly Schiff base complexes [126]. However, this review, even though restricted to $Co(DH)_2$ systems, is still quite extensive and topics selected for inclusion had to be restricted. For these same reasons, comparisons of various solutions studies were not made. A broader survey has appeared [105].

We have found the chemistry of organocobalt B_{12} models and the related chemistry of the non-organometallic compounds to be intriguing and informative transition-metal chemistry. As we hope that this review has demonstrated, these compounds, built on the $Co(DH)_2$ core, merit study in themselves. However, the biochemistry of cobalamins, currently incompletely understood and perhaps every bit as interesting as the models, has lured many investigators, including ourselves, into the study of the simpler organocobalt compounds where more definitive, if not as directly applicable, information can be obtained. The relevance of this cobaloxime chemistry to B_{12} is the subject of the next section.

E. IMPLICATIONS FOR B_{12} BIOCHEMISTRY

Some aspects of the relationship of B_{12} models to B_{12} biochemistry have recently been reviewed [112–117,247,248]. The biochemical steps of greatest interest to the transition-metal chemist are the Co–C bond cleavage step and the rearrangement reactions of the substrate [105,248]. Cobaloximes exhibit almost the full range of properties exhibited by other models, except that five-coordinate species have not been identified crystallographically. It is difficult to prepare an extensive variety of six-coordinate Schiff-base complexes [126] and no other series of models have been characterized with the large variety of axial ligands employed for cobaloximes. Prior to a consideration of the relevance of cobaloxime chemistry to B_{12} biochemistry, we first consider some aspects of B_{12} biochemistry. The reader is referred to the extensive review literature for more details [112–117,247,248].

(i) B_{12}-dependent processes

The reactions catalyzed by enzymes dependent on coenzyme B_{12} appear diverse but all can be categorized as vicinal 1,2-H interchanges according to either eqn. (13) or eqn. (14), with $X = NH_2$, COSCoA, $C(=CH_2)CO_2^-$, $CH(NH_3^+)CO_2^-$ (eqn. (13)) and $X = OH$ or NH_2 (eqn. (14)).

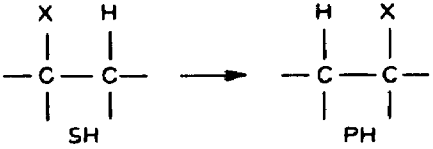

(13)

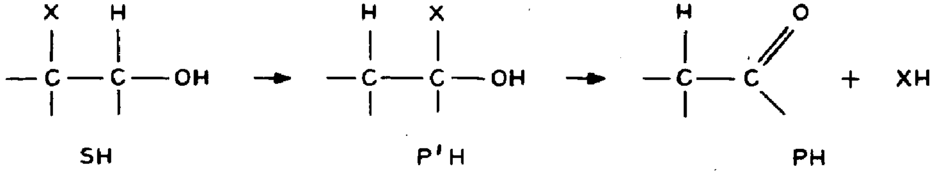

(14)

The ten known enzymic reactions represented by eqns. (13) and (14) are classified as follows [247]: class A if X is a migrating C group (eqn. (13)); class B if X is a migrating N group (eqn. (13)); and class C for the irreversible process in eqn. (14).

Examples of these processes are given in eqns. (15), (16), and (17).

Class A

(15)

Class B

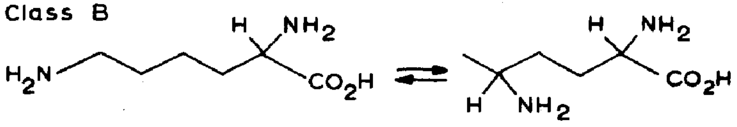

(16)

Class C

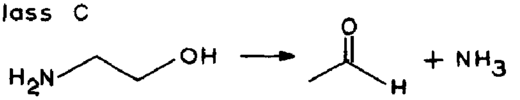

(17)

(ii) Role of cobalt

Halpern has suggested that one can view the role of coenzyme B_{12} as an "organic radical carrier" [249], since it is known that in the holoenzyme the coenzyme undergoes Co–C bond cleavage to generate cobal(II)amin (B_{12r}) and 5′-deoxyadenosyl radical. This cleavage is particularly evident when substrate (SH) is present [247]. The coenzyme is fairly stable in the absence of light. Upon mixing a B_{12}-dependent enzyme, such as diol dehydrase, with the coenzyme, conformational changes take place in both the enzyme and coenzyme and it is thought that this conformational change "triggers" the Co–C bond cleavage [41,49,57,69,81,112,126,250–256]. A better description might be that the conformational change "cocks" the "gun" and that the addition of substrate finally triggers the mechanism which leads to cleavage. These concepts are shown schematically in Scheme 2.

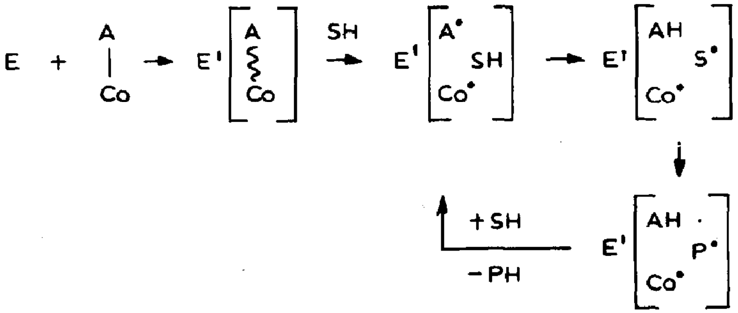

Scheme 2: Simplified description of B_{12}-dependent catalysis. E = apoenzyme; Co–A = coenzyme B_{12}; E′[ ] = conformationally changed enzyme and its active site pocket; Co ~~ A = conformationally changed coenzyme with a weakened Co–C bond; Co· = B_{12} r; A· = 5′-deoxyadenosine radical, enzyme bound; S· and P· are substrate and product radicals.

The predominant EPR-active species are substrate derived [247]. The possibility that Co–C bond formation occurs after the formation of $S^{\cdot}$ by the combination of B_{12}r and $S^{\cdot}$ has caused much speculation and controversy. However, there is essentially universal agreement that the Co–C bond cleaves and that this process is promoted by a conformational change.

(iii) Cleavage step and model compounds

Unfortunately, no direct information exists on the nature of the conformational change of the coenzyme. One can conceive of various factors which could contribute to the cleavage and test these ideas with models. With little to guide us from the enzymic studies, the present authors [41,49,57,69,81,126] and others [112,247–255] have put forward various ideas, most of which can be and have been evaluated with cobaloximes.

We will now list these possibilities and then discuss them in the same order. Thus the enzyme could induce (a) a corrin distortion which increases steric interaction with 5′Ado; (b) a change in the position of the benzimidazole which induces a corrin distortion as in (a); (c) a corrin distortion which lengthens the Co–N (benzimidazole) bond; (d) a direct lengthening or shortening of the Co–C bond. Of course, combinations of effects are also possible.

(a) Corrin distortion–steric cis *influence*

This was the first idea proposed [41,49,69,250–256]. The experimental evidence derives from the observation that changes in the corrin side-chains, such as the conversion of an amide to a carboxyl group, led to analogues which were much less active than the coenzyme [250–252]. Since an inductive effect could not account for the change in activity, it was suggested that the coenzyme side-chains held the coenzyme to the enzyme and that the conformational change in turn involved the corrin.

In cobalamins, it was known that steric factors influenced Co–C bond stability since, for example, isopropyl cobalamin is unstable [255]. Perhaps the isopropyl group influenced the corrin ring pucker or otherwise caused a distortion at Co which weakened the Co–C bond.

Cobaloximes provided an experimental test of these ideas. In 1979, we examined the structure of pyCo(DH)$_2$i-C$_3$H$_7$ (Fig. 20) [41]. This compound was remarkable in that the Co–C bond length was 2.085 Å, the longest such

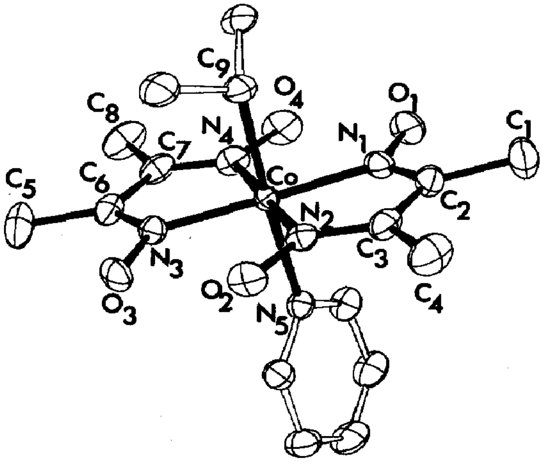

Fig. 20. ORTEP drawing of pyCo(DH)$_2$i-C$_3$H$_7$; from ref. 41.

bond ever observed. In addition, there was no distortion of the rest of the cobaloxime, suggesting a similar lengthening in Co–C bond length in isopropyl cobalamin. This conclusion has now been widely accepted [112,248,249,254], although there is still no direct evidence for such lengthening in isopropyl cobalamin.

In a pioneering study of steric effects, the structure of $PPh_3Co(DH)_2i\text{-}C_3H_7$ appeared to reveal the effect on the Co–C bond length of the distortion (butterfly bending) of the $Co(DH)_2$ moiety [49]. The Co–C bond length (although inaccurate owing to disorder) was 2.22 Å and the α bending towards $i\text{-}C_3H_7$ was 14°. These values can be compared with those in the py analogue of 2.085 Å and 4°. However, the structure of the closely related PPh_3 compound with $R = 2\text{-}C_4H_9$ [79] reveals much less distortion ($\alpha = 5°$ and Co–C = 2.11 Å). Since the two PPh_3 compounds have almost identical solution properties, it must be concluded that packing forces modulate the distortions.

Nevertheless, the relationship between Co–C bond length and α bending has been established for the series $LCo(DH)_2CH_2CMe_3$. With L of increasing bulk (H_2O, py, PMe_3, PPh_3) the Co–C bond lengths and α bending increase from 2.044 to 2.111 Å and −7 to 2°, respectively. For the related series with R = Me, the Co–C distances vary only from 1.978 to 2.026 Å but the α bending changes from −4 to +14°.

The above results for CH_2CMe_3 and $i\text{-}C_3H_7$ compounds clearly demonstrate a relationship between L bulk and Co–C bond length. It was assumed that Co–C bond energies decrease with increasing Co–C bond length and this assumption is strongly supported by the work of Halpern and co-workers on $LCo(DH)_2CHMePh$ compounds [218].

This relationship between Co–C bond energy and equatorial ligand distortion suggests a possible mechanism for Co–C bond homolysis in enzyme processes [69]. A small rotation about the Co–N bond of the benzimidazole caused by the protein could induce a distortion sufficient to promote Co–C bond cleavage.

(b) Benzimidazole-induced corrin distortion

The benzimidazole in coenzyme B_{12} lies over six-membered chelate rings and the Co–N(3)–C angles are unsymmetrical to avoid contact of the benzimidazole six-membered ring with the corrin [113]. Any distortion which moved the benzimidazole over the five-membered chelate ring [126] or increased interaction of the benzimidazole six-membered ring with the corrin could induce a change in corrin pucker which could weaken the Co–C bond by enhancing repulsive interactions between the corrin and the 5′-deoxyadenosine. No crystallographic evidence currently exists for this type of relationship, although the relationship of the orientation of planar L ligands with respect to the size of the equatorial chelate rings has been considered [126].

(c) Corrin distortion with Co–N bond lengthening

The most clear-cut relationship between Co–C bond energy and a structural parameter is that between the Co–C bond strength and axial Co–N bond length [81,126]. This relationship has led us to point out that a lengthening of the Co–N bond by a corrin distortion could also promote Co–C bond cleavage. A good axial donor stabilizes the Co(III) oxidation state [217] and lengthening of the Co–N bond decreases electron donation and destabilizes Co(III).

(d) Direct lengthening or shortening of the Co–C bond

If, via interaction of the benzimidazole side chain with the enzyme, the conformational change involved a lengthening of the Co–N bond, the Co–C bond cleavage would be favored. Conceivably, Co–N bond shortening by a similar process could weaken the Co–C bond by a direct *trans* influence. The Co–C bonds in P donor complexes do appear to be slightly longer than those in N donor complexes [79]. Such compression could also increase benzimidazole corrin interactions, leading to a STI which will also weaken the Co–C bond. A counteracting aspect of such a shortening would be an increase in Co(III) stability.

(e) Direct lengthening or angular distortion of the Co–C bond

The simplest conceivable conformational effect would be direct stress on the Co–C bond. Interaction of the 5′Ado with the enzyme could lead to a "pulling" or "bending" of the Co–C bond which would weaken it. Work with substituted R groups [41,57,69,81,246,257] reveals that the Co–C bond can be stretched easily and, therefore, the enzyme may be able to do this directly. Rather large distortions of Co–C–C bond angles were found in $LCo(DH)_2neo\text{-}C_5H_{11}$ compounds (Fig. 21). For L = py the value for the Co–C–C angle is 130° [57]. Neopentyl derivatives of cobalamins are known to be rather unstable [254,258], as are neopentyl derivatives in some B_{12} model systems [259,260]. However, in cobaloximes, neopentyl compounds appear to be relatively stable.

In summary, several reasonable alternatives exist for the nature of the conformational change which induces Co–C bond cleavage. More work is required on both model systems and the enzymes in order to define better the nature of the most important effects. Until such time, the above discussion should be considered to be primarily a basis for stimulating further studies.

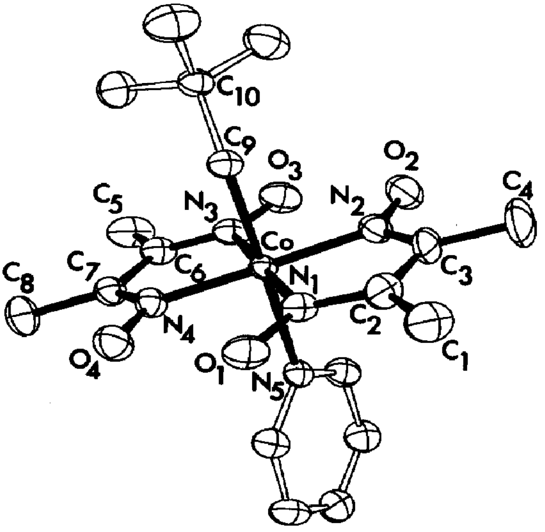

Fig. 21. ORTEP drawing of $pyCo(DH)_2CH_2CMe_3$; from ref. 57.

(iv) Rearrangement step

The majority of work in this area was reviewed by Finke [248] in this journal. The rearrangements may be that of enzyme-bound $S^{\cdot}$ with no participation by Co. Most model studies have involved the formation of organocobalt compounds with an alkyl group poised for rearrangement. For example, Retey [261] has studied the rearrangement of $Co{-}CH_2{-}C(CH_3)(CO_2Et)_2$ compounds upon photolysis. One role that one can conceive for the cobalt moiety would be to induce steric strain into the alkyl group and thus induce rearrangement. As discussed above, there are angular distortions induced in alkyl groups bound to cobaloximes. Such a distortion could position the alkyl group for rearrangement, if the substrate radical forms a direct bond to Co. We have examined the structures of $LCo(DH)_2CH_2C(CH_3)(CO_2Et)_2$ with $L = py$ and PPh_3 and have found no evidence for distortion [79]. However, most Co–C intermediates derived from B_{12} enzyme substrates would be more sterically constrained than these particular model species. It is clear from the instability of the isopropyl cobalamin compound relative to the stability of most $LCo(DH)_2i\text{-}C_3H_7$ compounds, that steric factors are probably more important in cobalamins than in cobaloximes. While this relationship suggests that a Co–C bonded intermediate would be more strained and, hence, more prone to undergo rearrangement, it also makes it less likely that such intermediates would form in the first place. In any case, it certainly is less likely that a knowledge of organocobalamin structures will be helpful in understanding the rearrangement step than that such knowledge will be helpful in understanding the Co–C bond cleavage step.

ACKNOWLEDGEMENTS

The authors are grateful to NIH (GM 29225) for a grant awarded to L.G.M., and to C.N.R. (Rome) and M.P.I. (Rome) for grants awarded to L.R. We are grateful to our past and present co-workers for their contributions to these studies, especially Drs. Epps, Ramsden, Calligaris, Stewart, Sandercock, Trogler, P. Marzilli, Nardin, and Zangrando. We also thank Drs. K.L. Brown, Costa, Crumbliss, Espenson, and Puxeddu for providing unpublished data. L.G.M. thanks the Alexander von Humboldt Foundation for a Senior U.S. Scientist Award which facilitated his contribution to this review.

REFERENCES

1 P.G. Lenhert, J. Chem. Soc. Chem. Commun., (1967) 980; axial bonds are as quoted by J.P. Glusker (see ref. 113).
2 M.W. Bartlett and J.D. Dunitz, Helv. Chim. Acta, 54 (1971) 2753.
3 A. Chiaroni and C. Pascard-Billy, Bull. Soc. Chim. Fr., (1973) 781.
4 W.W. Adams and P.G. Lenhert, Acta Crystallogr., Sect. B, 29 (1973) 2412.
5 Y. Ohasi, Y. Sasada, Y. Tashiro, Y. Ohgo, S. Takeuchi and J. Yoshimura, Bull. Chem. Soc. Jpn., 46 (1973) 2589.
6 A.L. Crumbliss, J.T. Bowman, P.L. Gaus and A.T. McPhail, J. Chem. Soc. Chem. Commun., (1973) 415.
7 M.M. Botoshanskii, Yu.A. Simonov and T.I. Malinovskii, Izv. Akad. Nauk Mold. SSR, (1973) 39; Chem. Abstr., 80 (1973) 41857y.
8 S. Bruckner and L. Randaccio, J. Chem. Soc. Dalton Trans., (1974) 1017.
9 L.P. Battaglia, A. Bonamartini-Corradi, C. Grasselli Palmieri, M. Nardelli and M.E. Vidoni Tani, Acta Crystallogr., Sect. B, 30 (1974) 1114.
10 A.V. Ablov, A.A. Dvorkin, Y.A. Simonov, O.A. Bologa and T.I. Malinovskii, Dokl. Akad. Nauk SSSR, 217 (1974) 89 (English translation).
11 D.L. McFadden and A.T. McPhail, J. Chem. Soc. Dalton Trans., (1974) 363.
12 L. Randaccio and E. Zangrando, Cryst. Struct. Commun., 3 (1974) 565.
13 P.D. Ginderow, Acta Crystallogr., Sect. B, 31 (1975) 1092.
14 D.A. Stotter, G.M. Sheldrick and R. Taylor, J. Chem. Soc. Dalton Trans., (1975) 2124.
15 D. Dodd, M.D. Johnson, I.P. Steeples and E.D. McKenzie, J. Am. Chem. Soc., 98 (1976) 6399.
16 L.G. Marzilli, L.A. Epps, T. Sorrell and T.J. Kistenmacher, J. Am. Chem. Soc., 97 (1975) 3351.
17 I. Leban, Vestn. Slov. Kem. Drus., 22 (1975) 27; Chem. Abstr., 86 (1975) 64008s.
18 M.M. Botoshanskii, Yu.A. Simonov, T.I. Malinovskii and M.A. Simonov, Dokl. Chem., 225 (1975) 625 (in English).
19 M.M. Botoshanskii, Yu.A. Simonov, T.I. Malinovskii and M.A. Simonov, Sov. Phys. Crystallogr., 20 (1975) 34 (in English).

20 Y.A. Simonov, A.A. Dvorkin, A.V. Ablov, T.I. Malinovskii and O.A. Bologna, Koord. Khim., 1 (1975) 1284.

21 A.A. Dvorkin, Yu.A. Simonov, O.A. Bologa and A.V. Ablov, Dokl. Akad. Nauk SSSR, 220 (1975) 156 (in English translation).

22 M.M. Botoshanskii, Yu.A. Simonov and T.I. Malinovskii, Izv. Akad. Nauk Mold. SSR, (1975) 24; Chem. Abstr., 84 (1975) 187849h.

23 G.J. Palenik, D.A. Sullivan and D.V. Naik, J. Am. Chem. Soc., 98 (1976) 1177.

24 C. Giannotti, C. Fontaine, A. Chiaroni and C. Riche, J. Organomet. Chem., 113 (1976) 57.

25 A. Bigotto, E. Zangrando and L. Randaccio, J. Chem. Soc. Dalton Trans., (1976) 96.

26 Y. Ohashi and Y. Sasada, Nature (London), 267 (1977) 142.

27 Y. Ohashi and Y. Sasada, Bull. Chem. Soc. Jpn., 50 (1977) 1710.

28 Y. Ohashi and Y. Sasada, Bull. Chem. Soc. Jpn., 50 (1977) 2863.

29 E.D. McKenzie, Inorg. Chim. Acta, 29 (1978) 107.

30 T. Saito, Bull. Chem. Soc. Jpn., 51 (1978) 169.

31 Y. Ohashi, Y. Sasada and Y. Ohgo, Chem. Soc. Jpn. Chem. Lett., (1978) 457.

32 Y. Ohashi, Y. Sasada and Y. Ohgo, Chem. Soc. Jpn. Chem. Lett., (1978) 743.

33 A. Clearfield, R. Gopal, R.J. Kline, M. Sipaki and L.O. Urban, J. Coord. Chem., 8 (1978) 5.

34 M.M. Botoshanskii, Yu.A. Simonov, A.V. Ablov, T.I. Malinovskii, G.P. Syrtsova and L.N. Istru, J. Struct. Chem., 19 (1978) 427.

35 L.A. Nemchinova, Yu.A. Simonov, A.V. Ablov, T.I. Malinovskii and O.A. Bologa, Sov. J. Coord. Chem., 4 (1978) 86.

36 M.M. Botoshanskii, Yu.A. Simonov, A.V. Ablov, T.I. Malinovskii and O.A. Bologa, Dokl. Chem., 240 (1978) 296 (English translation).

37 Yu.A. Simonov, M.M. Botoshanskii, T.J. Malinovskii, A.V. Ablov and L.A. Nemchinova, Sov. J. Coord. Chem., 4 (1978) 830.

38 N. Bresciani-Pahor, M. Calligaris and L. Randaccio, Inorg. Chim. Acta, 27 (1978) 47.

39 G.D. Stucky and J.S. Swanson, personal communication.

40 N. Bresciani-Pahor, M. Calligaris, L. Randaccio and L.G. Marzilli, Inorg. Chim. Acta, 32 (1979) 181.

41 L.G. Marzilli, P.J. Toscano, L. Randaccio, N. Bresciani-Pahor and M. Calligaris, J. Am. Chem. Soc., 101 (1979) 6754.

42 Yu.A. Simonov, M.M. Botoshanskii, A.V. Ablov, L.N. Istru, C.P. Syrtsova and T.L. Malinovskii, Sov. Phys. Crystallogr., 24 (1979) 274.

43 A.I. Shkurpelo and Yu.A. Siminov, Izv. Akad. Nauk Mold. SSR, (1979) 46.

44 M.J. Heeg and R.C. Eder, Inorg. Chem., 19 (1980) 932.

45 N. Bresciani-Pahor, M. Calligaris and L. Randaccio, Inorg. Chim. Acta, 39 (1980) 173.

46 Yu.A. Simonov, A.I. Shkurpelo and T.I. Malinovskii, Izv. Akad. Nauk Mold. SSR, (1980) 37.

47 A.I. Shkurpelo, Yu.A. Simonov and O.A. Bologa, Sov. Phys. Crystallogr., 25 (1980) 739.

48 N.E. Takach, E.M. Holt, N.W. Alcock, R.A. Henry and J.H. Nelson, J. Am. Chem. Soc., 102 (1980) 2968.

49 L. Randaccio, N. Bresciani-Pahor, P.J. Toscano and L.G. Marzilli, J. Am. Chem. Soc., 102 (1980) 7372.

50 T. Saito, H. Urabe and Y. Sasaki, Transition Met. Chem., 5 (1980) 35.

51 Yu.A. Simonov, A.J. Skurpelo, N.M. Camus, E.L. Belokoneva and J.D. Camus, Koord. Khim., 6 (1980) 1107 (in Russian).

52 Y. Ohashi, Y. Sasada, S. Takeuchi and Y. Ohgo, Bull. Chem. Soc. Jpn., 53 (1980) 627.

53 Y. Ohashi, Y. Sasada, S. Takeuchi and Y. Ohgo, Bull. Chem. Soc. Jpn., 53 (1980) 1501.
54 N. Bresciani-Pahor, M. Calligaris and L. Randaccio, J. Organomet. Chem., 184 (1980) C53.
55 T. Saito, Y. Tsurita and Y. Sasaki, Inorg. Chem., 19 (1980) 2365.
56 R.C. Elder, A. Nerone and J.C. Barrick, Acta Crystallogr., Sect. B, 36 (1980) 2428.
57 L. Randaccio, N. Bresciani-Pahor, P.J. Toscano and L.G. Marzilli, J. Am. Chem. Soc., 103 (1981) 6347.
58 L. Randaccio, N. Bresciani-Pahor, P.J. Toscano and L.G. Marzilli, Inorg. Chem., 20 (1981) 2722.
59 N. Bresciani-Pahor, M. Calligaris, G. Nardin and L. Randaccio, Gazz. Chim. Ital., 111 (1981) 147.
60 P.J. Toscano, C.C. Chiang, T.J. Kistenmacher and L.G. Marzilli, Inorg. Chem., 20 (1981) 1513.
61 N. Bresciani-Pahor, L. Randaccio, P.J. Toscano, A.C. Sandercock and L.G. Marzilli, J. Chem. Soc. Dalton Trans., (1982) 129.
62 N. Bresciani-Pahor, L. Randaccio, P.J. Toscano and L.G. Marzilli, J. Chem. Soc. Dalton Trans., (1982) 567.
63 S. Alvarez and C. Lopez, Inorg. Chim. Acta, 64 (1982) L99.
64 D. Schomburg, personal communication.
65 M. Van Hooste, A.T.H. Lenstra, M. Kwiecinski and S. Tyrlik, Transition Met. Chem., 7 (1982) 50.
66 N. Bresciani-Pahor, M. Calligaris, L. Randaccio and P.J. Toscano, J. Chem. Soc. Dalton Trans., (1982) 1009.
67 T. Kurihara, Y. Ohashi and Y. Sasada, Acta Crystallogr., Sect. B, 38 (1982) 2484.
68 N. Bresciani-Pahor, G. Nardin, L. Randaccio and E. Zangrando, Inorg. Chim. Acta, 65 (1982) L143.
69 N. Bresciani-Pahor, M. Calligaris, G. Nardin and L. Randaccio, J. Chem. Soc. Dalton Trans., (1982) 2549.
70 A.T.H. Lenstra, J.F.J. Van Loock, S.K. Tyrlik and H. Stapowska, Bull. Soc. Chim. Belg., 91 (1982) 917.
71 N. Bresciani-Pahor, L. Randaccio and P.J. Toscano, J. Chem. Soc. Dalton Trans., (1982) 1559.
72 L. Boscarol, Dh. Thesis, University of Trieste, 1982.
73 N. Bresciani-Pahor, J.D. Orbell and L. Randaccio, Croat. Chem. Acta, 57 (1984) 433.
74 N. Bresciani-Pahor, M. Calligaris, L. Randaccio, L.G. Marzilli, M.F. Summers, P.J. Toscano, J. Grossman and D. Liotta, Organometallics, (1985) in press.
75 M.N. Ponnuswany and J. Trotter, Acta Crystallogr., Sect. C, 39 (1983) 726.
76 M. Megnanisi-Belombe, H. Endres and E. Rossato, Acta Crystallogr., Sect. C, 39 (1983) 705.
77 N. Bresciani-Pahor, L. Randaccio, M. Summers and P.J. Toscano, Inorg. Chim. Acta, 68 (1983) 69.
78 A.T.H. Lenstra, H.J. Beise and S.H. Tyrlik, personal communication.
79 L. Randaccio, N. Bresciana-Pahor, J.D. Orbell, M. Calligaris, M.F. Summers, B. Snyder, P.J. Toscano and L.G. Marzilli, Organometallics, (1985) in press.
80 L.G. Marzilli, M.F. Summers, J.H. Ramsden, N. Bresciani-Pahor and L. Randaccio, J. Chem. Soc. Dalton Trans., (1984) 511.
81 M.F. Summers, P.J. Toscano, N. Bresciani-Pahor, G. Nardin, L. Randaccio and L.G. Marzilli, J. Am. Chem. Soc., 105 (1983) 6259.
82 T. Kurihara, Y. Ohashi and Y. Sasada, Acta Crystallogr., Sect. B, 38 (1982) 2484.

83 Y. Ohashi, K. Yanagi, T. Kurihara, Y. Sasada and Y. Ohgo, J. Am. Chem. Soc., 104 (1982) 6353.

84 R. Kergoat, M.M. Kubicki, J.E. Guerchais and J.A.K. Howard, J. Chem. Res., (1982) 340.

85 Y. Ohashi, A. Uchida, Y. Sasada and Y. Ohgo, Acta Crystallogr., Sect. B, 39 (1983) 54.

86 T. Kurihara, Y. Ohashi, Y. Sasada and Y. Ohgo, Acta Crystallogr., Sect. B, 39 (1983) 243.

87 T. Kurihara, A. Uchida, Y. Ohashi, Y. Sasada, Y. Ohgo and S. Baba, Acta Crystallogr., Sect. B, 39 (1983) 431.

88 X. Solans, M. Font-Altaba and J.L. Brianso, Z. Kristallogr., 162 (1983) 305.

89 See ref. 88.

90 D. Lenoir, H. Dauner, I. Ugi, A. Gieren, R. Hubner and V. Lamm, J. Organomet. Chem., 198 (1980) C39.

91 J. Schaffler, B. Deppisch and J. Rétey, Chem. Ber., 115 (1982) 2229.

92 R.R. Whittle, Ph.D. Thesis (Diss. Abstr. Int., 42 (1981) 1884B.

93 A.V. Ablov and I.D. Samus, Dokl. Chem., 146 (1962) 872; 193 (1970) 333.

94 Yu.A. Simonov, A.A. Dvorkin, O.A. Bologa, A.V. Ablov and T.I. Malinovskii, Dokl. Chem., 210 (1973) 433 (English translation).

95 D.L. McFadden, Ph.D. Thesis (Diss. Abstr. Int., 3376 (1976) B36).

96 I.F. Burstein, Yu.A. Simonov, B.M. Shchedrin, T.I. Malinovskii and V.N. Shafranskii, Dokl. Akad. Nauk SSSR, 222 (1975) 83.

97 S.T. Malinovskii, Yu.A. Simonov, A.V. Ablov, N.M. Samus and T.I. Malinovskii, Dokl. Akad. Nauk SSSR, 236 (1977) 1357.

98 L.A. Nemchinova, Yu.A. Simonov, A.V. Ablov, T.I. Malinovskii and O.A. Bologa, Sov. J. Coord. Chem., 4 (1978) 86.

99 L.M. Minichuk, M.J. Mombourquette, F.W.B. Einstein and A.C. Willis, Inorg. Chim. Acta, 63 (1982) 189.

100 N.W. Alcock, M.P. Atkins, B.T. Golding and P.J. Sellars, J. Chem. Soc. Dalton Trans., (1982) 337.

101 F. Kubel and J. Strahle, Z. Naturforsch., Teil B, 36 (1981) 441.

102 F. Kubel and J. Strahle, Z. Naturforsch., Teil B, 37 (1982) 272.

103 G.D. Fallon and B.M. Gatehouse, Cryst. Struct. Commun., 7 (1978) 263.

104 W.R. Cullen, D. Dolphin, F.W.B. Einstein, L.M. Minichuk and A.C. Willis, J. Am. Chem. Soc., 101 (1979) 6898.

105 P.J. Toscano and L.G. Marzilli, Prog. Inorg. Chem., 31 (1984) 105.

106 G. Costa, G. Mestroni, T. Licari and E. Mestroni, Inorg. Nucl. Chem. Lett., 5 (1969) 561.

107 J.H. Dimmit and J.H. Weber, Inorg. Chem., 21 (1982) 700.

108 D. Dodd and M.D. Johnson, J. Organomet. Chem., 52 (1973) 1.

109 J.M. Pratt and P.J. Craig, Adv. Organomet. Chem., 11 (1973) 331.

110 N.M. Samus and A.V. Ablov, Coord. Chem. Rev., 28 (1979) 177.

111 G.N. Schrauzer, Acc. Chem. Res., 1 (1968) 97.

112 D. Dolphin (Ed.), B_{12}, Vols. 1 and 2, Wiley, New York, 1982.

113 J.P. Glusker, in D. Dolphin (Ed.), B_{12}, Vol. 1, Wiley, New York, 1982, p. 23.

114 K.L. Brown, in D. Dolphin (Ed.), B_{12}, Vol. 1, Wiley, New York, 1982, p. 245.

115 H.P.C. Hogenkamp, in D. Dolphin (Ed.), B_{12}, Vol. 1, Wiley, New York, 1982, p. 295.

116 J. Halpern, in D. Dolphin (Ed.), B_{12}, Vol. 1, Wiley, New York, 1982, p. 501.

117 B.T. Golding, in D. Dolphin (Ed.), B_{12}, Vol. 1, Wiley, New York, 1982, p. 543.

118 C.L. Raston, D.W. Skelton and A.H. White, Aust. J. Chem., 33 (1980) 1519.

119 G.A. Jeffrey, J.R. Ruble and J.A. Pople, Acta Crystallogr., Sect. B, 38 (1982) 1975.

120 N. Bresciani-Pahor, M. Calligaris, P. Delise, G. Dodie, G. Nardin and L. Randaccio, J. Chem. Soc. Dalton Trans., (1976) 2478.
121 N. Bresciani-Pahor, M. Calligaris, G. Nardin and L. Randaccio, Acta Crystallogr., Sect. B, 34 (1978) 1360.
122 N. Bresciani-Pahor, M. Calligaris, G. Nardin, L. Randaccio and D. Viterbo, Acta Crystallogr., Sect. B, 35 (1979) 2276.
123 A. Clearfield, R. Gopal, R.J. Kline, M. Sipski and L.O. Urban, J. Coord. Chem., 7 (1978) 163.
124 M. Calligaris, G. Nardin and L. Randaccio, Inorg. Nucl. Chem. Lett., 8 (1972) 477.
125 M. Calligaris, G. Nardin and L. Randaccio, J. Chem. Soc. A, (1972) 1433.
126 M.F. Summers, L.G. Marzilli, N. Bresciani-Pahor and L. Randaccio, J. Am. Chem. Soc., 106 (1984) 4478.
127 G. De Alti, V. Galasso, A. Bigotto and G. Costa, Inorg. Chim. Acta, 3 (1969) 533.
128 L.G. Marzilli, P.J. Toscano, J.H. Ramsden, L. Randaccio and N. Bresciani-Pahor, Adv. Chem. Ser., 196 (1982) 85.
129 C.A. Tolman, Chem. Rev., 77 (1977) 313.
130 We also find that this relationship seems to extend to C donors. See data in refs. 30 and 50.
131 J.S. Dewar, H. Kollmar and W.K. Li, J. Chem. Educ., 52 (1975) 305.
132 G. Gilli and V. Bertolasi, J. Chem. Educ., 60 (1983) 630.
133 J.P. Birk, P.B. Chock and J. Halpern, J. Am. Chem. Soc., 90 (1968) 6959.
134 W.K. Wilmarth, K.R. Ashley, J.C. Harmon, J. Fredricks and A.L. Crumbliss, Coord. Chem. Rev., 51 (1983) 225.
135 A.V. Ablov and M.P. Filippov, Russ. J. Inorg. Chem., 7 (1962) 525.
136 K.L. Brown, J. Am. Chem. Soc., 101 (1979) 6600.
137 K.L. Brown and R.K. Hessley, Inorg. Chem., 19 (1980) 2410.
138 A.B. Cartano and L.L. Ingraham, Bioinorg. Chem., 7 (1977) 351.
139 K.L. Brown and D. Jinkerson, J. Organomet. Chem., 164 (1979) 203.
140 K.L. Brown, J. Chem. Soc. Chem. Commun., (1981) 598 and references therein.
141 G.N. Schrauzer and E. Deutsch, J. Am. Chem. Soc., 91 (1969) 3341.
142 A. Bakac and J.H. Espenson, Inorg. Chim. Acta, 30 (1978) L329.
143 A. Bakac and J.H. Espenson, Inorg. Chem., 19 (1980) 242.
144 P. Abley, E.R. Dockal and J. Halpern, J. Am. Chem. Soc., 95 (1973) 3166.
145 K.L. Brown, D. Lyles, M. Pencovici and R.G. Kallen, J. Am. Chem. Soc., 97 (1975) 7338.
146 K.L. Brown, D. Chernoff, D.J. Keljo and R.G. Kallen, J. Am. Chem. Soc., 94 (1972) 6697.
147 A.V. Ablov and M.P. Filippov, Russ. J. Inorg. Chem., 5 (1960) 1311.
148 B.A. Bovykin, Russ. J. Inorg. Chem., 17 (1972) 89.
149 G.P. Syrtsova, Russ. J. Inorg. Chem., 17 (1972) 91.
150 R.W. Taft, in M.S. Newman (Ed.), Steric Effects in Organic Chemistry, Wiley, New York, 1956, Ch. 13.
151 T.G. Appleton, H.C. Clark and L.E. Manzer, Coord. Chem. Rev., 10 (1973) 335.
152 H.A.O. Hill and K.G. Morallee, J. Chem. Soc. A, (1969) 554.
153 W.C. Trogler, R.C. Stewart, L.A. Epps and L.G. Marzilli, Inorg. Chem., 13 (1974) 1564.
154 L.G. Marzilli, P. Politzer, W.C. Trogler and R.C. Stewart, Inorg. Chem., 14 (1975) 2389.
155 M.M. Gofman and V.I. Nefedov, Inorg. Chim. Acta, 28 (1978) 1.
156 R.C. Stewart and L.G. Marzilli, Inorg. Chem., 16 (1977) 424.
157 P.J. Toscano, unpublished results.
158 H.M. McConnell, J. Chem. Phys., 27 (1957) 226.

159 J.P. Fox, R. Banninger, R.T. Proffitt and L.L. Ingraham, Inorg. Chem., 11 (1972) 2379.

160 (a) R.J. Guschl and T.L. Brown, Inorg. Chem., 13 (1974) 959. (b) T.L. Brown, L.M. Ludwick and R.S. Stewart, J. Am. Chem. Soc., 94 (1972) 384.

161 C. Bied-Charreton and A. Gaudemer, Tetrahedron Lett., (1969) 4189.

162 (a) W.C. Trogler and L.G. Marzilli, Inorg. Chem., 14 (1975) 2942. (b) W.C. Trogler and L.G. Marzilli, J. Am. Chem. Soc., 96 (1974) 7589.

163 (a) C.A. Streuli, Anal. Chem., 32 (1960) 985. (b) W.A. Henderson and C.A. Streuli, J. Am. Chem. Soc., 82 (1960) 5791.

164 C.A. Tolman, J. Am. Chem. Soc., 92 (1970) 2953.

165 D.N. Hendrickson and W.L. Jolly, Inorg. Chem., 9 (1970) 1197.

166 M.D. Johnson and G.J. Lewis, J. Chem. Soc. A, (1970) 2153.

167 R.C. Stewart, unpublished results.

168 J.A. Mosbo, J.R. Pipal and J.G. Verkade, J. Magn. Reson., 8 (1972) 243.

169 J. Mosbo and J.G. Verkade, J. Magn. Reson., 8 (1972) 250.

170 H.A.O. Hill, K.G. Morallee and R.E. Collis, J. Chem. Soc. Chem. Commun., (1967) 888.

171 G.N. Schrauzer and R.J. Windgassen, J. Am. Chem. Soc., 88 (1966) 3738.

172 R.D. Gillard and G. Wilkinson, J. Chem. Soc., (1963) 6041.

173 P.J. Toscano and L.G. Marzilli, Inorg. Chem., 18 (1979) 421.

174 J.A. Kargol, R.W. Crecely, J.L. Burmeister, P.J. Toscano and L.G. Marzilli, Inorg. Chim. Acta, 40 (1980) 79.

175 M.F. Summers, unpublished results.

176 C. Bied-Charreton, B. Septe and A. Gaudemer, Org. Magn. Reson., 7 (1975) 116.

177 J. Huet and A. Gaudemer, Org. Magn. Reson., 20 (1982) 4.

178 J.F. Nixon and A. Pidcock, Ann. Rev. NMR Spectrosc., 2 (1969) 345.

179 C.W. Fong and M.D. Johnson, J. Chem. Soc. Perkin Trans., 2 (1973) 986.

180 D. Dodd, M.D. Johnson and C.W. Fong, J. Chem. Soc. Dalton Trans., (1974) 58.

181 K.L. Brown and L. Lu, Inorg. Chem., 20 (1981) 4178.

182 R.A. LaRossa and T.L. Brown, J. Am. Chem. Soc., 96 (1974) 2072.

183 B.E. Reichert and B.O. West, J. Chem. Soc. Chem. Commun., (1974) 177.

184 G.N. Schrauzer, L.P. Lee and J.W. Sibert, J. Am. Chem. Soc., 92 (1970) 2997.

185 A. Blanco-Labra, A. Cartano, M. Chu and L.L. Ingraham, Bioinorg. Chem., 4 (1975) 99.

186 D. Dodd and M.D. Johnson, J. Chem. Soc. Dalton Trans., (1973) 1218.

187 R.A. Firth, H.A.O. Hill, J.M. Pratt, R.G. Thorp and R.J.P. Williams, J. Chem. Soc. A, (1968) 2428.

188 K.L. Brown and A.W. Awtrey, Inorg. Chem., 17 (1978) 111.

189 S.C. Chan and P.Y. Leang, Aust. J. Chem., 22 (1969) 2569.

190 V.R. Vijayaraghavan and M. Santappa, J. Inorg. Nucl. Chem., 36 (1974) 163.

191 D.N. Hague and J. Halpern, Inorg. Chem., 6 (1967) 2059.

192 P.H. Tewari, R.W. Gaver, H.K. Wilcox and W.K. Wilmarth, Inorg. Chem., 6 (1967) 611.

193 J.M. Palmer and E. Deutsch, Inorg. Chem., 14 (1975) 17.

194 L. Seibles and E. Deutsch, Inorg. Chem., 16 (1977) 2273.

195 K.L. Brown and R.G. Kallen, J. Am. Chem. Soc., 94 (1972) 1894.

196 H.G. Tsiang and W.K. Wilmarth, Inorg. Chem., 7 (1968) 2535.

197 L.G. Marzilli, J.G. Salerno and L.A. Epps, Inorg. Chem., 11 (1972) 2050.

198 L.A. Epps and L.G. Marzilli, J. Chem. Soc. Chem. Commun., (1972) 109.

199 L.G. Marzilli, R.C. Stewart, L.A. Epps and J.B. Allen, J. Am. Chem. Soc., 95 (1973) 5796.

200 L.G. Marzilli, Inorg. Chem., 11 (1972) 2504.

201 G. Costa, G. Tauzher and A. Puxeddu, Inorg. Chim. Acta, 3 (1969) 41.

202 R.J. Guschl and T.L. Brown, Inorg. Chem., 12 (1973) 2815.

203 L.M. Ludwick and T.L. Brown, J. Am. Chem. Soc., 91 (1969) 5188.

204 R.J. Guschl, R.S. Stewart and T.L. Brown, Inorg. Chem., 13 (1974) 417.

205 W.C. Trogler, R.C. Stewart and L.G. Marzilli, J. Am. Chem. Soc., 96 (1974) 3697.

206 R.C. Stewart and L.G. Marzilli, J. Am. Chem. Soc., 100 (1978) 817.

207 When NH groups are present [81,208] or the ligand is bulky [61,81], the value of the competition ratio k_1/k_2 deviates from unity.

208 F.R. Jensen and R.C. Kiskis, J. Am. Chem. Soc., 97 (1975) 5820.

209 J.H. Ramsden, Ph.D. Thesis, Johns Hopkins University, 1980.

210 A. Sandercock, unpublished data.

211 Ref. 204 contains dynamic NMR information on $P(OMe)_3Co(DH)_2R$ in C_6H_5Br and calculated values for k_1 at 110°C. The values are as follows (s^{-1}): $CH_2{-}SiMe_3$, 380*; CH_3, 48 ± 5; CH_2F, 35 ± 5; CHF_2, 24 ± 4; CF_3, 3.0 ± 0.7; CH_2Cl, 8.4 ± 1; $CHCl_2$, 3.4*; CH_2Br, 35 ± 1; $CHBr_2$, 1.8 ± 0.7. Errors in starred values are discussed in ref. 204. Five bond couplings (P–H) are also given but the value for CH_3 appears to be in error.

212 J.H. Espenson and R. Russell, Inorg. Chem., 13 (1974) 7.

213 R. Dreos Garlatti, G. Tauzher and G. Costa, Inorg. Chim. Acta, 70 (1983) 83.

214 J.A. Ewen and D.J. Darensbourg, J. Am. Chem. Soc., 98 (1976) 4317.

215 R. Dreos Garlatti, G. Tauzher and G. Costa, Inorg. Chim. Acta, 71 (1983) 9.

216 W.C. Trogler, L.A. Epps and L.G. Marzilli, Inorg. Chem., 14 (1975) 2748.

217 F.T.T. Ng, G.L. Rempel and J. Halpern, J. Am. Chem. Soc., 104 (1982) 621.

218 F.T.T. Ng, G.L. Rempel and J. Halpern, Inorg. Chim. Acta, 77 (1983) L165.

219 A. Adin and J.H. Espenson, J. Chem. Soc. Chem. Commun., (1971) 653.

220 J. Halpern and P.F. Phelan, J. Am. Chem. Soc., 94 (1972) 1881.

221 P.W. Schneider, P.F. Phelan and J. Halpern, J. Am. Chem. Soc., 91 (1969) 77.

222 K.L. Brown and M. Ngamelue, J. Organomet. Chem., 243 (1983) 339.

223 K.L. Brown and E. Zahonyi-Budo, Inorg. Chem., 20 (1981) 1264.

224 K.L. Brown and E. Zahonyi-Budo, J. Am. Chem. Soc., 104 (1982) 4117.

225 R.L. Courtright, R.S. Drago, J.A. Nusz and M.S. Nozari, Inorg. Chem., 12 (1973) 2809.

226 A.W. Herlinger and T.L. Brown, J. Am. Chem. Soc., 94 (1972) 388.

227 G. Costa, A. Puxeddu and G. Tauzher, Inorg. Nucl. Chem. Lett., 4 (1968) 319.

228 G. Costa, A. Puxeddu and E. Reisenhofer, Collect. Czech. Chem. Commun., 36 (1970) 1065.

229 R.G. Finke, B.L. Smith, M.W. Droege, C.M. Elliott and E. Hershenhart, J. Organomet. Chem., 202 (1980) C25.

230 C.M. Elliott, E. Hershenhart, R.G. Finke and B.L. Smith, J. Am. Chem. Soc., 103 (1981) 5558.

231 M.D. Le Hoang, Y. Robin, J. Devynck, C. Bied-Charreton and A. Gaudemer, J. Organomet. Chem., 222 (1981) 311.

232 A.L. Crumbliss and R.D. Morgan, unpublished results.

233 J. Halpern, M.S. Chan, J. Hanson, T.S. Roche and J.A. Topich, J. Am. Chem. Soc., 97 (1975) 1606.

234 I. Levitin, A.L. Sigan and M.E. Vol'pin, J. Chem. Soc. Chem. Commun., (1975) 469.

235 P. Abley, E.R. Dockal and J. Halpern, J. Am. Chem. Soc., 94 (1972) 659.

236 J. Halpern, J.A. Topich and K.I. Zamaraev, Inorg. Chim. Acta, 20 (1976) L21.

237 A.V. Benedetti, E.R. Dockal, H.L. Chum and T. Rabockai, J. Electroanal. Chem., 133 (1982) 45.

238 G.A. Nikitaeva, A.T. Nikitaev, K.I. Zamaraev, A.L. Sigan, I.Ya. Levitin and M.E. Vol'pin, J. Struct. Chem., 19 (1978) 243.

239 R.H. Magnuson, J. Halpern, I.Ya. Levitin and M.E. Vol'pin, J. Chem. Soc. Chem. Commun., (1978) 44.
240 M.E. Vol'pin, I.Ya. Levitin, A.L. Sigan, J. Halpern and G.M. Tom, Inorg. Chim. Acta, 41 (1980) 271.
241 H.L. Chum, E.R. Dockal and T. Rabockai, J. Electroanal. Chem., 63 (1975) 197.
242 G. Costa, A. Puxeddu, C. Tavagnacco and R. Dreos Garlatti, Inorg. Chim. Acta, 89 (1984) 65.
243 S. Bruckner, M. Calligaris, G. Nardin and L. Randaccio, Inorg. Chim. Acta, 3 (1969) 278.
244 D.M. Palade, T.N. Volokh, N.A. Breslauskaya and T.N. Golyshina, Russ. J. Inorg. Chem., 15 (1970) 1401.
245 A. Bakac and J.H. Espenson, J. Am. Chem. Soc., 106 (1984) 5197.
246 N. Bresciani-Pahor, L.G. Marzilli, L. Randaccio, P.J. Toscano and E. Zangrando, J. Chem. Soc. Chem. Common., (1984) 1508.
247 B.M. Babior and J.S. Krouwer, CRC Crit. Rev. Biochem., 6 (1979) 35.
248 R.G. Finke, D.A. Schiraldi and B.J. Mayer, Coord. Chem. Rev., 54 (1984) 1.
249 J. Halpern, Pure Appl. Chem., 55 (1983) 1059.
250 T. Toraya, E. Krodel, A.S. Mildvan and R.H. Abeles, Biochemistry, 18 (1979) 417.
251 J.S. Krouwer, B. Holmquist, R.S. Kipnes and B.M. Babior, Biochim. Biophys. Acta, 153 (1980) 612.
252 D.L. Anton, P.K. Tsai and H.P.C. Hogenkamp, J. Biol. Chem., 255 (1980) 4507.
253 M.R. Hollaway, H.A. White, K.N. Joblin, A.W. Johnson, M.F. Lappert and O.C. Wallis, Eur. J. Biochem., 82 (1978) 143.
254 S.M. Chemaly and J.M. Pratt, J. Chem. Soc. Dalton Trans., (1980) 2259, 2267, 2274.
255 J.H. Grate and G.N. Schrauzer, J. Am. Chem. Soc., 101 (1979) 4601 and references therein.
256 J. Halpern, Ann. N.Y. Acad. Sci., 239 (1974) 2.
257 Unpublished results.
258 J.H. Grate, J.W. Grate and G.N. Schrauzer, J. Am. Chem. Soc., 104 (1982) 1588.
259 T.-T. Tsou, M. Loots and J. Halpern, J. Am. Chem. Soc., 104 (1982) 623.
260 R.G. Finke, B.L. Smith, B.J. Mayer and A.A. Molinero, Inorg. Chem., 22 (1983) 3677.
261 G. Bidlingmaier, H. Flohr, V.M. Kempe, T. Krebs and J. Rétey, Angew. Chem., Int. Ed. Engl., 14 (1975) 822.
262 G. Dreos Garlatti, C. Tauzher and G. Costa, Inorg. Chim. Acta, 82 (1984) 197.
263 A. Fisher, W.J. Gallaway and J. Vaughan, J. Chem. Soc., (1964) 3591.